

Transient and Steady-State Thermodynamic Modeling of
Modular Data Centers

A Thesis
Presented to
The Academic Faculty

by

REHAN KHALID

In Partial Fulfillment
of the Requirements for the Degree
Master of Science in the
School of Mechanical Engineering

Georgia Institute of Technology

May 2016

Copyright © 2016 by Rehan Khalid

Transient and Steady-State Thermodynamic Modeling of Modular Data Centers

Approved by:

Dr. Yogendra K. Joshi, Advisor
School of Mechanical Engineering
Georgia Institute of Technology

Dr. Satish Kumar
School of Mechanical Engineering
Georgia Institute of Technology

Dr. Aaron P. Wemhoff
Department of Mechanical Engineering
Villanova University

Date Approved: April 18, 2016

To Mom & Dad,
Without whom
this would never have been possible

ACKNOWLEDGEMENTS

This project would not have been possible without the support of many people, first and foremost my parents. Also, many thanks to my adviser, Dr. Yogendra K. Joshi, who read my numerous revisions and helped make sense of the confusion. Moreover, thanks to my committee members, Dr. Aaron Wemhoff and Dr. Satish Kumar, who offered guidance and support. Next, thanks to the Georgia Institute of Technology, Woodruff School for providing me with numerous opportunities, world-class facilities and a congenial environment to complete this project. And last but certainly not least, thanks to my family and friends who endured this long process with me, always offering their love and support.

TABLE OF CONTENTS

ACKNOWLEDGEMENTS	iv
LIST OF TABLES	ii
LIST OF FIGURES	iii
LIST OF ABBREVIATIONS	vi
SUMMARY	vii
CHAPTER 1: INTRODUCTION	1
1.1 Modular Data Centers	1
1.2 History, Development & Current Trends in Modular Data Centers	2
1.3 Review of Cooling Techniques used in Portable Data Centers	3
1.4 Anatomy of a Modular Data Center.....	4
1.5 Huawei’s Modular Data Center (IDS 1000A)	5
1.6 Simulation Software.....	5
CHAPTER 2: NUMERICAL CODES USED	6
2.1 ASHRAE TC 9.9	6
2.2 ASHRAE Environmental Guidelines.....	6
2.3 Explanation of ASHRAE limits	9
Dry-bulb upper limit:	9
Upper moisture limit:	9
Lower moisture limit:	10
Acoustical noise levels:.....	10
2.4 ASHRAE 2011 Thermal Guidelines – Expanded Data Center Classes & Usage Guidance	10
2.5 New Environmental Class Definitions.....	13
A1.....	13
2.6 ASHRAE Standard 90.1	14
2.6.1 Applicability to Datacom	14
CHAPTER 3: STEADY-STATE RESPONSE.....	16
3.1 Data Center Selection.....	17
3.2 Modular Data Center Advantages.....	18
3.3 Modelling Tool Selection.....	18
3.4 Location and Climate	19
3.5 EnergyPlus Workflow.....	20

3.6	Model Development.....	20
3.6.1	Creating the Geometry	20
3.6.2	Internal Gains.....	21
3.6.3	PUE & Exergy Calculations	24
3.7	Timestep Analysis.....	31
3.8	Passive Cooling Techniques	38
3.8.1	Direct Evaporative Cooling	39
3.8.2	Free Air Cooling	41
3.9	Results & Discussion	46
3.10	Summary & Conclusions	50
CHAPTER 4: TRANSIENT RESPONSE		52
4.1	Introduction.....	52
4.2	Dynamic Server Model Development.....	52
4.3	Implementation of the Dynamic Server Model.....	54
4.4	Results.....	56
4.4.1	MLE+ Results	56
4.4.2	Un-modified Power.....	56
4.4.3	Power Savings.....	62
4.5	Timestep analysis for transient server model.....	67
4.6	Summary & Conclusion.....	70
CHAPTER 5: CONCLUSIONS		71
Appendix A: PERFORMANCE CURVES FOR DX SYSTEM MODELED AS A CRAC UNIT.....		73
Appendix B: SIMPLE TRANSIENT SERVER EXPERIMENT TO VALIDATE TRANSIENT MODEL		82
REFERENCES		93

LIST OF TABLES

Table 2.1: 2008 ASHRAE guidelines for data center equipment.....	8
Table 2.2: Comparison of ASHRAE's environmental and operating guidelines for ITE incoming air	9
Table 2.3: ASHRAE updated guidelines and new classes - 2011	10
Table 2.4: Comparison between 2011 and 2008 ASHRAE environmental classes and guidelines	12
Table 3.1: Huawei IDS 1000-A specifications	18
Table 3.2 Sources of heat gain within the data center	21
Table 3.3: DX cooling system specifications	22
Table 3.4: ASHRAE classes for IT equipment.....	23
Table 3.5: DX-evaporative cooling system specifications	40
Table 3.6: DX, Evaporative and Free Air Cooling performance summary, Phoenix, AZ.....	45
Table 3.7: Winter, Summer & Annual PUE values for DX Cooling.....	47
Table 3.8: Mechanical PUE values for Phoenix, AZ using all	48
Table 4.1: Variable exchange to and from EnergyPlus	55
Table 4.2: Server parameters calculated through MLE+	56
Table 4.3: CPU power modifier curves – original and modified.....	57
Table 4.4: Comparison of server transient parameters with varying timestep	69
Table B.1 : Transient server parameters for an unpowered server	85
Table B.2: Transient server parameters for an initially powered server.....	88
Table B.3: Comparison of numerical vs empirical transient server parameters	90

LIST OF FIGURES

Figure 1.1: Anatomy of a modular data center	4
Figure 2.1: ASHARE environmental operating guidelines for ITE – 2004	6
Figure 2.2: ASHARE environmental operating guidelines for ITE - 2008	7
Figure 2.3: 2011 ASHRAE Environmental classes for data com equipment	12
Figure 3.1: Container Data Center Layout Description	17
Figure 3.2: Selected locations across the US	19
Figure 3.3: Variation of Outdoor Dry-Bulb temperature with location.....	20
Figure 3.4: EnergyPlus Workflow	20
Figure 3.5: Geometry created using SketchUp.....	21
Figure 3.6: DX cooling system schematic	22
Figure 3.7: Variation of PUE with location for DX cooling.....	26
Figure 3.8: Variation of cooling coil total cooling rate for DX cooling.....	27
Figure 3.9: Variation of cooling coil power consumption with location for DX cooling	27
Figure 3.10: CRAC total power consumption for DX cooling.....	28
Figure 3.11: CRAC SCOP variation with location for DX cooling	28
Figure 3.12: Variation of HVAC total power consumption for DX cooling	29
Figure 3.13: Variation of exergy destruction with location for DX cooling	29
Figure 3.14: Server temperature difference across the four locations for DX cooling.....	30
Figure 3.15: Server temperature across the four locations for DX cooling	31
Figure 3.16: Comparison of PUE values against different timesteps for DX cooling.....	32
Figure 3.17: Comparison of total HVAC power agaist timestep for DX cooling	32
Figure 3.18: Comparison of cooling coil power consumption agaist	33
Figure 3.19: Comparison of cooling coil power consumption agaist	33
Figure 3.20: Percentage error for DX cooling PUE values by	34
Figure 3.21: Percentage error for DX cooling HVAC power consumption	35
Figure 3.22: Percentage error for DX cooling coil power consumption.....	35
Figure 3.23: Percentage error for DX cooling exergy destruction, Phoenix, AZ	36
Figure 3.24: Percentage error for DX cooling PUE values by	36
Figure 3.25: Percentage error for DX cooling HVAC power consumption	37

Figure 3.26: Percentage error for DX cooling coil power consumption.....	37
Figure 3.27: Percentage error for DX cooling exergy destruction, Chicago, IL	38
Figure 3.28:DX-Direct Evaporative Cooling HVAC schematic	39
Figure 3.29: DX-Free Air Cooling HVAC schematic as	41
Figure 3.30: Variation of PUE with cooling system, Phoenix, AZ	42
Figure 3.31: Variation of CRAC total power consumption with.....	42
Figure 3.32: Variation of HVAC total power consumption	43
Figure 3.33: Variation of Cooling Coil total cooling rate, Phoenix, AZ	43
Figure 3.34: Variation of Cooling coil total power consumption, Phoenix, AZ	44
Figure 3.35: Evaporative Cooler pump power & water usage, Phoenix, AZ	44
Figure 3.36: Variation of exergy destruction with cooling system, Phoenix, AZ	45
Figure 3.37: IT equipment inlet temperature for the three cooling systems	46
Figure 3.38: IT equipment inlet relative humidity for the three cooling systems.....	47
Figure 3.39: Comparison of annual total facility and HVAC system.....	49
Figure 3.40: Comparison of HVAC power consumption as a	49
Figure 4.1: Control volume for a server treated as a blackbox	53
Figure 4.2: CPU loading schedule	57
Figure 4.3: CPU power modifier curve output	58
Figure 4.4: CPU power dissipation.....	59
Figure 4.5: HVAC power consumption	60
Figure 4.6: Server Inlet and Exit Temperature	61
Figure 4.7: Server Temperature calculated using MLE+	61
Figure 4.8: Server Temperature increasing with rising demand.....	62
Figure 4.9: Comparison of HVAC power between EP & transient model	63
Figure 4.10: Server Temperature decreasing with a drop in demand	64
Figure 4.11: Comparison of HVAC power between EP & transient model.....	64
Figure 4.12: Power Savings by following transient server profile	65
Figure 4.13: Extrapolated annual energy savings for both cases.....	66
Figure 4.14: Expected financial savings for both cases	66
Figure 4.15: Variation in percentage error of server temperature with timestep.....	67
Figure 4.16: Variation in percentage error of exit air temperature	68

Figure 4.17: Variation in percentage error of exit air temperature	68
Figure 4.18: Variation in percentage error of total HVAC power with timestep	69
Figure B.1: Variation of server inlet air temperature with time	85
Figure B.2: Variation of CPU & fan power dissipation with time	86
Figure B.3: Variation of server inlet & exit air temperature with time	86
Figure B.4: Variation of server temperature with time.....	87
Figure B.5: Variation of server & exit air temperature with time	87
Figure B.6: Variation of CPU & fan power dissipation with time	88
Figure B.7: Variation of server inlet & exit air temperature with time	89
Figure B.8: Variation of server & exit air temperature with time	89
Figure B.9: Variation of CPU & fan power for an initially	91
Figure B.10: Variation of server inlet & exit temperature.....	91
Figure B.11: Variation of server & exit air temperature.....	92

LIST OF ABBREVIATIONS

CRAC	Computer room air conditioner
CRAH	Computer room air handler
CSV	Comma-separated values
EMS	Energy management system
EP	EnergyPlus
DCE+	Data Center EnergyPlus
DEC	Direct evaporative cooling
DX	Direct expansion
HVAC	Heating, ventilation, and air conditioning
IDF	Input data file
IEC	Indirect evaporative cooling
IT	Information technology
NREL	National Renewable Energy Laboratory
PLR	Part Load Ratio
PUE	Power utilization effectiveness
SCOP	Sensible coefficient of performance
T	Temperature
UPS	Uninterruptible power system
VAV	Variable air volume
WUE	Water utilization effectiveness
Subscript °	Ambient
Superscript °	Degree

SUMMARY

Modular data centers are fast becoming the industry norm. Standardized, rapidly fabricated, easily transported and quickly deployed as compared to regular brick and mortar data centers, they are rapidly replacing the big and bulky regular data centers as a means of deploying cloud-based capability across the globe. The trend for these data centers was on the decline a decade or so ago, but since the year 2007, they are picking pace again. Nowadays, even regular data centers are being manufactured as clusters of modular centers, with each modular data center acting as a unit cell or an individual “brick in the wall”. The biggest advantage that comes with such a design is in terms of modularity, followed by ease of deploy-ability. In terms of modularity, whenever the need is felt, additional modular data centers or “cells” can be incorporated into the structure to enhance overall capacity. The way this modularity is achieved is that individual containers come together to form a cluster, and then individual clusters are grouped together and housed in a brick-and-mortar facility to form a complete data center, with a central power source. Additional clusters can be added whenever the need for increasing the capacity is felt. Moreover, if a change in location is desired, individual clusters can be taken out and transported to another location to be deployed and supply data center capacity at the new location. The PUE and similar metrics of such a facility can be calculated and controlled relatively easily.

The ease of transportation means that these mobile data centers have to deal with various climates. Depending on the application for which they have to be used, the climate and topography can vary from cold and mountainous to hot, harsh and barren; from cold and windy to hot and humid. These varying weather conditions, not just seasonally but also location based, demand that data center cooling systems be prepared to handle such conditions.

This study hence considers Huawei’s IDS 1000A (All-in-One) container data center and analyses its base cooling system, which is DX cooling, for four different climatic conditions across the United States. These range from cold and dry in Chicago, IL to hot and humid in Tampa, FL and from the cold mountains of Golden, Colorado to the hot and arid deserts of Phoenix, Arizona. The study suggests that the base cooling system does best in the cold weathers of Chicago, IL and Golden, CO and does worst in Phoenix, AZ, in terms of the calculated summer and winter PUE values. Thus, it is chosen as the location for further analysis.

For this purpose, the base cooling system is augmented, in turn, with two additional cooling techniques, namely Direct Evaporative Cooling (DEC) and Free Air Cooling, using an outside air-economizer. The results suggest that for Phoenix, AZ, DX cooling augmented with direct evaporative cooling (DEC) works best which is intuitive, given that desert coolers perform very well in dry and arid climate, such as that of Phoenix. 38% savings in terms of annual total facility power consumption can be realized by adapting a passive cooling technique such as DEC in conjunction with DX cooling, as opposed to running DX cooling alone. This massively cuts down on utility costs over the span of a full year. Moreover, by utilizing the relatively cooler night air and, running the system in economizer mode when feasible, can result in power savings of up to 36% in Phoenix as compared to running on DX cooling alone.

Data centers are power hungry by design and hence lots of effort are put into finding effective ways to save power in a data center and cut down on utility bills. A major question that is the focus of tremendous amounts of research and development is whether to instantly ramp up cooling at times of increasing demand or ramp up slowly over a small time period, thereby saving some power.

For this purpose, the transient model as proposed by Erden et al. [5] was implemented in MLE+ and co-simulated with EnergyPlus. The transient model takes into account the thermal mass of the server by assuming that it has an associated thermal capacitance, C_s and time constant, τ . The findings are interesting in the sense that while EnergyPlus quickly ramps up the cooling power in response to an increase in CPU loading (demand), which reduces the inlet air temperature to the servers in order to maintain the zone temperature and meet the return air setpoint, the transient model suggests that the server temperature and hence the exit air temperature actually lags the inlet air temperature, depending on the value of the calculated time constant. This leads to the fact that server power dissipation will also not increase instantly to the higher level but rather increase gradually at a decreasing rate, eventually achieving steady-state at a higher temperature. Thus, the cooling system can actually respond in a corresponding manner by delaying the output cooling rate, so as to meet the increasing server temperature. Profiles for the server temperature have been plotted and corresponding profiles for the HVAC system have been suggested based on the rising server temperature (server power dissipation). This delayed response from the cooling system will result in small power savings during the instants in which the server is powering up/demand is

going up. However, in the case of demand going down, the corresponding server power can be either decreased instantly to the desired lower level, in order to save power or decrease the power slowly, which will potentially offset any savings gained earlier by ramping up slowly.

In essence, data center power consumption continues to double every 7 years. At this rate, global data center energy consumption will increase by a factor of 2^5 or 32 times that of today. With depleting energy resources and increasing power requirements, it is necessary that cost effective measures to curb not only energy consumption but also environmental emissions such as CO and NO_x be pursued and implemented aggressively.

CHAPTER 1

INTRODUCTION

1.1 Modular Data Centers

Modular data centers are a portable method of deploying data center capacity. They consist of standardized and pre-built components and are thus easier and cheaper to build than regular data centers. They can be readily customised to suit the needs of the manufacturer and the terrain in which they are going to be deployed.

Modular data centers come in two form factors, either containerised data centers or flexible data centers [1]. Containerised data centers, also known as portable modular data centers, pack data center equipment into a standard shipping container and the container is then transported to a desired location. They typically come outfitted with their own cooling systems. Flexible data centers, on the other hand, are composed of pre-fabricated components which are then transported to and quickly assembled on site and added to the existing infrastructure when needed. Modular data centers are hence designed for rapid deployment.

Modular data centers are used in terrains where grid connected brick and mortar data centers can either not be built, such as oil fields and other harsh terrains, or they are used to enhance the capability of existing infrastructure by adding pre-configured modules. Since they consume significant energy, with typical 20%-50% towards cooling, this calls for systematic ways to monitor and control their power consumption.

Modular or container data centers offer scalable data center capacity and multiple power and cooling options. The modules can be assembled and shipped anywhere in the world to be added, integrated or retrofitted into the customer's existing data center footprint. They are also energy efficient and some like the Microsoft Generation 4 modular data center are highly energy efficient. Since they are made from standardized components, their Power Usage Effectiveness (PUE) values can be easily calculated and controlled. Moreover, they are high-density computing clusters for storing and processing large amounts of data over the cloud and for multiple purposes such as telecommunications, Internet Service Providers and large IT companies for storing customer data over the cloud.

The benefits of modular data centers over the regular brick and mortar ones include deployment and delivery of data center capacity at a lower cost than traditional construction methods. Also, modularising the data center into standard parts and assembling it on site reduces the construction time from years to a matter of months.

The data center industry currently focuses on initiatives to reduce its enormous energy consumption and minimize its adverse environmental impact. Hence, keeping this need in mind, this study aims at developing steady-state energy and exergy destruction models for modular data centers using four different cooling approaches: direct expansion cooling, direct and indirect evaporative cooling, and free air cooling. Sources of inefficiency are identified via exergy destruction calculations in the hot and cold aisles of the data center.

1.2 History, Development & Current Trends in Modular Data Centers

Modular data centers started from Sun Microsystems project codenamed Black Box [2]. There are several manufacturers of modular data centers in the market now. These include OEMs such as IBM, HP & Dell as well as other big players are emerging onto the scene including software giants Microsoft, Google and Facebook [3]. Microsoft's *Generation 4* modular data center is extraordinarily energy efficient and operates without water, relying entirely on air-side economisers for cooling [4]. Microsoft has also developed a "*Data Center in a Box*" approach, which they are offering in their new state-of-the-art facility outside of Chicago. Furthermore, Microsoft also offer another version of their modular data centers called the *IT-PAC* (Pre-assembled components) [5].

Rackable Systems (RACK), on the other hand, use water cooling for their *ICE Cube*. However, they are now shifting to air-cooled versions, designed to offer deployment options in scenarios where water hook-ups may not be readily available [6]. IBM offers their Portable Modular Data Center. Similarly, Verari Systems offer their own version of a Container Data Center [7]. Schneider Electric offers their own version of MDC's called the *EcoBreeze*, which has a separate cooling module from the main data center equipment module. This innovative modular data center implements adaptable cooling based on environmental conditions and automatically selects either indirect evaporative cooling or air-to-air heat exchange, depending on the external environment [8]. Similarly, Hewlett-Packard offer what they call a *DataPod*, their own version of a modular data center [9], [10].

1.3 Review of Cooling Techniques used in Portable Data Centers

Manufacturers of portable or modular data centers normally use Direct Expansion (DX) cooling to cool the equipment within their data center. Examples of these include Huawei and a few others. Other containerized data center manufacturers, such as Astek, use liquid cooling as the primary means to cool their data center; they utilize in-row liquid cooling using chillers [11]. Other modern and innovative techniques for cooling these data centers include liquid CO₂ cooling systems for high density data center applications. This rack mounted technology uses fans to pull air through equipment cabinets and into contact with a CO₂ refrigerant circulated through a vertical coil. The CO₂ is pumped in at a pressurized liquid state of 15°C into the vertical cooling coil. The cooling capacity of these systems is similar to water at this temperature and pressure.

In comparison to that, “in traditional computer systems, you have a mechanical chiller outside that delivers cold water into the data center, where air-conditioned units blow cold air under a raised floor to try to keep computer components from overheating”, says Hammond at the National Renewable Energy Laboratory (NREL). *“From a data center perspective, that’s not very efficient; it’s like putting your beverage on the kitchen table and then going outside to turn up the a/c to get your drink cold”* [12].

In addition to that, another innovative technique currently being used in the data center industry includes the use of warm-water liquid cooling. Using this technique, relatively warm water at 75 °F (23.88°C) is supplied to the servers, as opposed to traditionally using cold air at 15°C. The water, thus being supplied, is nearly at room temperature and hence does not need to be cooled or over-cooled, depending on the situation. This “warm water” is then used to “cool” the servers, whereby the water returning from the high performance cluster to the chiller is in excess of 100°F (37.78 C). This hot water is then the primary source of heat for Energy Systems Integration Facility’s (ESIF) offices and laboratory spaces at NREL. The 75°F design point is a higher starting temperature for computer cooling, allowing NREL to eliminate compressor cooling systems and instead use cooling towers. In addition, the pump energy needed to move liquid in the cooling system is much less than the fan energy needed to move air in a traditional data center. Moreover, water is about 1000 times more effective than air in terms of the thermodynamics, or heat exchange [13].

1.4 Anatomy of a Modular Data Center

A modular data center has many of the features that a regular brick and mortar data center has, such as IT equipment including servers, networking equipment, energy management and monitoring system as well as other equipment including power supply, back-up power equipment and fire protection system. The servers are housed in racks and the racks are assembled in a hot and cold aisle configuration, just as a regular data center. Figure 1.1 below shows a container data center that is still in assembly phase. The key features of a modular data centers are:

- Made from standard shipping containers (either 20' or 40' in length).
- Have insulation in the walls and roofs to prevent transfer of heat.
- Have a damping system installed in the base to protect the ITE from shocks during transportation.
- Are mounted on a special platform with basement below it, which is prepared simultaneously as the data center is assembled in order to reduce installation time.
- In the all-in-one types, the cooling, power and networking system are all contained within the same physical space (even though they may be partitioned from each other).
- Contain a door for entry and exit.
- Equipped with state-of-the-art security systems such as biometric identification [14].



Figure 1.1: Anatomy of a modular data center

1.5 Huawei's Modular Data Center (IDS 1000A)

Huawei's IDS 1000A container data center is chosen for the purpose of this study. Huawei's data centers come in two forms, the All in One (A-type) and Cluster (C-type). The A-type consist of a single container housing the servers, power and networking equipment as well as the cooling system. The default cooling system for the A-type containers is direct expansion (DX) cooling, with the indoor units contained behind the server racks and the outdoor units contained within the container at one end, with vents in the container for the fans to cool the condenser. The C-type consists of three connected containers, with a container each for the servers, power & networking equipment and the cooling system. The default cooling system for the C-type is also Direct Expansion (DX) [15].

1.6 Simulation Software

The core simulation software used for this study is EnergyPlus, an open source software from the U.S. Department of Energy [16]. EnergyPlus is used as the simulation engine within the in-house software package Data Center EnergyPlus (DCE+), which modifies EnergyPlus input data and reads EnergyPlus results to calculate data center metrics such as the Power Usage Effectiveness (PUE) values for the summer and winter design days. These values are averaged in DCE+ to calculate an overall PUE for the entire run period.

CHAPTER 2

NUMERICAL CODES USED

2.1 ASHRAE TC 9.9

The American Society for Heating, Refrigeration and Air-Conditioning, ASHRAE's, Technical Committee 9.9 (TC 9.9) is concerned with all aspects of mission critical facilities, technology spaces, and electronic equipment/systems. This includes data centers, computer rooms/closets, server rooms, raised floor environments, high-density loads, emergency network operations centers, telecom facilities, communications rooms/closets, and electronic equipment rooms/closets.¹

2.2 ASHRAE Environmental Guidelines

ASHRAE's environmental guidelines for incoming air were established in 2004 and are shown in the following psychrometric chart.

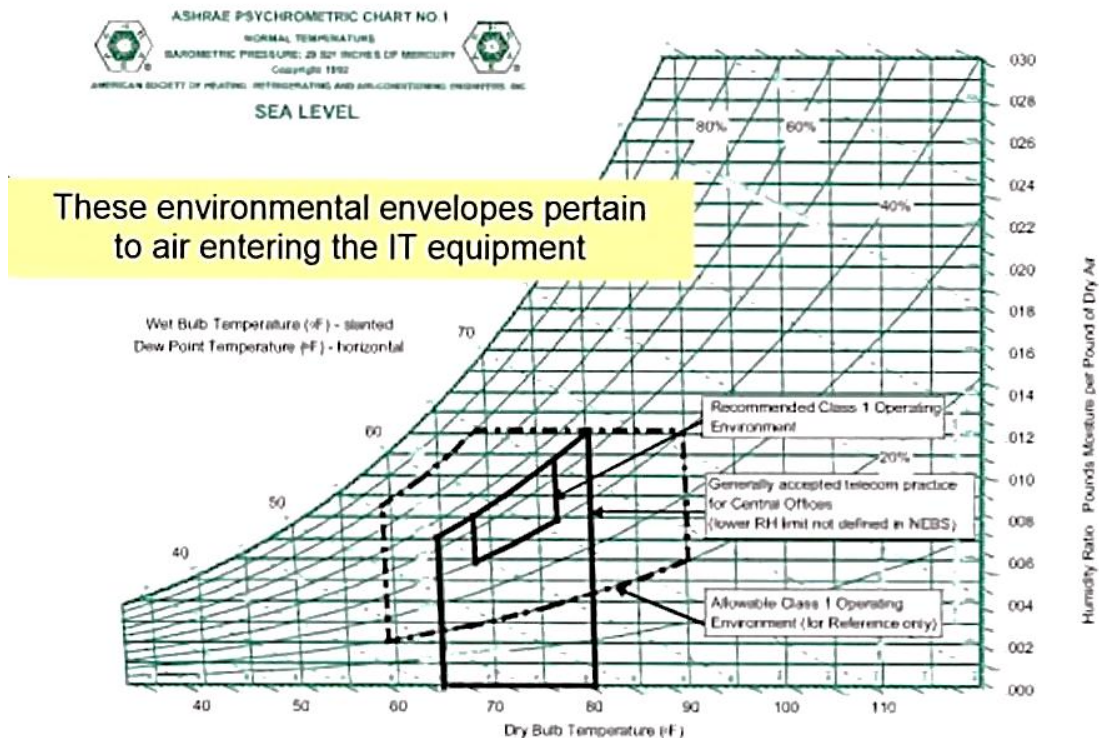


Figure 2.1: ASHARE environmental operating guidelines for ITE – 2004

¹ Source: <http://tc0909.ashraetcs.org/functions.php>

These guidelines were then relaxed in 2008 to allow for a greater range of environmental operating conditions, without compromising on functionality of the equipment. However, it is to be kept in mind that these operating conditions specify either the recommended or allowable operating conditions for data center, or data com, equipment; they do not specify the optimum operating conditions which are dependent on other factors such as thermal management (TM) and other control algorithms used for the IT equipment as well as geographical location, external weather and cooling technique employed to cool the data center and its equipment. Figure 2.2 shows the updated operating envelope [17]. Table 2.1 on the next page shows ASHRAE’s 2008 thermal guidelines for data centers.

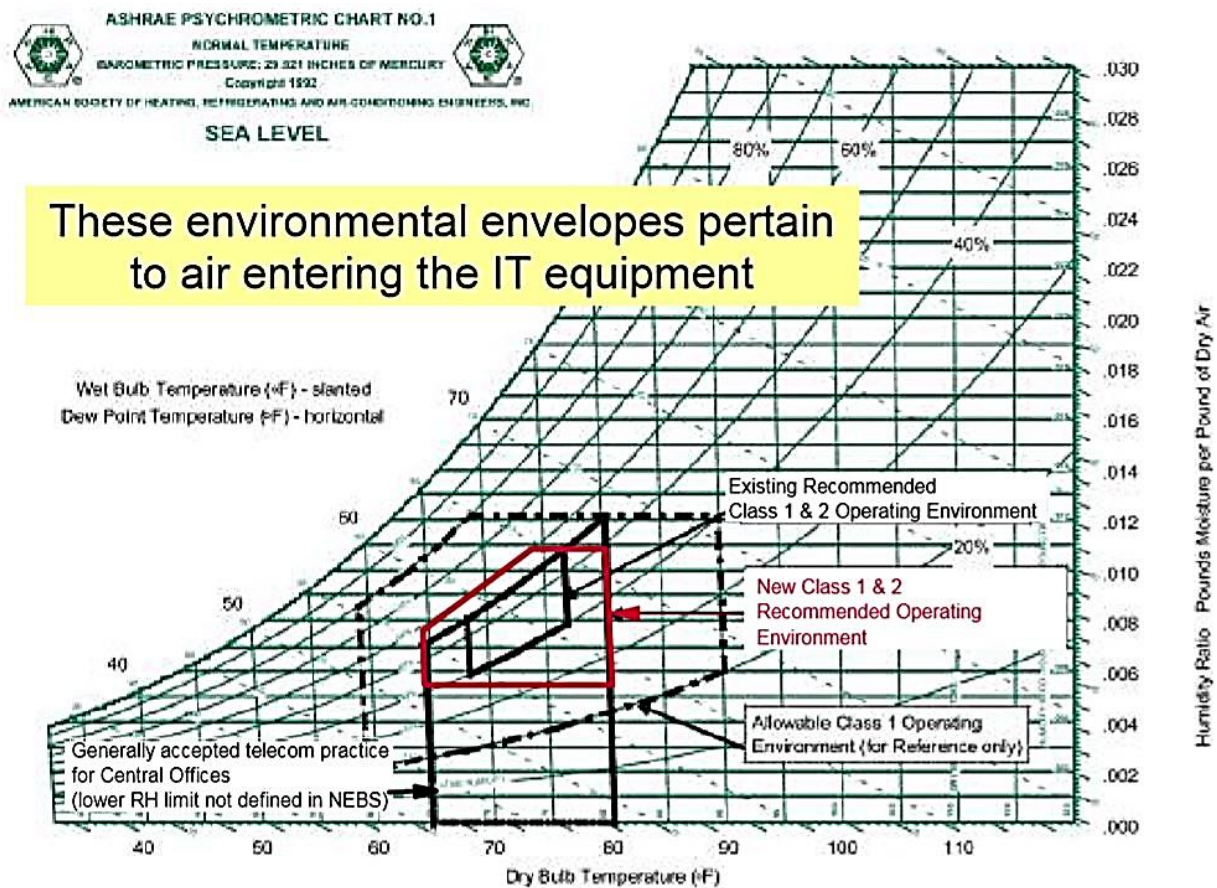


Figure 2.2: ASHARE environmental operating guidelines for ITE – 2008

Table 2.1: 2008 ASHRAE guidelines for data center equipment

Equipment Environment Specifications										
Product Operation										
Dry Bulb Temperature (°C)		Humidity Range, Non-Condensing		Maximum Dew Point (°C)	Maximum Elevation (m)	Maximum Rate of Change (°C/h)	Product Power Off			
Allowable	Recommended	Allowable (% RH)	Recommended				Dry-Bulb Temperature (°C)	Relative Humidity (%)	Maximum Dew Point (°C)	
1	15 to 32	18 to 27	20 to 80	5.5°C DP to 60% RH and 15°C DP	3050	5/20	17	5 to 45	8 to 80	27
2	10 to 35	18 to 27	20 to 80	5.5°C DP to 60% RH and 15°C DP	3050	5/20	21	5 to 45	8 to 80	27
3	5 to 35	NA	8 to 80	NA	3050	NA	28	5 to 45	8 to 80	29
4	5 to 40	NA	8 to 80	NA	3050	NA	28	5 to 45	8 to 80	29

Guidelines for incoming air were established in 2004 and then revised in 2008 while keeping all equipment manufacturers' and hardware vendors on board. Table 2.1 below summarizes the differences between the two guidelines:

Table 2.2: Comparison of ASHRAE's environmental and operating guidelines for ITE incoming air

	2004 version	2008 version
Low End Temperature	20°C (68°F)	18°C (64.4°F)
High End Temperature	25°C (77°F)	27°C (80.6°F)
Low End Moisture	40% RH	5.5°C DP (41.9°F)
High End Moisture	55% RH	60% RH & 15°C DP (59°F DP)

2.3 Explanation of ASHRAE limits

It should be noted that the temperature range specified above is for inlet air conditions for Datacom equipment unless otherwise specified. The specified conditions generally prevail in the majority of the data center; however, the temperature of the incoming air is higher near the top of the racks than at the bottom, due to wake effect and mixing of the cooler incoming and hot return air as it moves from the cold plenum at the bottom to the hot plenum at the top, especially if the return hot air does not have a direct path to the CRAC because that promotes air mixing. The higher temperatures at the top also lead to reduced humidity levels near the top.

Dry-bulb lower limit: The lower end dry-bulb temperature has been decreased from 20 to 18°C. This is done to increase the control range of the building energy management system. Moreover, this reduces the use of hot return air for mixing and rely more on the fraction of the outside air. However, this should not be taken as a reason for reducing operating or setpoint temperatures, especially if the temperature recorded is that of return air, because this may lead to overcooling, higher energy costs and freezing of cooling coils.

Dry-bulb upper limit: The reason for increasing the dry-bulb upper limit to 27°C is to increase the number of economizer running hours per year. This has the effect of reducing energy consumed. However, it should be kept in mind that acoustical/noise level of the entire HVAC system is greatly enhanced. This will be discussed in detail later.

Upper moisture limit: The upper moisture level has been reduced slightly to slow down the process of corrosion and provide an adequate safeguard for server components such as disk and tape drives.

Lower moisture limit: The reason for reducing this is to find a humidity level low enough so as not to require humidification from the HVAC system and save on associated water usage and energy costs.

A secondary reason is to prevent buildup of electrostatic discharge (ESD) which occurs because of air drying up. So a lower level is chosen to cater to these conditions without excessively drying up the air. However, the effects of ESD and moisture level are not yet completely understood and research is being done by ASHRAE to come up with an optimum level, which may be adopted in the future.

Acoustical noise levels: Acoustical noise is a major issue faced by data center operators, especially when the recommended upper dry-bulb temperature has been increased by 2°C in the 2008 guidelines. This can potentially lead to an increase of 3-5 dB in noise level within the data center due to the operation of the air movers. However, it is still not certain whether there will be a considerable increase in noise levels because it's not known what effect the increase in temperature will have on the air movers.

2.4 ASHRAE 2011 Thermal Guidelines – Expanded Data Center Classes & Usage Guidance

Table 2.3 below shows ASHRAE’s new environmental classes for data center equipment operation.

Table 2.3: ASHRAE updated guidelines and new classes - 2011

Classes (a)	Equipment Environment Specifications							
	Product Operation					Product Power Off		
	Dry Bulb Temperature (°C)	Humidity Range, Non-Condensing	Maximum Dew Point (°C)	Maximum Elevation (m)	Maximum Rate of Change (°C/h)	Dry-Bulb Temperature (°C)	Relative Humidity (%)	Maximum Dew Point (°C)
Recommended (applies to all A classes; individual data centers can choose to expand this range based on guidelines presented in the document ASHRAE 90.1 – datacom equipment)								
A1 to A4	18 to 27	5.5°C DP to 60% RH and 15°C DP						
Allowable								

Table 2.3 continued

A1	15 to 32	20% to 80% RH	17	3050	5/20	5 to 45	8 to 80	27
A2	10 to 35	20% to 80% RH	21	3050	5/20	5 to 45	8 to 80	27
A3	5 to 40	-12°C DP & 8% RH to 85% RH	24	3050	5/20	5 to 45	8 to 85	27
A4	5 to 45	-12°C DP & 8% RH to 90% RH	24	3050	5/20	5 to 45	8 to 90	27
B	5 to 35	8% RH to 80% RH	28	3050	NA	5 to 45	8 to 80	29
C	5 to 40	8% RH to 80% RH	28	3050	NA	5 to 45	8 to 80	29

Note that in 2011, ASHRAE created two new classes A3 and A4 in order to facilitate data center owners. The other four classes, namely A1, A2, B and C remain the same as were in 2008 and have just been renamed for the sake of clarity and to avoid confusion.

These new classes, along with the existing renamed ones are shown in Fig. 2.3 below [18]:

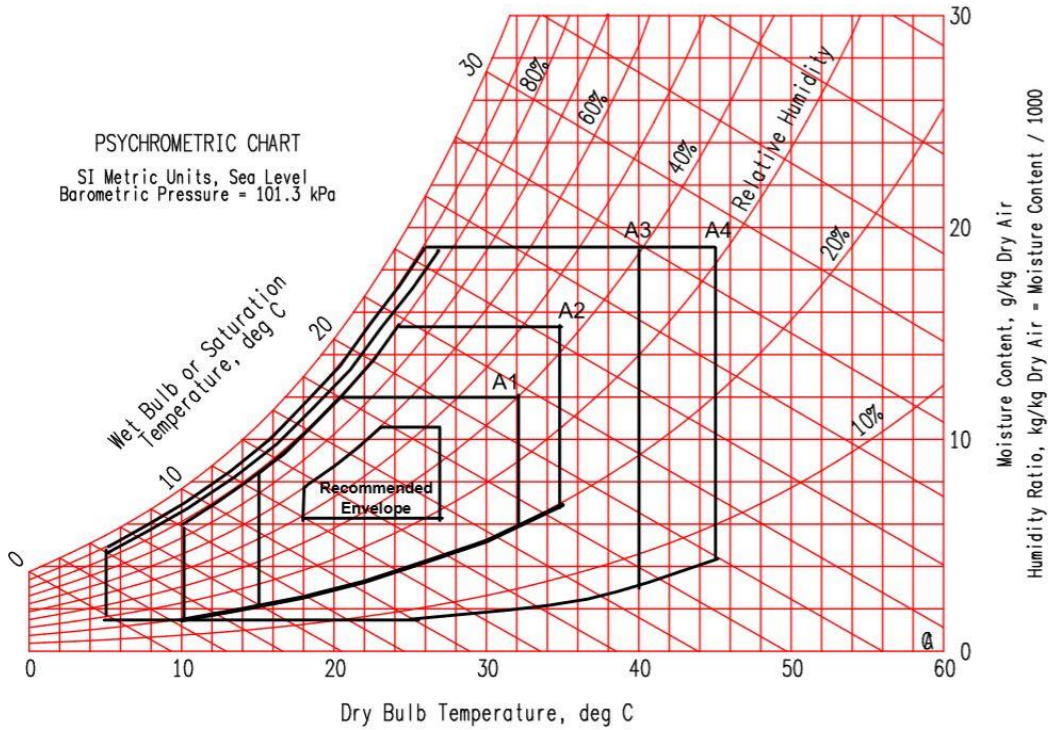


Figure 2.3: 2011 ASHRAE Environmental classes for data com equipment

Table 2.4 below compares the environmental classes and their degree of control from 2011 to that of 2008.

Table 2.4: Comparison between 2011 and 2008 ASHRAE environmental classes and guidelines

2011 classes	2008 classes	Applications	IT equipment	Environmental Control
A1	1	Datacenter	Enterprise Servers, Storage Products	Tightly controlled
A2	2		Volume Servers, Storage Products, personal computers, workstations	Some control
A3	NA		Volume Servers, Storage Products, personal computers, workstations	Some control
A4	NA		Volume Servers, Storage Products, personal computers, workstations	Some control

Table 2.4 continued

B	3	Office, home, transportable environment, etc.	Personal computers, workstations, laptops, and printers	Minimal control
C	4	Point-of-sale, industrial, factory, etc.	Point-of-sale equipment, ruggedized controllers, or computers & PDAs	No control

2.5 New Environmental Class Definitions

A1: This refers to ASHRAE’s old class 1 and typically refers to a data center environment or mission critical operations with very tight environmental control parameters (temperature, relative humidity and dew point). Typical products designed for this class include enterprise servers and storage products.

A2: This refers to ASHRAE’s old class 2 and typically refers to an information technology space/office/lab environment with some control of environmental parameters (temperature, relative humidity and dew point). Typical products designed for this class include volume servers, storage products, personal computers and workstations.

A3/A4: These are two new classes that have been created under ASHRAE’s 2011 environmental guidelines for Datacom equipment. These classes typically refer to an information technology space/office/lab environment with some control of environmental parameters (temperature, relative humidity and dew point). Typical products designed for this class include volume servers, storage products, personal computers and workstations.

B: This refers to ASHRAE’s old class 3 and typically refers to an office/home environment with minimal control of environmental parameters (temperature only). Typical products designed for this class include personal computers, workstations, laptops and printers.

C: This refers to ASHRAE’s old class 4 and typically refers to a point-of-sale or light industrial or factory environment offering weather protection, sufficient winter heating and ventilation. Types of products include point-of-sale equipment, ruggedized controllers, computers and PDA’s.

2.6 ASHRAE Standard 90.1

This document provides energy standards for buildings except low-rise residential buildings. It offers detailed guidelines for the minimum energy design and construction of new buildings, new and existing systems, building spaces and existing buildings. Thus, it provides a comprehensive guide for engineers and researchers in the building design and construction industry. The section of this code that pertains to data centers and related equipment was established in 2010, seeing the growing trend of the data center industry and a need to cut down on the power used and increase energy efficiency.

The three main components of Standard 90.1-2010 compliance are as follows:

1. Mandatory provisions—applies to all projects
2. Prescriptive (code minimum) or performance path (known as the Energy Cost Budget Method [ECB])—must comply with one or the other
3. Appendix G—exceeding 90.1 prescriptive requirements (generally used for LEED® certification; however, LEED for data centers was not available as of the publication of [19]).

Section 6 of ASHRAE Standard 90.1-2010 contains mandatory provisions for HVAC systems.

2.6.1 Applicability to Datacom

ASHRAE Standard 127 is the rating standard used to establish performance rating requirements for HVAC systems intended for use in computer room applications. Standard 127 was first published in 1988, was revised in 2001 and 2007, and is being revised again for the 2013 update to Standard 90.1 to further address requirements of computer room air-conditioning equipment. This is the applicable standard for Datacom equipment included in ASHRAE 90.1-2010 [20].

ASHRAE Table 6.8.1K applies to HVAC equipment intended for computer rooms as rated by ANSI/ASHRAE Standard 127-2007, Method of Testing for Rating Computer and Data Processing Room Unitary Air Conditioners (ASHRAE 2007)—typical CRAC and CRAH HVAC equipment only. Other types of commercial HVAC equipment (air-handling units, rooftop units, chillers, heat exchangers, etc.) applied to data centers must meet the requirements of Tables 6.8.1A through 6.8.1J and their associated rating standards, as appropriate. Any HVAC equipment used in Datacom applications that is not addressed by these tables and associated rating standards is

exempt from mandatory equipment efficiency requirements. Examples of equipment that are exempt include all types of source cooling options (in the row, above the electronic equipment frames, on or in cabinets, etc.), hybrid chillers, evaporative cooling and humidification solutions, absorption chillers, and other types of liquid cooling applications.

The data center chosen for this study contains volume servers. They are compared against ASHRAE class A3 (2011) for environmental control pertaining to cold aisle temperature, which should lie in the 5-35 °C and relative humidity, which should lie in the 8-80% range.

CHAPTER 3

STEADY-STATE RESPONSE

This work discusses the impact of various cooling techniques on the performance of modular data centers. Regular brick and mortar style data centers are common throughout the industry but modular data centers are emerging as an upcoming trend to enhance existing data center capacity, or deploy new capability in remote locations. In traditional air cooled data centers, an external mechanical chiller delivers cold water inside to cool the hot air. However, modular data centers, especially the all-in-one type discussed in this paper, cannot have components external to the system since that comes at the expense of mobility. Moreover, modular data centers also do not rely on the raised floor plenum for supplying cold air. These factors make a modular data center different from a conventional one. However, the traditional hot and cold aisle arrangement of information technology (IT) equipment, as well as augmenting the base cooling system with additional cost effective cooling methodologies are also employed in modular data centers.

Only a select few studies specific to modular data centers are seen in the literature. Ham et al. [21] found that air side economization for modular data centers could have significant savings (up to 67%) for specific climate regions. Further work by Ham et al. [22] on the optimum supply air temperature for modular data centers shows the optimum temperature to be in the 18-23°C range. They conclude that increasing the temperature any further increases the overall energy consumption since the reduction in chiller energy is offset by the increase in CRAH fan energy. Similar work on the use of fresh-air for cooling container data centers by Endo et al. [23] showed that depending on the location, fresh air alone is not suitable to maintain the data center within ASHRAE's allowable range for data centers. Their work suggests that supplementing it with evaporative cooling and waste heat from the data center can be used to effectively cool the facility even when the characteristics of fresh air was outside the allowable server settings. Similarly, Zhang et al. [24] review the work done on free air cooling for data centers in general using airside, waterside and heat pipe free cooling. They conclude that out of the three, heat pipe free cooling systems show the greatest energy efficiency and cooling capacity because of their ability to transfer heat through small temperature differences without the use of external energy and absence of any moving parts, thus making them virtually maintenance free. Quoneh et al. [25] compare the

performance and efficiency of container data centers with that of raised- floor data centers. Their study concludes that containers achieve 80% and 42% saving in cooling and facility power respectively of that of a raised-floor data center and that raised-floor data centers can approach the efficiency of a container at low utilizations while using a single cooling optimization. Depoorter et al. [26] study the effect of location on data center efficiency and its use as a renewable energy supply measure. They study five locations across Western Europe with climatic conditions ranging from Mediterranean-like in Barcelona, Spain to the freezing cold in Stockholm, Sweden. Their study suggest that PUE's rise in the summer months due to lesser availability of outside air with suitable conditions. Moreover, they note maximum energy consumption to be tied with demand on the data center and occurs around mid-day. Thus they suggest a smart IT management system to shift the load from peak hours to times in which electricity tariff is cheaper to save energy and cut down on utility cost.

3.1 Data Center Selection

This study considers Huawei's 1000A modular data center [27]. Figure 3.1 shows the anatomy of this data center. Its construction & HVAC specifications are provided in Table 1.

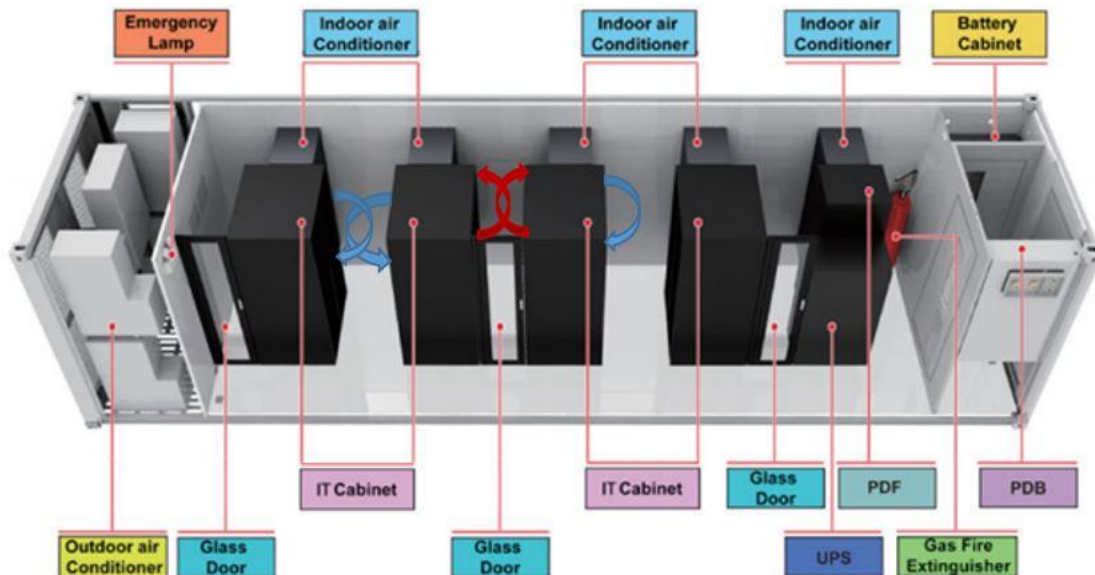


Figure 3.1: Container Data Center Layout Description

Table 3.1: Huawei IDS 1000-A specifications

	Sub Feature	IDS1000-A40
Size	External Dimensions (LxWxH)	12196*2438*2896(mm)
	Typical Power Capacity (rated)	60kW
	Typical Rack Capacity	8 IT Racks (4 cabinets + 1 redundant)
Power	Power Density per Rack	5kW per rack (actual)
Cooling	Technology	DX type horizontal flow A/C units
	Containment	Hot and Cold aisle isolation
	Cooling Capacity	12.5kW per unit
	Humidity	Optional humidifier
Design	Design target PUE	+ 1.6 at full load
Operation Parameters	Cold Aisle temperature	18-27 C within sensor tolerance
	Humidity Range	20% to 80% RH
Construction	Base Construction	40" standard ISO shipping container
	Insulation	Polyurethane: top-75mm, side-40mm

3.2 Modular Data Center Advantages

Modular data centers have several advantages as compared to regular brick and mortar data centers. Firstly, they are manufactured using standard shipping containers, retrofitted to suit the needs of the environment and purpose for which they are going to operate. Moreover, standard containers have the benefit of being pre-engineered, highly integratable, relatively low cost, fast moving, with deployment times of a week or so. Finally, they are highly customizable to suit the needs of the data center operator.

3.3 Modelling Tool Selection

The simulation software employed for this study is EnergyPlus v8.4 [28], an open-source software managed by National Renewable Energy Laboratory (NREL). The advantage of EnergyPlus over other modelling tools, such as DOE2.2, is that it uses a heat balance method for heat transfer calculations, which is more accurate when compared to other methods such as the weighting factor

approach. Moreover, EnergyPlus accounts simultaneously and iteratively for all building thermal loads and effects of HVAC systems at each time step, rather than sequentially, like in DOE 2.2 [9]. The geometry of the data center is modelled using Google's SketchUp, another free software package that provides a graphical user interface as opposed to specifying individual coordinates, as in EnergyPlus.

3.4 Location and Climate

Figure 3.2 below shows the selected locations across the US.



Figure 3.2: Selected locations across the US

Chicago, IL and Golden, CO were selected as prime locations for data center activity, with Tampa, FL and Phoenix, AZ chosen to simulate harsh environments and add detail to the comparison. The climate ranges from moist and cold in Chicago, to hot and dry in Phoenix. In general, the eastern half of the U.S. is in a moist climate zone while the western half is in a dry climate zone, except for the pacific coast, which is in a marine climate. Figure 3.3 compares the outdoor dry-bulb temperature for each of the four chosen locations.

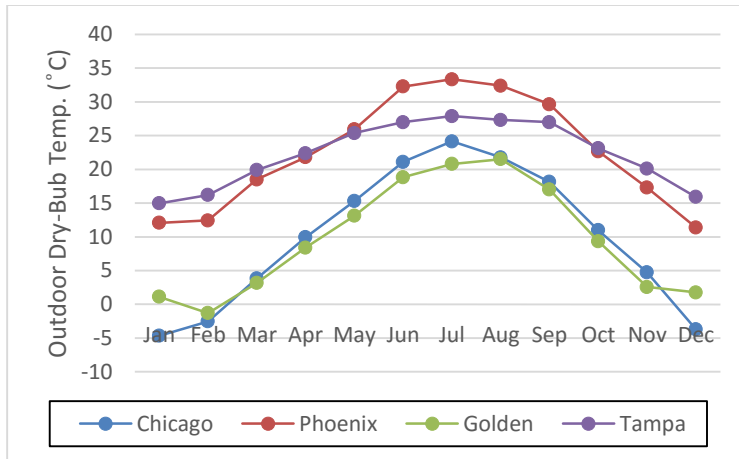


Figure 3.3: Variation of Outdoor Dry-Bulb temperature with location

3.5 EnergyPlus Workflow

The entire model workflow is summarized in Figure 3.4 below. For standard building models, modelling work starts with creating the geometry using SketchUp. Then EnergyPlus native, or any third-party software such as OpenStudio, can then be used to define the internal loads and HVAC system. The entire model specifications are contained in an input data file (IDF). EnergyPlus runs the file and outputs the results in the form of a comma separated value (CSV) file, which can be accessed using any commercial spreadsheet software.

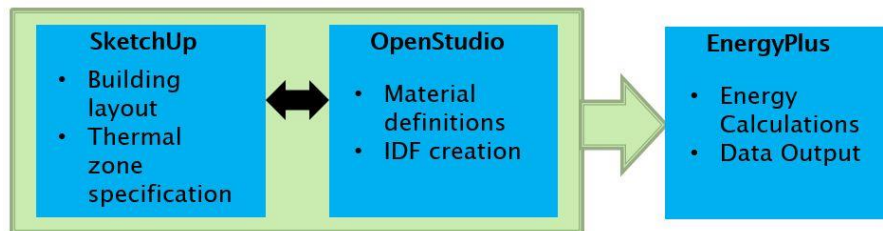


Figure 3.4: EnergyPlus Workflow

3.6 Model Development

3.6.1 Creating the Geometry

The geometry of the given size and construction was created using SketchUp. Four back-to-back, dual rack IT cabinets were modelled, with a fifth cabinet housing UPS equipment in one rack and a redundant IT rack for backup, thus creating three hot aisles, in the middle of the racks, and three cold aisles. Three thermal zones were also created within SketchUp. Each cold aisle was one

thermal zone, named Cold Zone, and the hot aisle was a second thermal zone, named Hot Zone. The outdoor air conditioner units as well as the networking & power room was a third non air-conditioned neutral zone. Two thermostats were similarly defined, one for the hot zone and the other for the cold zone. The geometry created using SketchUp is shown in Figure 3.5 below.

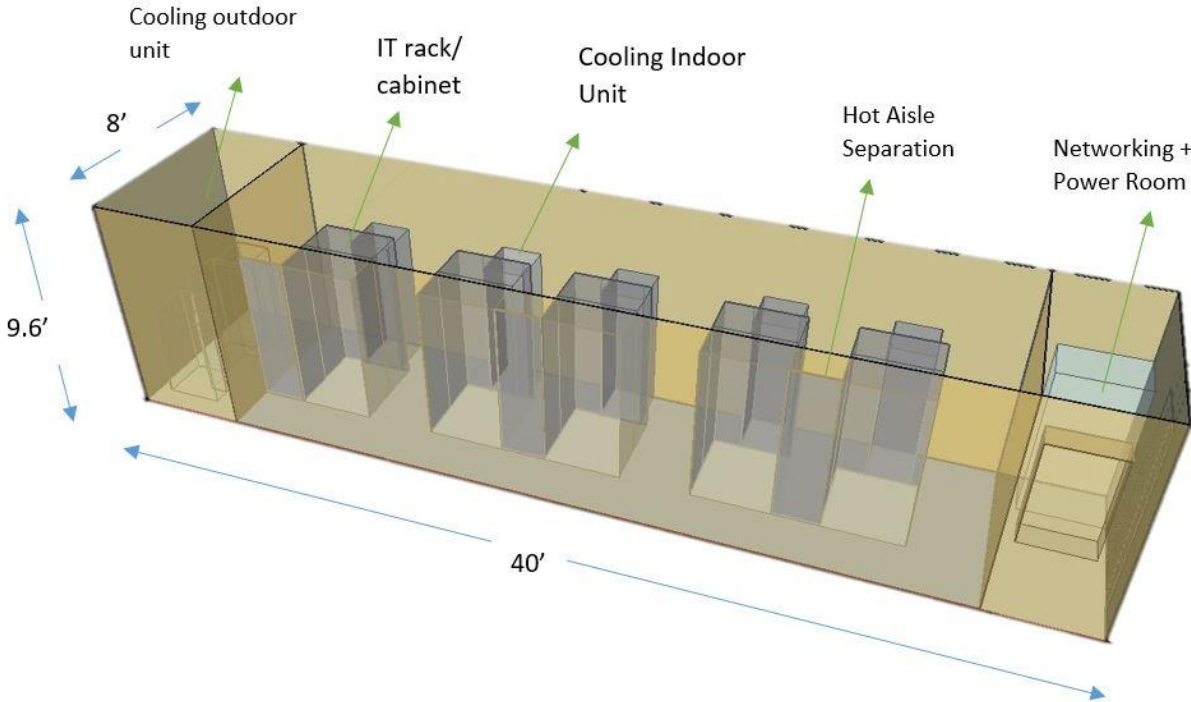


Figure 3.5: Geometry created using SketchUp

3.6.2 Internal Gains

Lights and IT equipment were specified as sources of electric load. Table 2 lists the sources of heat gain along with their other characteristics.

Table 3.2 Sources of heat gain within the data center

Source	Number of Units	Design Power (W)
Servers	320	300
Lights	--	300 (total)

The number of servers within the facility and the power dissipation of each server was specified using the object IT Equipment Air Cooled. Moreover, the design CPU power can be modified using a built-in curve which calculates the actual CPU power based on CPU loading (x) and inlet air temperature (y).

3.6.2.1 Cooling System - DX Cooling

A DX cooling system comprises of a vapour compression refrigeration cycle with either an air-cooled or liquid cooled condenser. As shown in Figure 3.1, the evaporator is contained within the conditioned space, while the condenser is mounted on the outside walls of the container (not shown in Figure 3.1) and cooled by the ambient air.

The HVAC schematic of a DX cooling system as detailed in EnergyPlus is shown in Figure 3.6 below. The specifications of the cooling system are provided in Table 3.

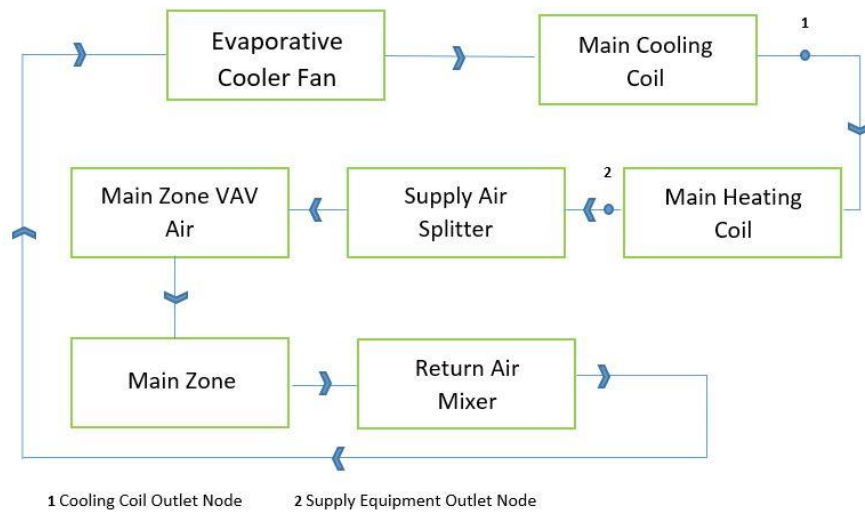


Figure 3.6: DX cooling system schematic

Table 3.3: DX cooling system specifications

Object	Specification
System type	DX type A/C with electric heating
Thermostat type	Dual-zone thermostat
Heating Setpoint	15°C

Table 3.3 continued

Cooling Setpoint	29.3°C
Design Supply Air Temp.	14°C
Supply Fan	Variable speed fan
Air distribution unit	Single-duct VAV with no reheat
Cooling coil COP	4.6

The supply fan and DX cooling coil rated power & flow rate were set to be autosized. This lets the software calculate their value based on the cooling/heating setpoints and design supply air temperature in order to meet the zone cooling load.

If the air temperature at the coil’s inlet is greater than the supply equipment outlet node setpoint temperature, node 2, and also greater than the cooling setpoint, the cooling coil works in order to meet that setpoint at its exit, i.e. node 1. And vice versa, in the opposite case the cooling coil will remain off and the heating coil would work in order to meet the zone heating setpoint.

ASHRAE’s environmental class A3 was specified as the guideline for incoming air to the servers and comparison of the HVAC system performance. Table 4 outlines the various classes for mission critical facilities by ASHRAE and their required operating conditions when the product is powered on.

Table 3.4: ASHRAE classes for IT equipment

Class	Recommended		Allowable	
	Dry-bulb Temp. (C)	Relative Humidity (%)	Dry-bulb Temp. (C)	Relative Humidity (%)
A1	18 to 27	5.5 C DP to 60% RH and 15 C DP	15 to 32	20 to 80

Table 3.4 continued

A2	18 to 27	5.5 C DP to 60% RH and 15 C DP	10 to 35	20 to 80
A3	N/A	N/A	5 to 35	8 to 80
A4	N/A	N/A	5 to 40	8 to 80

As per ASHRAE class A3 conditions, the inlet temperature and relative humidity for this cooling system were met 100% of the time.

3.6.3 PUE & Exergy Calculations

Within EnergyPlus, EMS (Energy Management System) allows the user to modify built-in functions such as schedules or setpoints for thermostats or actuate various pieces of hardware. It also allows the user to declare EnergyPlus variables as sensors and store their values to be used later on. Hence, using these values, the PUE of the data center, sensible coefficient of performance (SCOP) of the cooling coil and exergy destruction within the zone total airspace were calculated using EMS programs and reported at each timestep. The formulas are shown below.

$$PUE = \frac{\text{whole building power}}{\text{IT equipment power}} \quad (1)$$

$$SCOP = \frac{\dot{Q}_{DXcoil\ sens.} - Fan\ Sens.Heat}{Power\ DX\ Coil + Power\ Supply\ Fan} \quad (2)$$

$$T_s = T_{in} + \frac{T_{out} - T_{in}}{1 - e^{-1/(r_{server} * m_{server} * c_{pair})}} \quad (3)$$

$$\text{exergy} = n_{server} * (m_{server} * c_{pair} * \alpha) + \beta \quad (4)$$

Where

T_{in} is the server inlet temperature, in Kelvin

T_{out} is the server exit temperature, in Kelvin

T_{ref} is the reference temperature, 273.15 K

T_s is the server surface temperature, in Kelvin

n_{server} is the number of servers

m_{server} is the mass flow rate through each server

$c_{\text{p,air}}$ is the specific heat capacity at constant pressure of the cooling air

$$\alpha = \left(T_{\text{out}} - T_{\text{in}} - T_{\text{ref}} * \ln \frac{T_{\text{out}}}{T_{\text{in}}} \right)$$
$$\beta = \left(1 - \frac{T_{\text{ref}}}{T_s} \right) * q_{\text{server}}$$

Here T_{ref} should in fact be the instantaneous value of the ambient air temperature, since that is what limits heat flow, rather than the absolute zero temperature, which is what is used for the purpose of exergy calculations in this study. The server temperature and exergy calculations are referenced from [29], which describes a Matlab-based tool for thermodynamic analysis of data centers.

The server temperature, T_s , in (3), is calculated based on the inlet air characteristics and inherent inertia or resistance of the server to a change in temperature following any heating or cooling, called “ r_{server} ”. This is an empirically determined value and will vary from server to server depending on physical characteristics such as mass and volume. A value of 0.065 J/K is used for the purpose of this study.

Exergy destruction within the overall airspace is calculated using (4), where α and β are simply used to make the equation compact and fit in the given space; otherwise they play no role in the equation and are mere placeholders. Equation (4) here is a standard equation for calculating exergy destruction in any particular case, modified for a data center airspace to account for the total heat dissipation from all servers by accounting for the number of servers’ present, “ n_{server} ”. Like the standard exergy destruction equation, (4) utilizes the difference in air temperatures between the server inlet and exit as well as a reference temperature against which to compare or limit the amount of possible heat flow.

3.6.3.1 Results for DX Cooling

Output parameters from EnergyPlus are averaged and then plotted for each month across the four locations. Figure 3.7 – 3.13 compare the outdoor dry-bulb temperature, PUE values, CRAC & HVAC power consumption, DX coil power consumption and its SCOP and exergy destruction

across the four locations. As shown in the figures below, the general trend follows the variation in outdoor air temperature and hence a sinusoidal output is produced, with values peaking in the hot summer months of June & July and dropping in the cold winter months of December & January. As such, the cooling system (DX cooling) is powered on for a greater duration of time in the summer months, thus leading to greater power consumption of the DX cooling coil itself and hence the CRAC unit and the entire HVAC unit. As a result, mechanical PUE values tend to be higher in the summer months as opposed to the winter months. Moreover, since the DX system used in this study has an air-cooled condenser, its efficiency is directly affected by the outdoor dry-bulb temperature; a lower outdoor temperature means greater potential of heat transfer from the condenser coils and thus better performance of the overall DX system. Hence, its sensible coefficient of performance, SCOP, shows the opposite trend to that of the other variables; it goes down in the summer months when the ambient temperature is higher and vice versa for the cooler winter months, resulting in a upside down bell-curve, as shown in Figure 3.12.

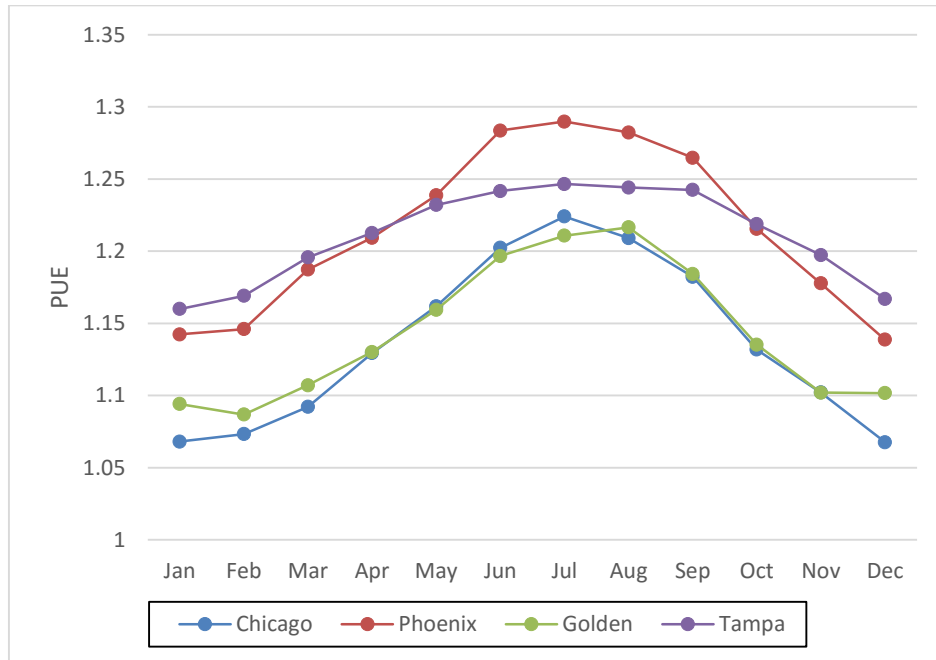


Figure 3.7: Variation of PUE with location for DX cooling

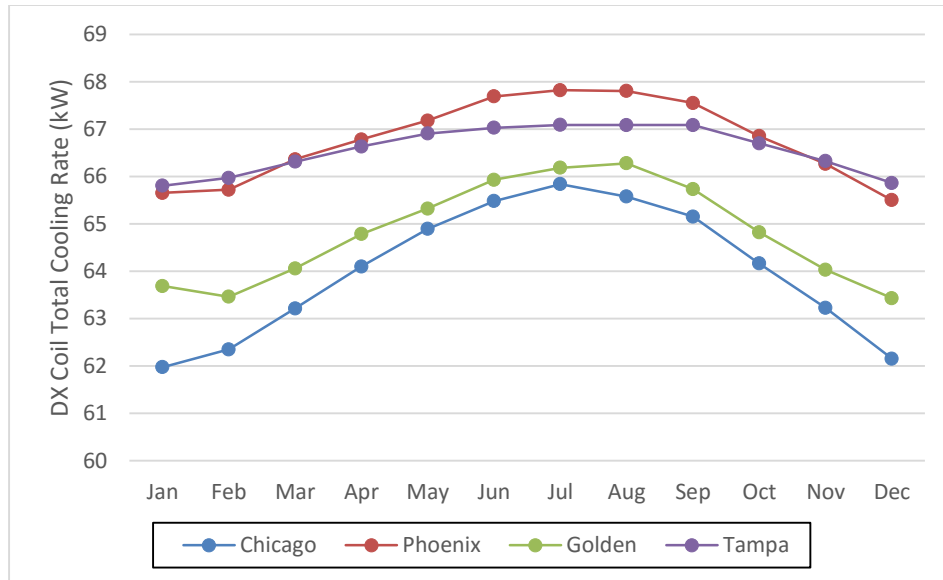


Figure 3.8: Variation of cooling coil total cooling rate for DX cooling

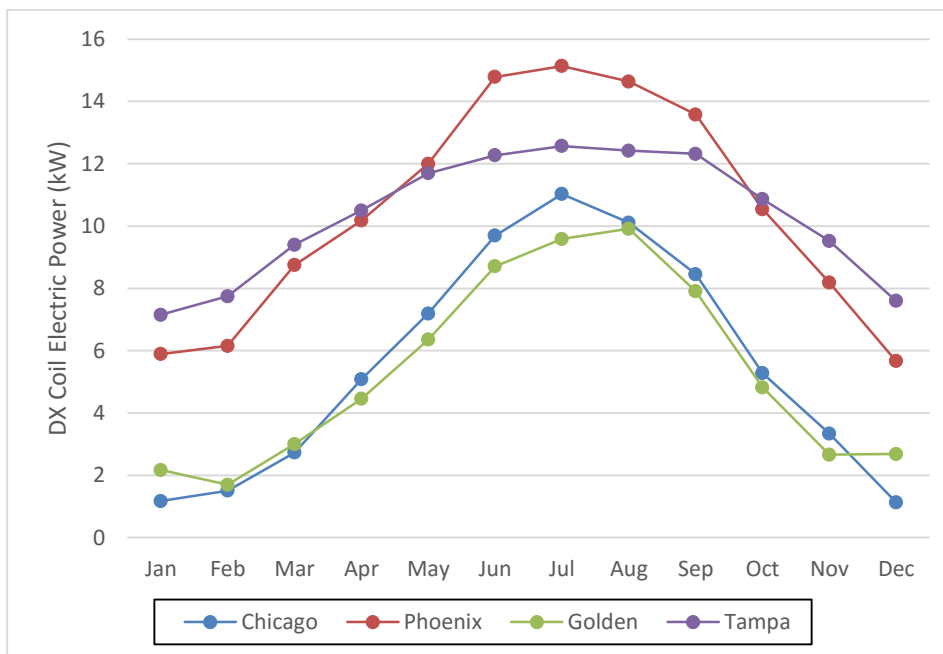


Figure 3.9: Variation of cooling coil power consumption with location for DX cooling

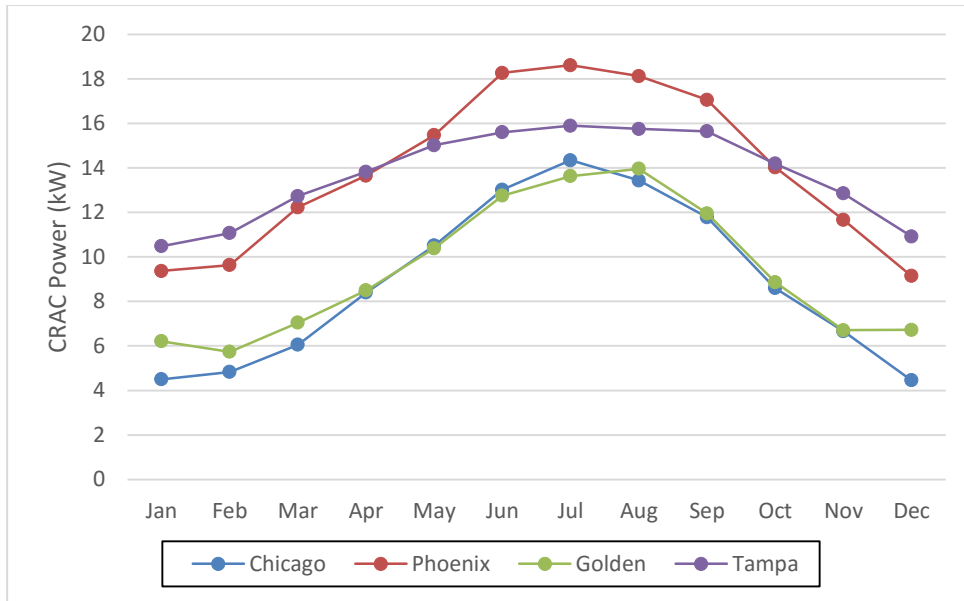


Figure 3.10: CRAC total power consumption for DX cooling

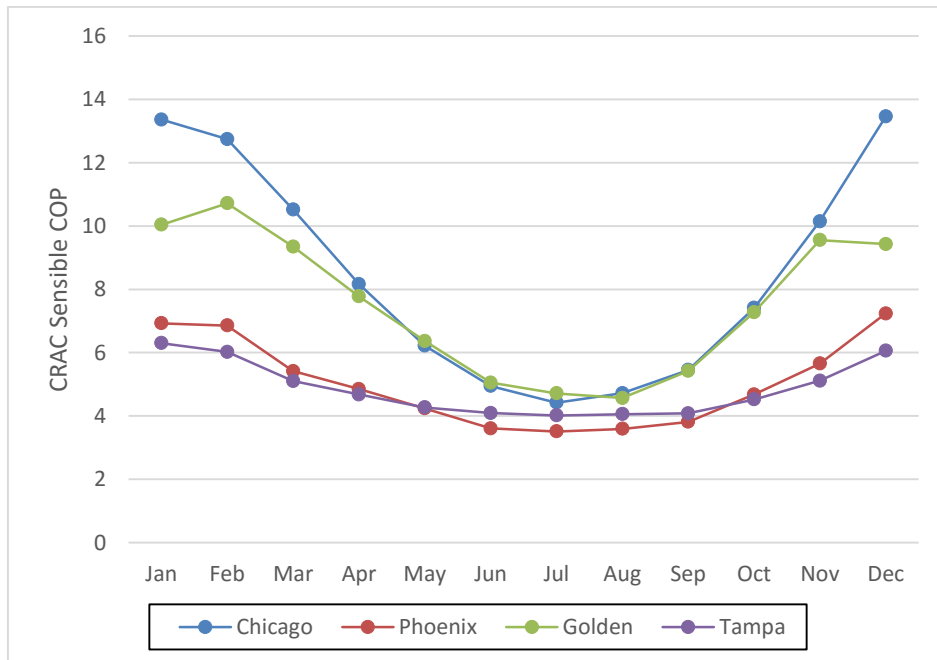


Figure 3.11: CRAC SCOP variation with location for DX cooling

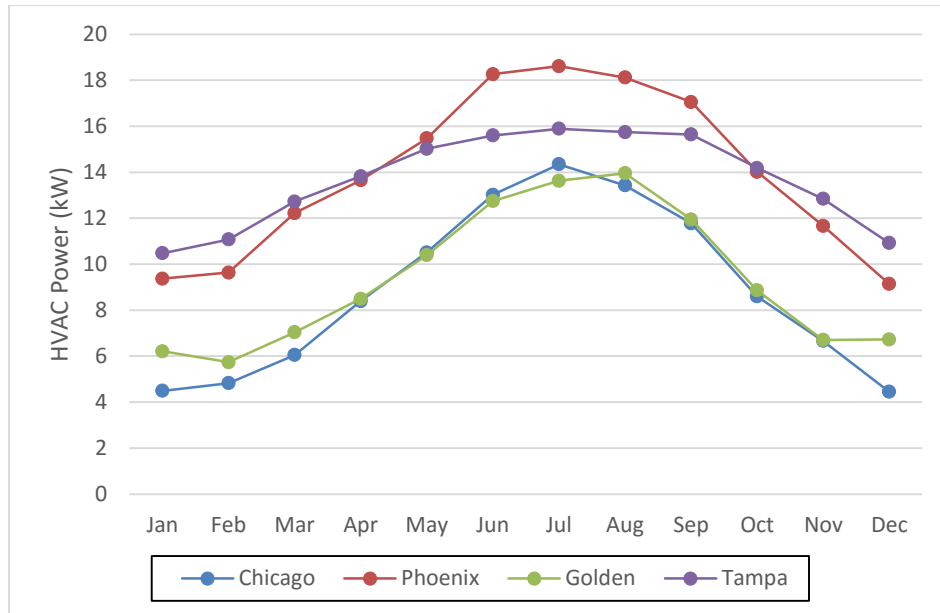


Figure 3.12: Variation of HVAC total power consumption for DX cooling

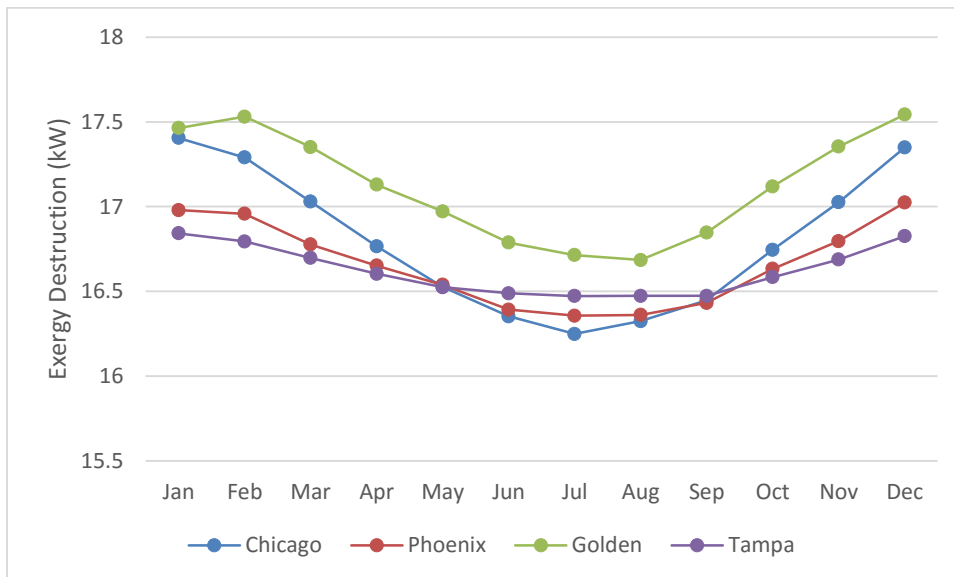


Figure 3.13: Variation of exergy destruction with location for DX cooling

As per the exergy destruction equation (4), two things effect exergy destruction within a data center airspace; one is the ambient or surrounding temperature in which your system is placed and second is the difference in air temperature between the server inlet and exit, ΔT .

The first temperature is important in that it provides a lower limit to which your temperature can drop, or in other words, an upper limit on your system efficiency. The temperature difference is important in that it determines the extent to which potential (exergy) is being utilized or wasted, depending on the situation at hand. In the case of a data center, the higher the exhaust temperature of a server, the more potential is being wasted since that hot air with greater energy is not being used to do any useful work, rather being cooled down again to a lower temperature.

Keeping these factors in mind, the trend shown in Figure 3.14 depicts that locations with higher ambient temperatures will have lower exergy destruction, since the reference temperature is higher. However, since in this case the reference temperature is held constant, the parameters that effect exergy destruction are the server inlet and exit temperature. A higher ΔT across the server would result in a higher value of the exergy destruction, keeping all other factors constant. Thus to explain the higher value of exergy destruction for the cooler locations of Chicago, IL and Golden, CO, it makes sense to compare the difference in server inlet-outlet temperatures across these locations. This trend is shown in Figure 3.15 below:

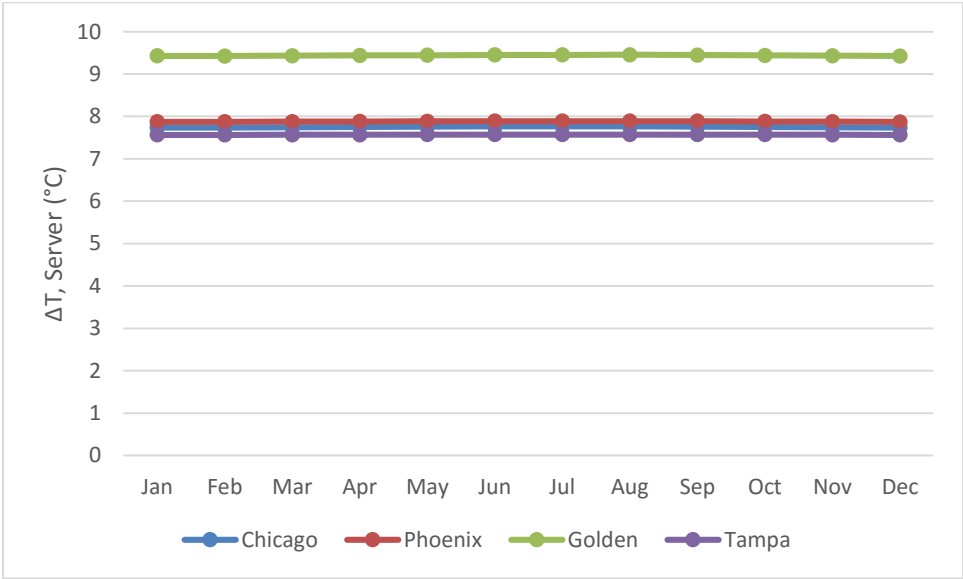


Figure 3.14: Server temperature difference across the four locations for DX cooling

As expected, the ΔT across the servers for the site location of Golden, CO is the highest, which increases the value of α in (4). This is because Golden, CO has cold to mild climate throughout

the year, and is in general colder than the other three locations. Thus, this allows the DX system to operate for a lower amount of time, which saves energy but makes the servers run a little hotter, by virtue of supplying cooling air at a slightly elevated temperature. Since the cooling coil is autosized and the return air setpoint (cooling setpoint) is fixed at 29.3 °C for all locations; this allows EnergyPlus to operate at slightly elevated inlet air temperatures which then raises the exit air temperature slightly further than the rest of the cases, resulting in a higher ΔT across the servers'. Moreover, this raises the temperature of the servers in this location as well, as determined by (3), and since T_{ref} is fixed, causes the value of β to go up, which further elevates the exergy destruction. A plot of the server temperature as calculated by EnergyPlus using equation (3) is shown in Figure 3.16 below.

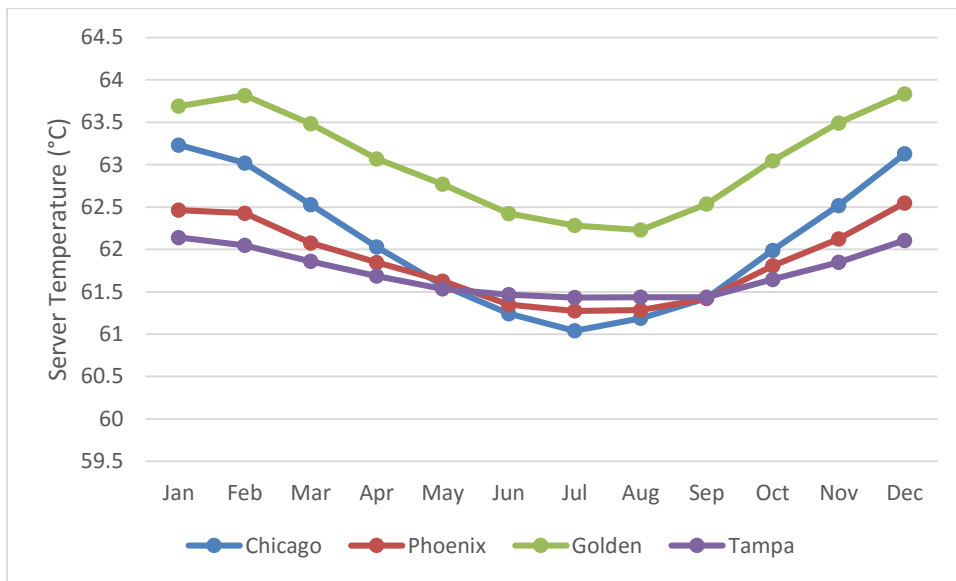


Figure 3.15: Server temperature across the four locations for DX cooling

3.7 Timestep Analysis

A timestep analysis was performed to determine the influence of changing timestep on parameter values and also to gauge whether convergence is achieved or not. The base timestep of one hour (1 hour) was compared against four other cases by decreasing the timestep to 30-minutes, 20-minutes, 10-minutes and 1-minute. 10-minutes is the default timestep for EnergyPlus, while 1-minute is the least timestep that EnergyPlus can simulate. The results for PUE values, total HVAC

power, cooling coil power consumption and exergy destruction are shown in Fig. 3.15 – 3.18 below.

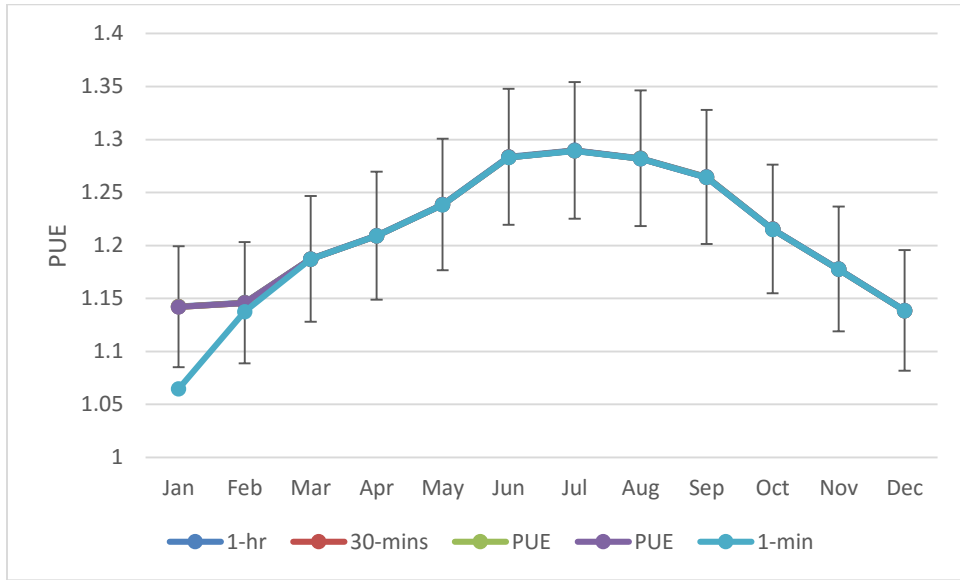


Figure 3.16: Comparison of PUE values against different timesteps for DX cooling

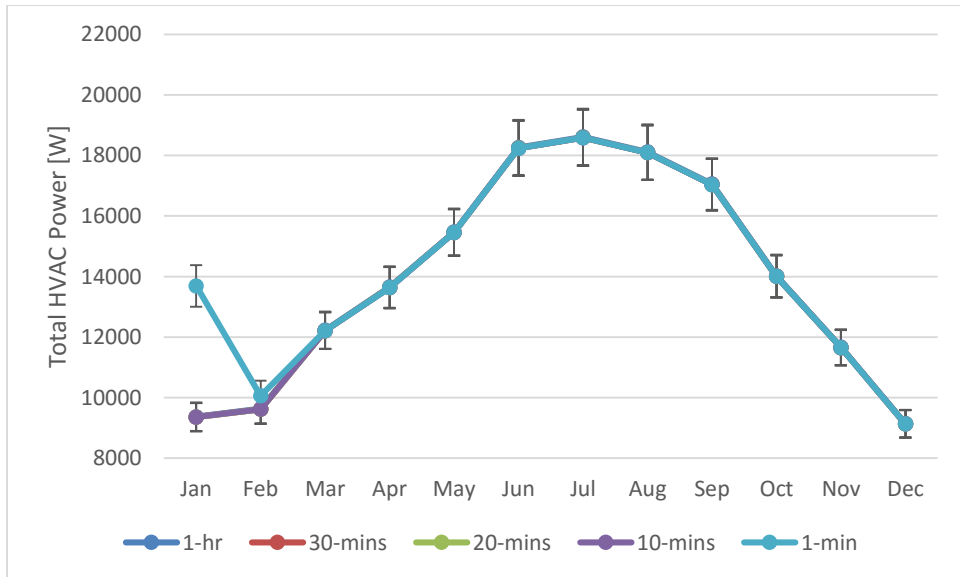


Figure 3.17: Comparison of total HVAC power against timestep for DX cooling

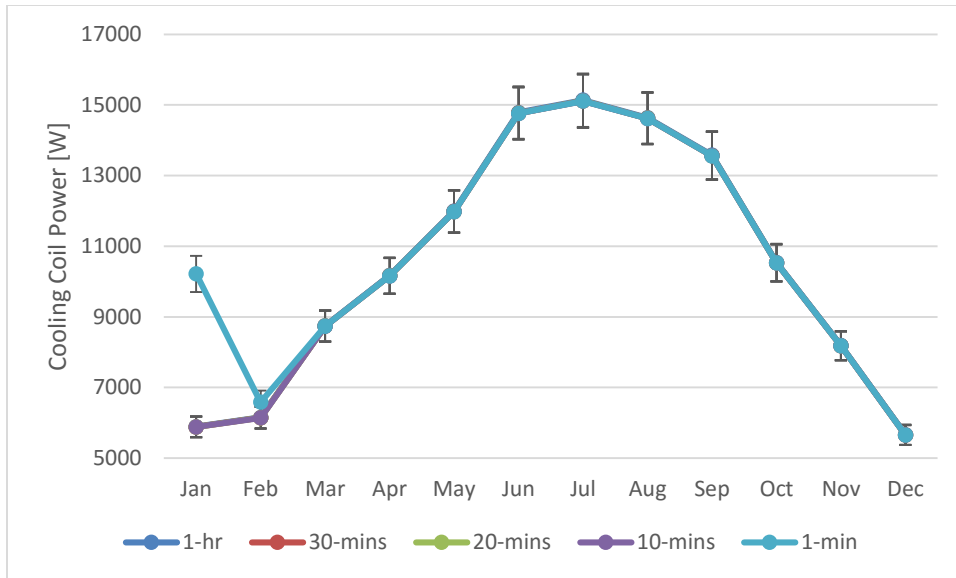


Figure 3.18: Comparison of cooling coil power consumption against timestep for DX cooling

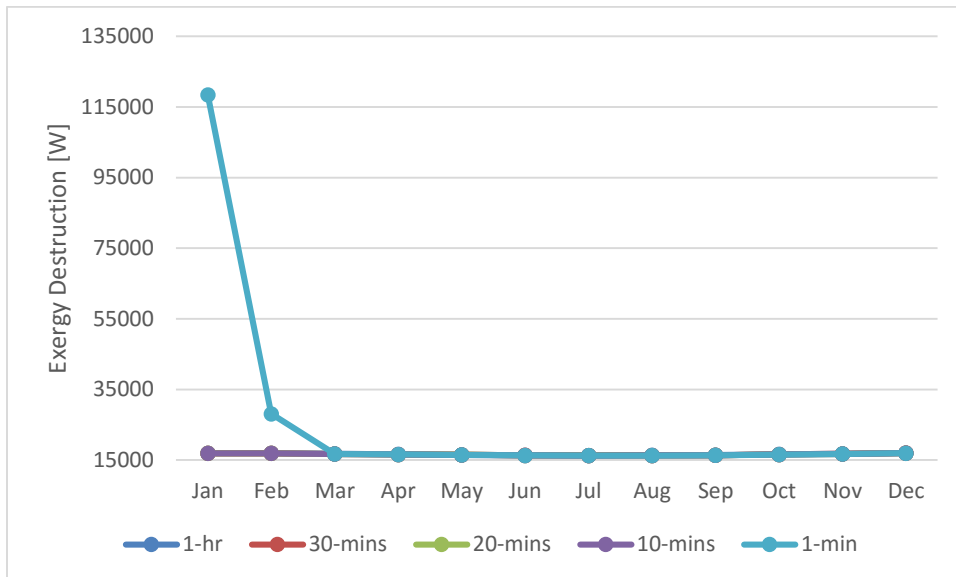


Figure 3.19: Comparison of cooling coil power consumption against timestep for DX cooling

Furthermore, an error analysis utilizing percentage error difference of the parameter values at each timestep versus the base timestep (1 hour) was also carried out. The results showed that there is

no significant change in parameter values by decreasing timestep from 1 hour down to 1 minute for the case of DX cooling in Phoenix, Arizona. However, the average values for January and February for the 1-minute case did not converge within the given conditions and surface temperature exceeded the set limit of 200 °C. Hence the maximum surface temperature limit had to be increased to 250 °C for convergence to occur. However, as can be seen from Fig. 3.15 – 3.18, the values reported for 1 minute timestep for the months of January and February were still relatively high (low in the case of PUE) as compared to other values. The rest of the values converged within the specified tolerance.

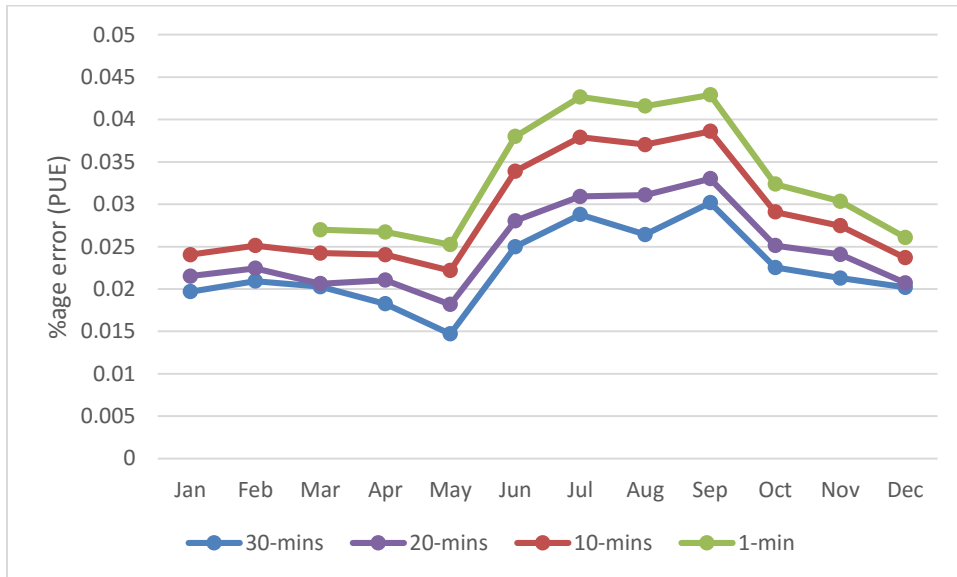


Figure 3.20: Percentage error for DX cooling PUE values by decreasing timestep, Phoenix, AZ

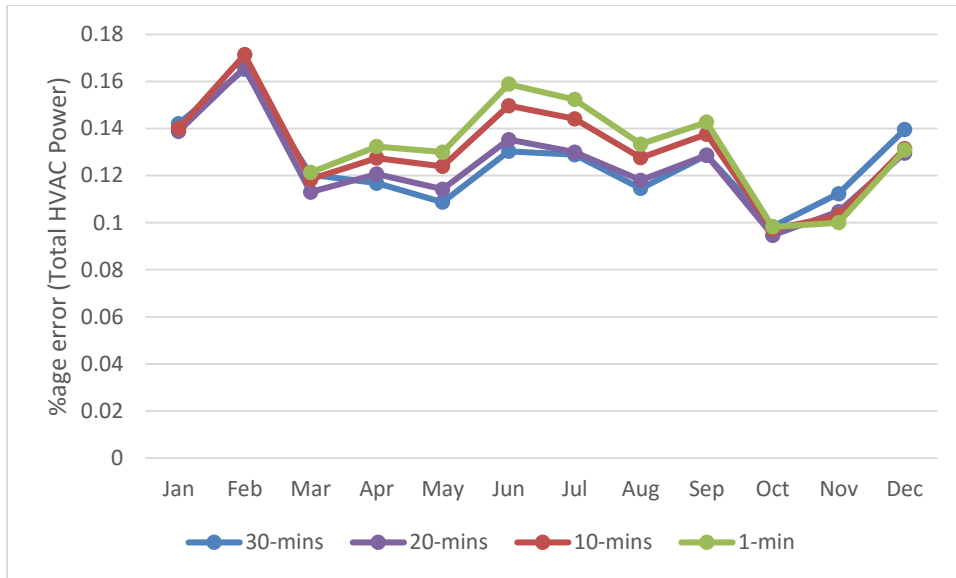


Figure 3.21: Percentage error for DX cooling HVAC power consumption values by decreasing timestep, Phoenix, AZ

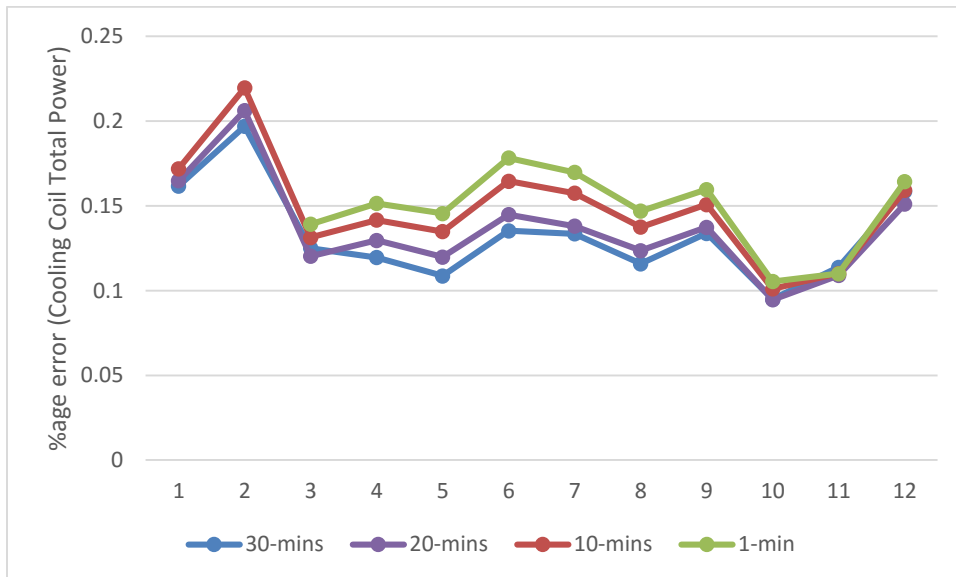


Figure 3.22: Percentage error for DX cooling coil power consumption values by decreasing timestep, Phoenix, AZ

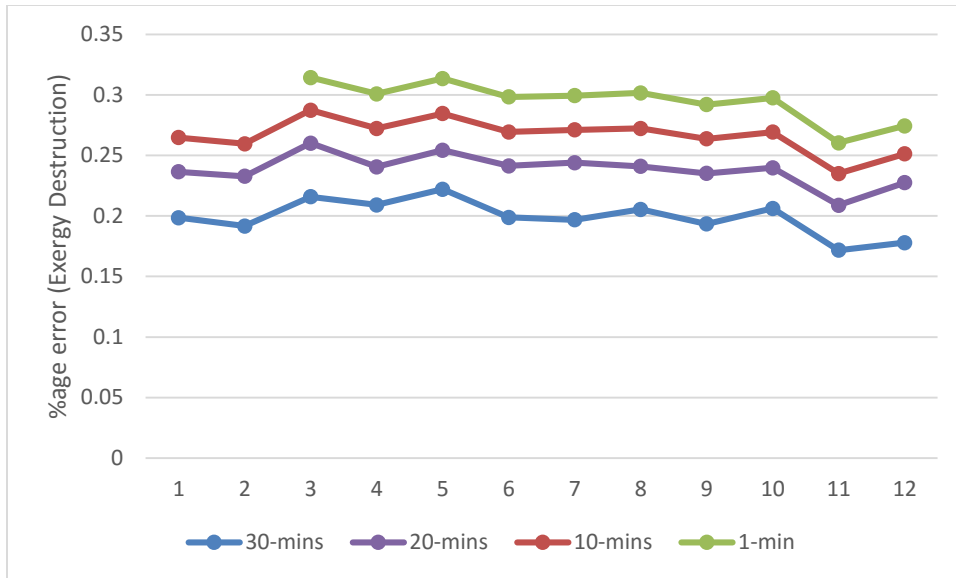


Figure 3.23: Percentage error for DX cooling exergy destruction, Phoenix, AZ

In order to ensure that the results are not location dependent i.e. the outside conditions do not play a significant role, the same error analysis was run for Chicago where the ambient conditions are much cooler than in Phoenix for the same time of the year. The results are shown in Figure 3.23 – 3.26 below.

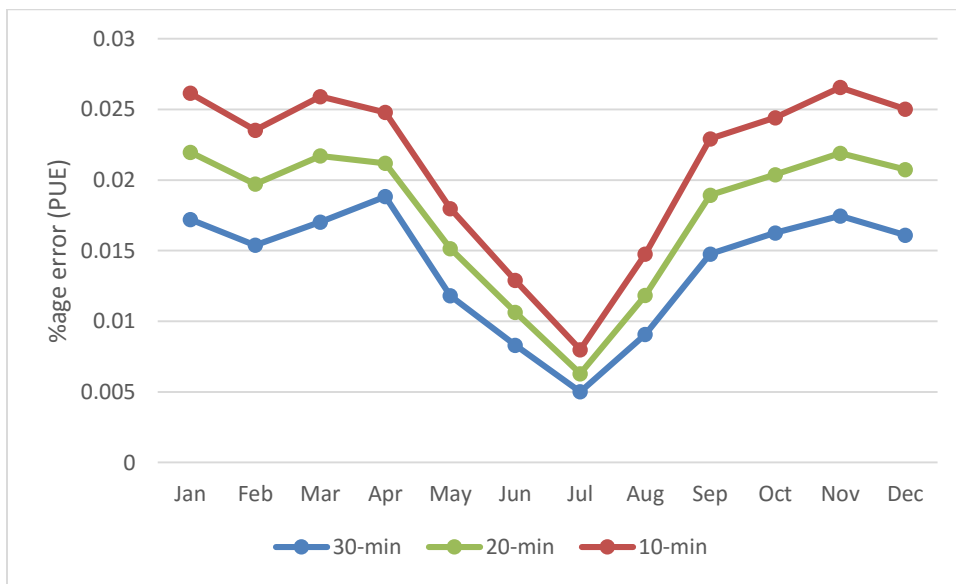


Figure 3.24: Percentage error for DX cooling PUE values by decreasing timestep, Chicago, IL



Figure 3.25: Percentage error for DX cooling HVAC power consumption values by decreasing timestep, Chicago, IL

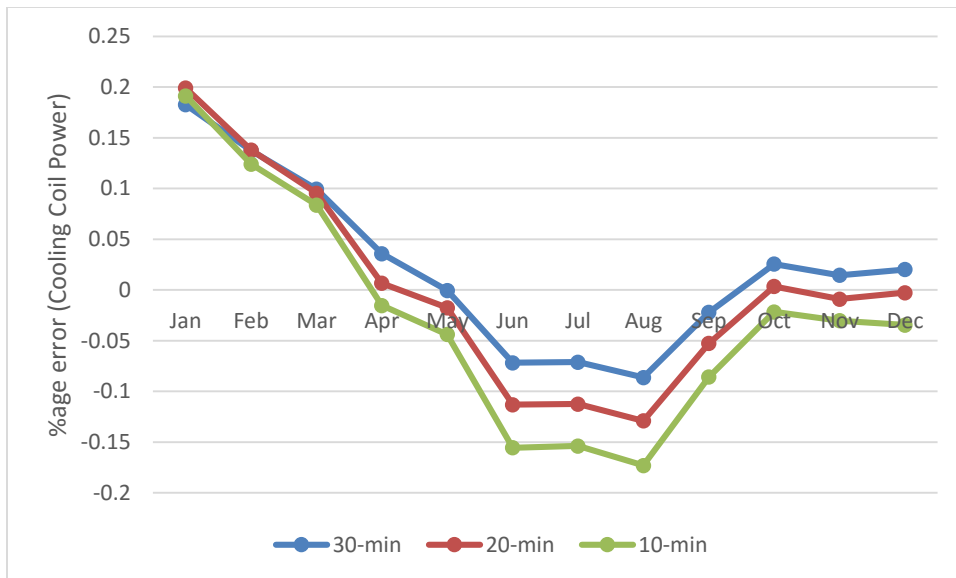


Figure 3.26: Percentage error for DX cooling coil power consumption values by decreasing timestep, Chicago, IL

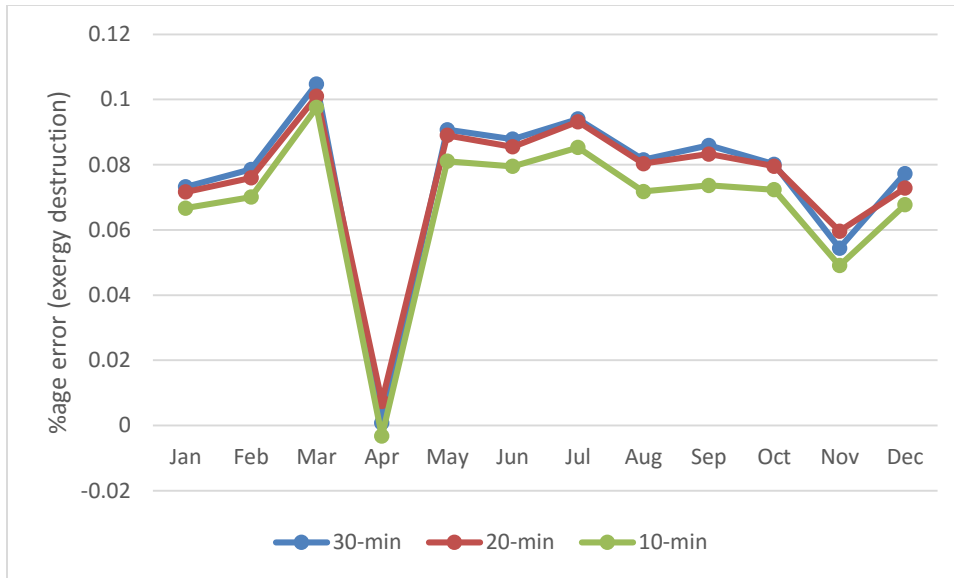


Figure 3.27: Percentage error for DX cooling exergy destruction, Chicago, IL

However, in this case, the results for 1 minute timestep simulation did not converge, even after increasing the surface temperature to 250 °C, and are hence not presented. The remaining trends are the same as for Phoenix, AZ, with a decrease in timestep leading to greater accuracy and thus a larger error as compared to the base case of 1 hour. The percentage error, however, is on the order of 0.1% for the 10-minute timestep, which is the most accurate out of all those compared. Thus, this error is negligible enough to not warrant any changes in the simulations itself.

3.8 Passive Cooling Techniques

As seen in the above analysis, the base cooling option (DX Cooling) is not the most viable option for every location, particularly in hot and dry climates like those of the south west United States (e.g. Phoenix, AZ) or hot and humid climates like those in the south east (e.g. Tampa, FL). Hence, depending on the climate in which to deploy your modular data center, additional cooling techniques on top of the base case can be added to enhance performance factors such as PUE & SCOP and reduce the HVAC and hence overall facility electricity consumption.

Passive cooling techniques such as evaporative cooling (direct and indirect) as well as free air cooling can be effectively employed in modular data centers to enhance cooling efficiency and reduce power consumption.

3.8.1 Direct Evaporative Cooling

Direct evaporative cooling is a technique to remove heat simply by evaporating water within an airstream. It differs from traditional mechanical cooling systems (such as DX CRAC units or chilled water CRAH units) in that they require practically no electricity to cool the air, making them an economical option to use in regions where the summers are dry. Moreover, if the ambient conditions permit, the incoming outdoor air can bypass the evaporative cooler and the system can operate in economizer mode as well, thus even saving power required to run the pump of the evaporative cooler. Figure 3.14 below shows the schematic a hybrid DX-Evaporative cooler system modelled in EnergyPlus:

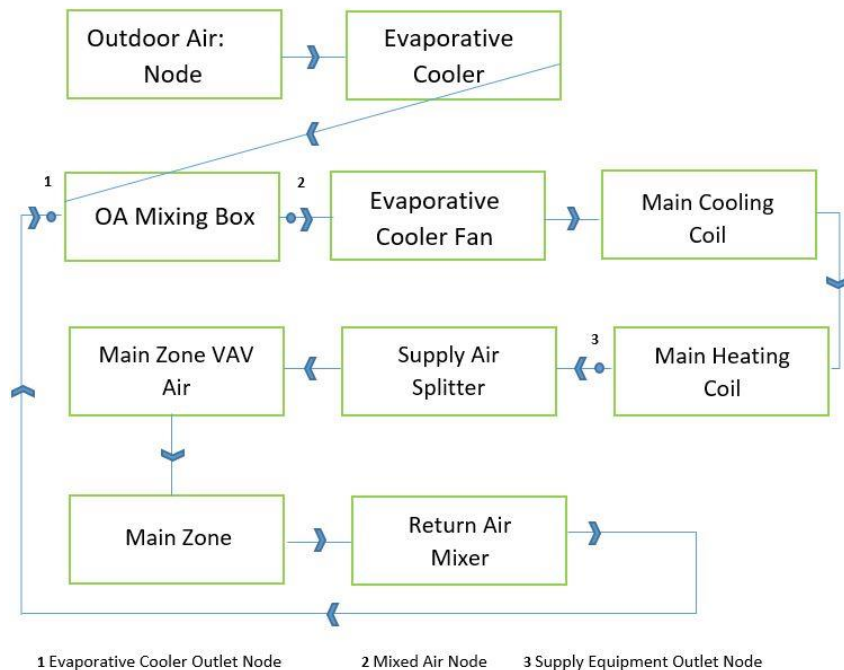


Figure 3.28:DX-Direct Evaporative Cooling HVAC schematic as displayed in EnergyPlus

Within EnergyPlus, the Evaporative Cooler Direct Research Special object is used to model this system. A separate availability schedule is specified to turn the evaporative cooler on and off, depending on the ambient air temperature. A sensor placed on the outdoor air node senses the ambient air and is controlled by the object Outdoor Air Controller. Based on the ambient temperature, the evaporative cooler operates as per the following logic:

- If $T_o < 12^\circ\text{C}$, then cut-off outside air
- If $12^\circ\text{C} < T_o \leq 28^\circ\text{C}$, run in economizer mode and mix with return air to meet zone cooling setpoint
- If $T_o > 28^\circ\text{C}$, run evaporative cooler

The evaporative cooler runs to meet the setpoint at its outlet, Node 1, which is equal to that of the supply equipment outlet node, Node 3. If this temperature is less, than it is mixed with the return air to meet the same setpoint at Node 2, the exit of the mixing box node. In case the temperature at Node 1 is greater than the return air temperature, the return air is exhausted using a relief valve located in the mixing box and the DX coil runs to meet the required setpoint. In this manner, the DX coil runs for a smaller fraction of time, thus saving a tremendous amount of electric power since the power consumption of the cooler pump is negligible compared to that of the DX coil's compressor. The specifications for the DX-evaporative cooling system are shown in Table 5 below:

Table 3.5: DX-evaporative cooling system specifications

Object	Specification
System type	Hybrid direct evaporative cooler & DX type A/C with electric heating
Thermostat type	Dual-zone thermostat
Heating Setpoint	15°C
Cooling Setpoint	29.3°C
Design Supply Air Temp.	14°C
Supply Fan	Single speed on/off fan
Air distribution unit	Single-duct VAV with no reheat
Cooling coil COP	4.6
Evaporative Cooler	
System efficiency	0.7
Rated Pump Power	30 W

3.8.2 Free Air Cooling

An air-side economizer brings outside air into the data center and distributes it to the servers. The hot zone return air is fed into a mixing box where it is mixed in proportion with the cooler outside air to achieve the required zone cooling setpoint.

The outdoor air controller uses the following logic to mix the outdoor and return air streams:

- If $T_o < 12^\circ\text{C}$ or $> 28^\circ\text{C}$, then cut-off outside air
- Else, mix with return air to meet supply outlet node setpoint

The hybrid DX-Free Air cooling system has the same specifications as that of the individual DX cooling system. The DX coil is set to autosize for all three cases.

The supply equipment outlet node is located after the main heating coil and is set to vary between 10 & 50°C , in order to meet the zone setpoint of 27°C . The large variation in supply equipment setpoint allows EnergyPlus to appropriately size the cooling coil. In case of oversizing, the cooling coil outlet temperature can fall below 2°C and frost may occur, damaging the coil. In case of under-sizing, the zone may overheat.

All objects that require outside air such as evaporative coolers have built-in filters to filter the outside air and limit particle contamination within the conditioned space. Figure 3.15 shows a DX cooling system with an outside air economizer.

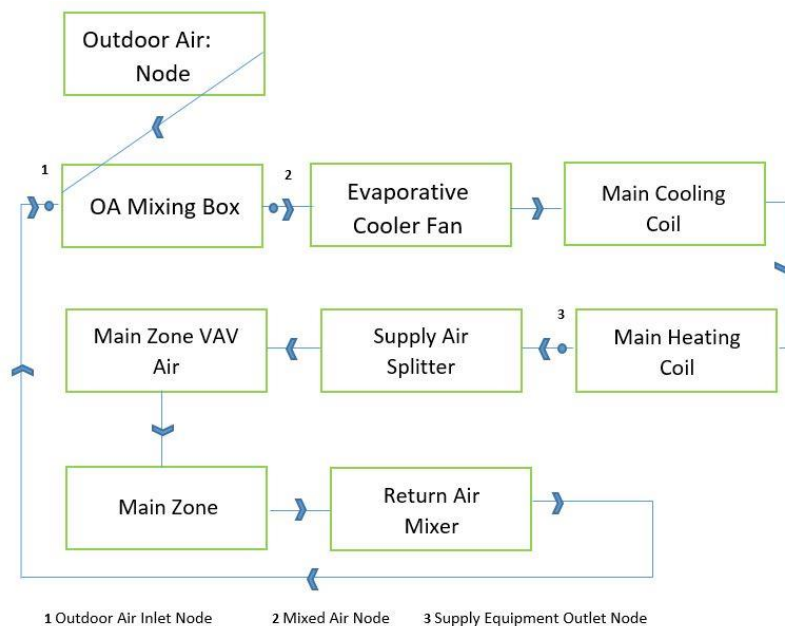


Figure 3.29: DX-Free Air Cooling HVAC schematic as displayed in EnergyPlus

The results from the DX cooling analysis suggested that Phoenix, AR, has the highest mechanical PUE and hence the most HVAC power consumption. Thus, it is chosen as the location for implementing these two cooling techniques. A comparison of the mechanical PUE results, CRAC total power and HVAC system power are shown in Figure 3.16 – 3.18 below:

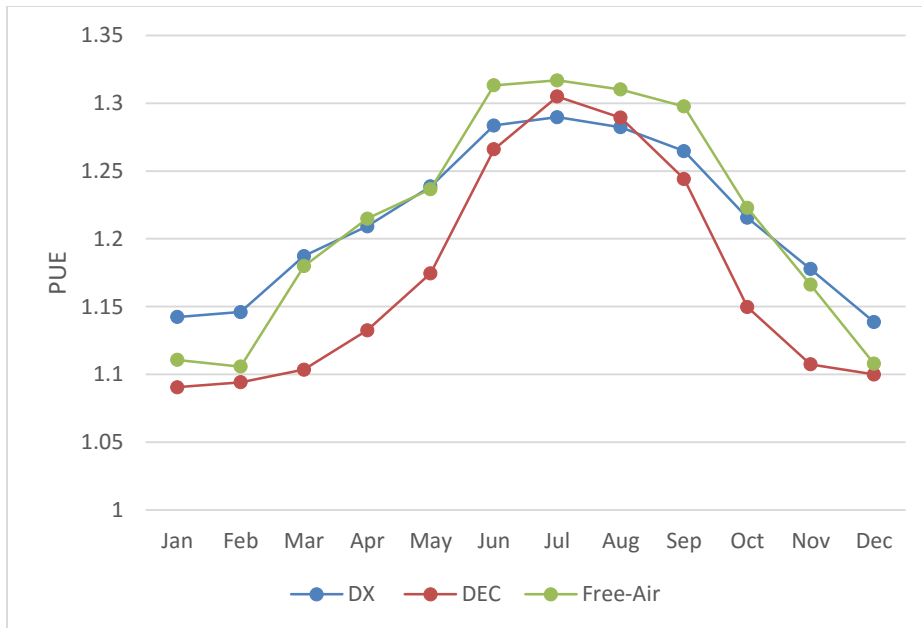


Figure 3.30: Variation of PUE with cooling system, Phoenix, AZ

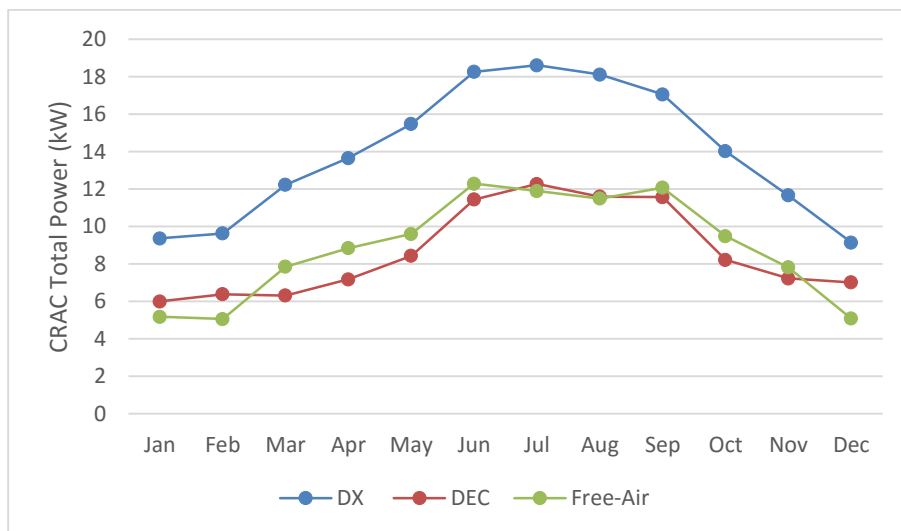


Figure 3.31: Variation of CRAC total power consumption with cooling system, Phoenix, AZ

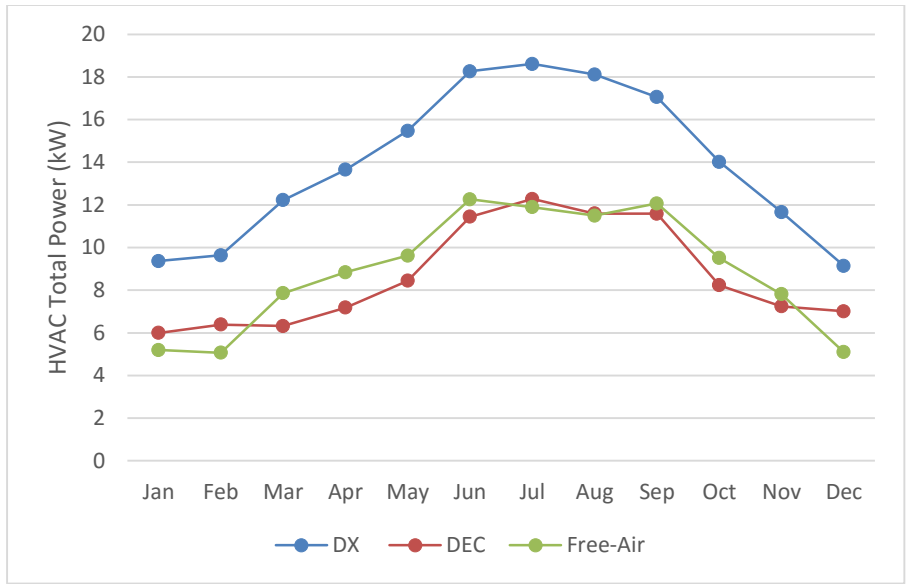


Figure 3.32: Variation of HVAC total power consumption with cooling system, Phoenix, AZ

As can be seen from the above figure, augmenting the base cooling system with either of these cooling techniques produces great savings in terms of HVAC power and hence elevates the mechanical cooling efficiency (mechanical PUE). Figure 3.19 – 3.22 present, DX coil total cooling rate and its power consumption, the evaporator cooler pump power, its volume of water used and lastly the exergy destruction for the facility for the three cooling systems:

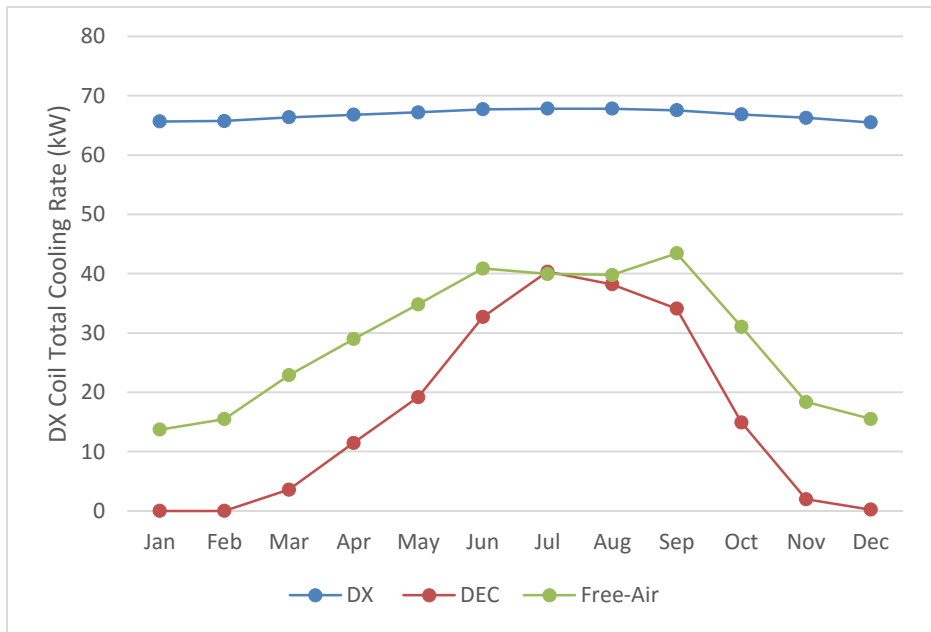


Figure 3.33: Variation of Cooling Coil total cooling rate, Phoenix, AZ

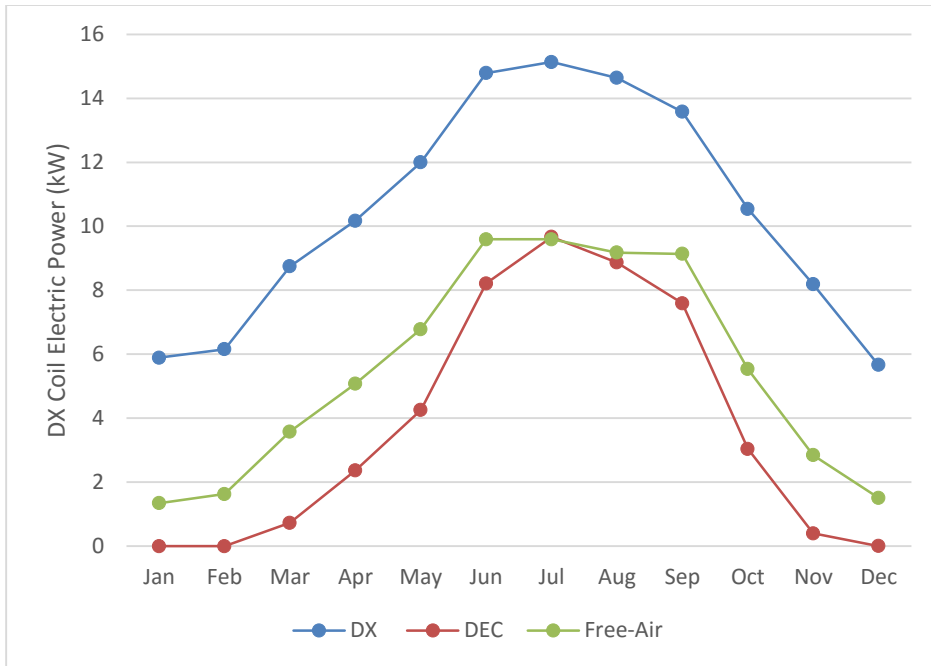


Figure 3.34: Variation of Cooling coil total power consumption, Phoenix, AZ

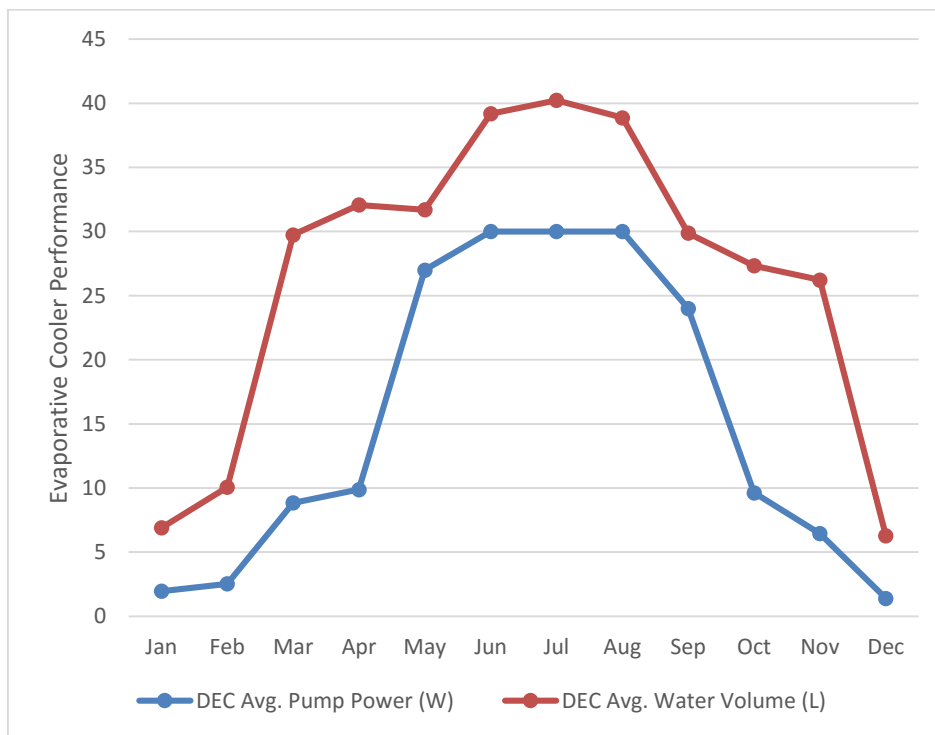


Figure 3.35: Evaporative Cooler pump power & water usage, Phoenix, AZ

The trend in evaporative cooler power also depicts the time for which it runs during the year. During the winter months of December through February, it is mostly powered off. However, in the summer months from May through August, it run throughout on full power because of the hot and dry outside air and hence maximum savings in terms of cooling power are reported during this period.

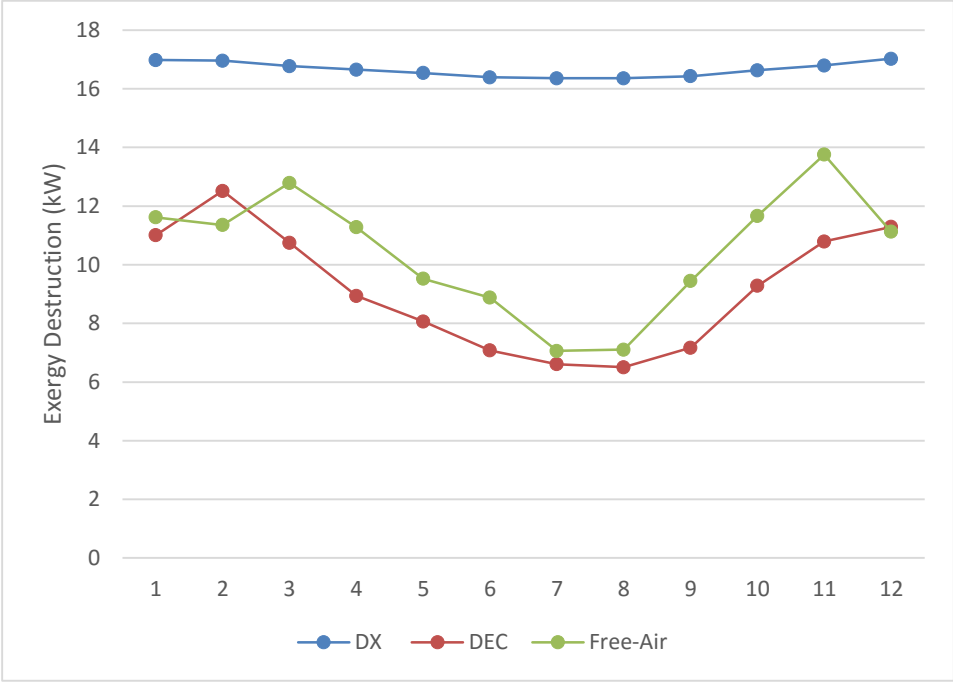


Figure 3.36: Variation of exergy destruction with cooling system, Phoenix, AZ

Table 6 summarizes the annual average performance of the three cooling techniques for Phoenix.

Table 3.6: DX, Evaporative and Free Air Cooling performance summary, Phoenix, AZ

Parameter	DX	DX + DEC	DX + Free Air
PUE	1.21	1.17	1.20
CRAC Power (kW)	13.96	8.65	8.91
HVAC Power (kW)	13.96	8.65	8.91

Table 3.6 continued

DX Coil Cooling Rate (kW)	66.77	16.47	28.79
DX Coil Power (kW)	10.48	3.78	5.50

3.9 Results & Discussion

The IT equipment inlet temperature profile and inlet relative humidity are compared against ASHRAE class A3 limits. The results are presented in Figure 3.23 & 3.24 below.

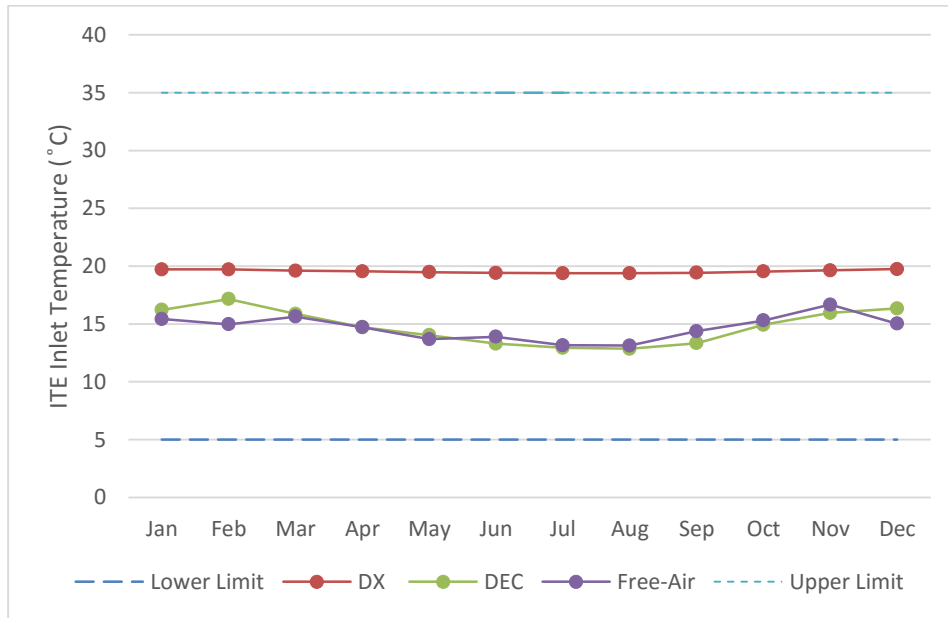


Figure 3.37: IT equipment inlet temperature for the three cooling systems

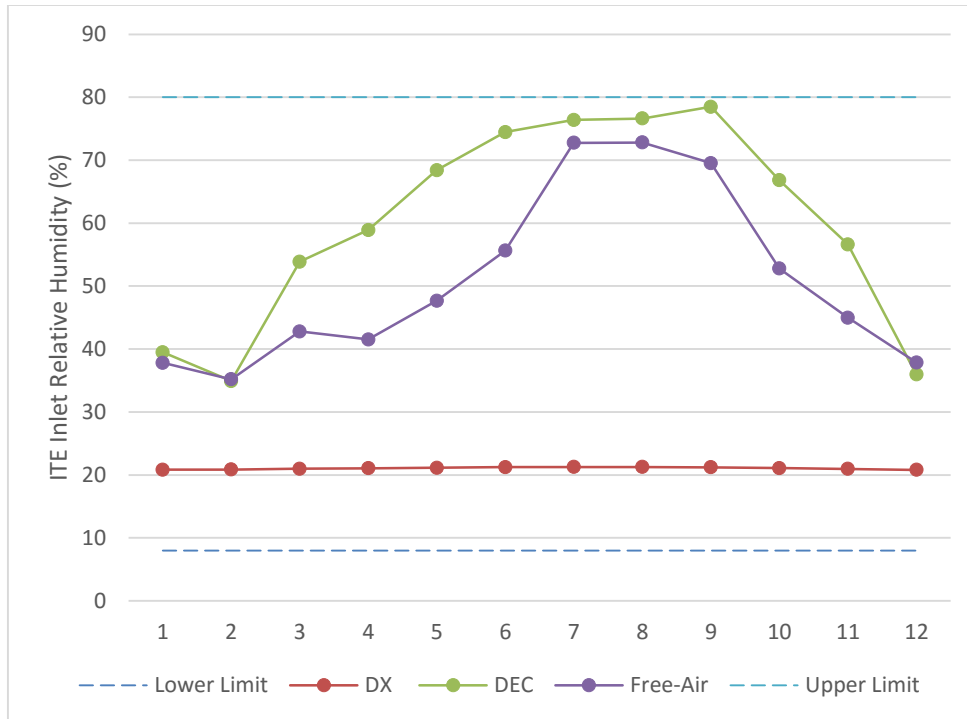


Figure 3.38: IT equipment inlet relative humidity for the three cooling systems

A summary of the mechanical PUE results for DX cooling are presented in Table 7 below.

Table 3.7: Winter, Summer & Annual PUE values for DX Cooling

Location	Winter PUE	Summer PUE	Annual PUE
Chicago, IL	1.08	1.20	1.14
Phoenix, AR	1.15	1.27	1.22
Golden, CO	1.10	1.20	1.14
Tampa, FL	1.17	1.24	1.21

The mechanical PUE values for the hybrid systems are summarised in Table 8 below:

Table 3.8: Mechanical PUE values for Phoenix, AZ using all three cooling techniques

Location	Winter PUE	Summer PUE	Annual PUE
DX	1.15	1.27	1.22
DX + DEC	1.09	1.26	1.17
DX + Free Air	1.13	1.29	1.21

In essence, for DX cooling, lowest PUE values are seen for Chicago, followed by Denver. The CRAC and HVAC power consumption are by far the lowest for Chicago. Similarly, its total cooling rate is the lowest of all, showing that it has to perform the least amount of work. Moreover, its coil power consumption (input power) and hence its SCOP are by far the lowest and highest respectively. Hence, DX cooling is very well suited for colder locations like Chicago where the cold outside air cools the condenser (air-to-air loop) better by raising the system’s efficiency.

As can be seen from Figure 3.16 – 3.22, the inclusion of additional cooling systems on top of the base case greatly reduce the load on the DX cooling system which helps to drastically lower its power consumption and total cooling rate. A comparison of the total facility electricity consumption and HVAC system power consumption is given in Figure 3.23. The results clearly demonstrate the savings in power consumption by adapting hybrid cooling approaches consisting of passive cooling techniques on top of the base cooling system. Considering the power consumption of DX cooling as the base case for comparison purpose, the power consumption of the other two cooling techniques as a percentage of the base case is shown in Figure 3.24.

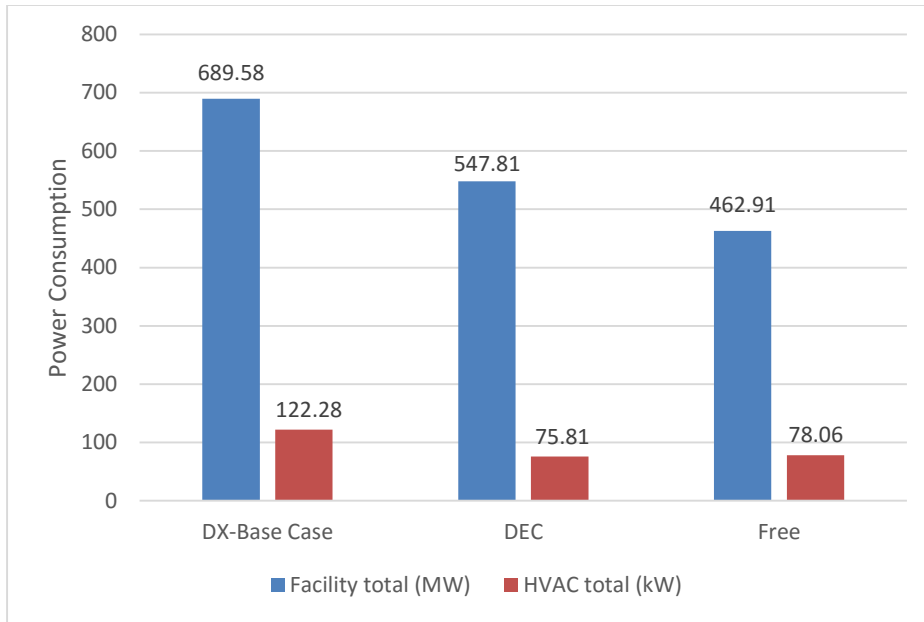


Figure 3.39: Comparison of annual total facility and HVAC system power consumption for Phoenix, AZ

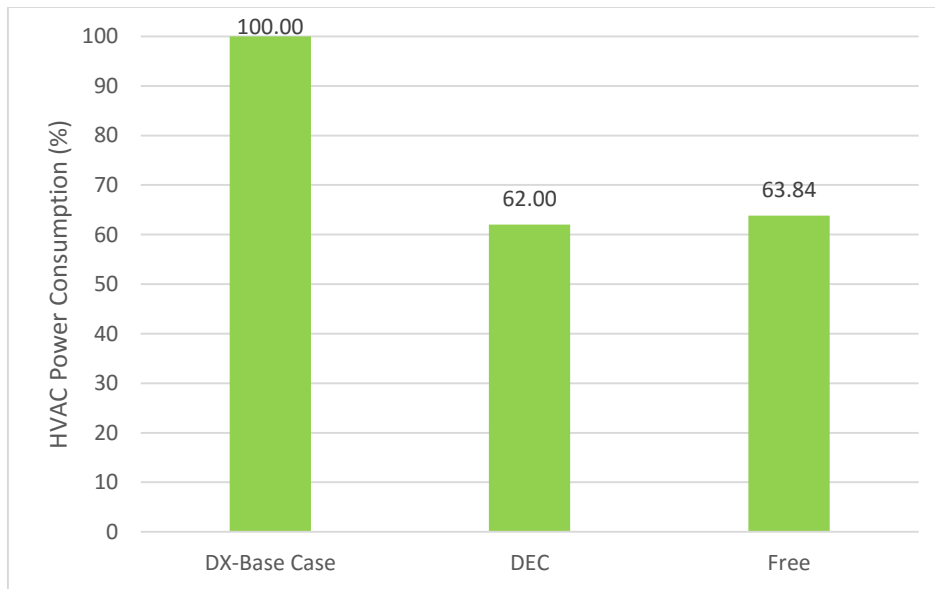


Figure 3.40: Comparison of HVAC power consumption as a percentage of the base case (DX cooling), Phoenix, AZ

The greatest savings are seen in the case of adapting an evaporative cooling approach, followed by that of free-air cooling. This is because the evaporator cooler can function in economizer mode as well as operate itself to meet the cooling load, thus saving excess power that is consumed by running the DX coil. This helps to enhance the PUE values. Moreover, the results show that for a hot and arid place like Phoenix, AR, evaporative cooling can work very well in the hot and dry summer months to adequately cool the facility and reduce power consumption and electricity cost. In case of a hybrid DX-evaporative cooling system, the colder night air can be used to run the system in economizer mode and save further energy.

Free air cooling is second best to evaporative cooling because of the relatively limited utilization of ambient air. Moreover, the results supplement the findings of Depoorter et al. [6] that PUE's for free-air cooling rise in the summer months due to lesser availability of outside air, as opposed to other techniques like direct evaporative cooling. However, in periods of time where outside air cannot be brought in to cool the facility, the only option is to run the power hungry DX coil. However, the extent to which each of these cooling techniques can be utilized depends on the outdoor dry and wet-bulb temperatures. In places where they are not suitable to run for extended periods of time, the cost of installing or modifying a facility may not overcome the energy savings that are brought about by utilizing these passive cooling techniques.

3.10 Summary & Conclusions

Energy usage modelling of various modular data center cooling systems has been undertaken using the open-source software EnergyPlus. Four locations across the United States have been initially modelled using the base system, DX cooling. The results suggest that in hotter climates near the southern belt, DX cooling alone is not adequate enough to meet the cooling demands. Hence augmenting the base system with additional techniques such as direct evaporative and free air cooling can produce energy savings of 38% and 36% respectively and help to take the load off the DX system. The results show that direct evaporative cooling has the most effect on reducing energy consumption in a hot and dry climate like Phoenix since the evaporative cooler pump power is negligible as compared to the DX system compressor power. Furthermore, free air cooling can be utilized when outdoor temperatures are suitable enough, either as a stand-alone cooling option or by using evaporative cooler in economizer mode.

The modelling work further suggests that the COP of the DX cooling coil significantly affects its power consumption and raising the COP from a typical value of 3 to 4.6 can reduce the peak summer PUE values from 1.65 down to 1.4. Furthermore, this work gives insight into an optimum IT equipment inlet temperature of 73-74°F, exceeding which will reduce the CRAC/HVAC system power but increase the server fan power, thus having a negative effect on overall energy consumption and hence PUE values. Thus, a trade-off exists between IT equipment and HVAC power and a balanced temperature for the facility has to be maintained in order to achieve optimum results.

Lastly, a second-law analysis of the conditioned airspace suggests that the biggest source of exergy generation is the server inlet temperature and the inlet-outlet temperature difference, ΔT . The greater the difference between these two, the more potential will be wasted. Simulation results suggest that by lowering the cooling setpoint (return air temperature), the server inlet temperature and hence the resulting server surface temperature can be reduced. Thus the amount of exergy created can be lowered while still maintaining PUE values since passive cooling techniques augment the base case, they can allow the data center to operate at lower temperatures without raising power consumption and hence utility costs.

CHAPTER 4

TRANSIENT RESPONSE

4.1 Introduction

In a typical data center, the servers contribute significantly to the thermal mass. This thermal mass has the ability to flatten swings in temperature variation inside the conditioned space, by absorbing energy following a sudden increase in workload, and releasing it with a certain delay, resulting in the moderation of the temperature rise during the transient. Hence, transient analysis of modular data centers needs to include the influence of thermal mass. The implementation of server thermal mass in models is important for development and deployment of control schemes.

Previous studies include a finite-difference server model by Pardey et al. [30] in conjunction with IBM. Their work is based on the individual analytical development by Pardey and VanGilder et al (2014) and Erden et al (2014). The goal of the present study is to implement a transient server thermal model, conjunction with an established energy modelling software package EnergyPlus. In order to do this integration, we have employed companion software that provides the appropriate input modification to enable a model of data centers, and post-processing of data center performance metrics. This paper discusses the transient server models and the complimentary software package to EnergyPlus, called DCE+.

4.2 Dynamic Server Model Development

Treating the server as a blackbox with a stream of cooling air flowing through the server (over the electronic components). This can be effectively modelled as a single-stream heat exchanger and hence the ϵ -NTU method used for heat exchangers is readily applied. The model in [31] can be mathematically expressed as follows:

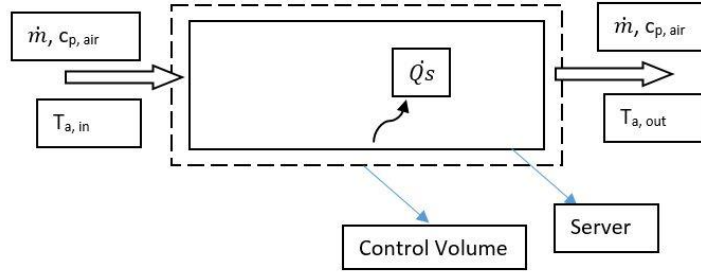


Figure 4.1: Control volume for a server treated as a blackbox

Energy balance for the server:

$$C_s \frac{dT_s}{dt} = \dot{Q}_s - \dot{C}_a(T_{a,out} - T_{a,in}) \quad (1)$$

Which in the steady-state reduces to

$$T_{a,ex} = \frac{\dot{Q}_s}{\dot{m}c_{p,a}} + T_{a,in} \quad (2)$$

Energy balance for the air stream:

Neglecting thermal storage in the air, the heat gained by the air is equal to that lost by the server times the server effectiveness of heat transfer. This leads to the expression:

$$\dot{C}_a(T_{a,out} - T_{a,in}) = \varepsilon \dot{C}_a(T_s - T_{a,in}) \quad (3)$$

Solving Equations (1) and (3) simultaneously gives

$$C_s \frac{dT_s}{dt} = \dot{Q}_s - K(T_s - T_{a,in}) \quad (6)$$

Where

$$K = \varepsilon \dot{C}_a \quad (7)$$

&

$$\tau = \frac{C_s}{K} \quad (8)$$

The capacitance C_s and effectiveness ε may be estimated using correlations from Pardey [1]:

$$C_s = 644M \quad (9)$$

$$\varepsilon = 1 - 13(\rho')^{-1.87} \quad (10)$$

where M is the server mass in kg and ρ' is the mass density of the server in kg/U, where 1U = 1.75”

The time derivative in Eq. (6) is discretized in EnergyPlus using forward differencing as

$$\frac{dT_s}{dt} = \frac{T_s - T_s^{old}}{\Delta t} \quad (11)$$

This approach allows for the updating of the server temperature in EnergyPlus as

$$T_s = \left(\frac{\tau}{\tau + \Delta t}\right) T_s^{old} + \left(\frac{\Delta t}{\tau + \Delta t}\right) \left[T_{a,in} + \frac{\Delta T_{ss}}{\varepsilon}\right] \quad (12)$$

Where

$$T_s^0 = T_{a,in}^0 + \frac{\Delta T_{ss}^0}{\varepsilon} \quad (13)$$

Furthermore, the exit air temperature is modified to the following form:

$$T_{a,out} = \left[1 + \varepsilon \left(\frac{\Delta t}{\tau + \Delta t}\right) - \varepsilon\right] T_{a,in} + \varepsilon \left(\frac{\tau}{\tau + \Delta t}\right) T_s^{old} + \left(\frac{\Delta t}{\tau + \Delta t}\right) \Delta T_{ss} \quad (14)$$

Where ΔT_{ss} is the steady-state temperature difference obtained by making the time derivative term in Eq. (1) equal to zero, thus giving:

$$\Delta T_{ss} = \frac{\dot{Q}_s}{\dot{m}c_{p,a}} \quad (15)$$

Equations (12) through (15) are the relevant equations for the Schneider model that are implemented in EnergyPlus using the built-in Energy Management System (EMS) through EnergyPlus Runtime Language (ERL).

4.3 Implementation of the Dynamic Server Model

The EnergyPlus software package is designed for commercial and residential buildings, but important differences exist between these types of buildings and data centers. In general, the amount of cooling load present in a data center is much more than that of a typical residential or commercial building, due to the presence of a large number of computer servers that are in continuous operation. Moreover, cooling demand from the HVAC system fluctuates more profoundly for a data center than a residential building, due to varying degree of computing load throughout a 24-hour cycle.

This variation of cooling load requires taking the thermal mass of the servers into account when calculating the total cooling load at any given instant of time. Since EnergyPlus does not take into account this additional factor, a second software called Matlab EnergyPlus (MLE+) was used to implement a transient scheme for air flow through the servers.

MLE+ is a Matlab-based software that performs co-simulation with EnergyPlus using a BACNET interface, built on the Buildings Virtual Control Test Bed (BCVTB). Data is exchanged between the two software at the timestep used by EnergyPlus in the current simulation session. MLE+ uses Matlab's built-in Java socket to communicate and exchange data with EnergyPlus. The required variables to be exchanged between the two software are specified in a separate configuration (CGF) file. Using MLE+, the user can either implement control schemes not built into EnergyPlus or process, analyse or plot data that has been calculated by EnergyPlus. Furthermore, variables calculated in Matlab can be sent to EnergyPlus as Schedule Values using the built-in schedule option or they can be used to modify EnergyPlus values by using an EnergyPlus actuator, if one is available. Finally, the biggest advantage that MLE+ offers is the development and debugging capabilities of Matlab and the ease of interfacing them with a building model developed outside in EnergyPlus.

Thus using MLE+, the above scheme was coded in Matlab and interfaced with EnergyPlus using MLE+. The following variables were exchanged between the two software, as shown in Table 1 below:

Table 4.1: Variable exchange to and from EnergyPlus

EnergyPlus output variable	EnergyPlus input variable
Server Inlet Temperature (C)	Server Temperature
Server Mass Flow Rate (kg/s)	Server Exit Air Temperature
Server Power Dissipation (W)	--
Server Fan Rise in Air Temperature (C)	--

The variables appearing in the EnergyPlus output variables column are those that are calculated by EnergyPlus directly and then sent over to MLE+ to be used elsewhere; hence they are listed as

output. The variables in the input column are those that are calculated by MLE+ and then sent to EnergyPlus and are written as schedule values, for comparison purpose, in the output file.

4.4 Results

4.4.1 MLE+ Results

For the purpose of this transient analysis, the server with cooling air flowing through it is modelled as a single-flow heat exchanger, where the heated electronic components mounted on a printed circuit board exchange heat with the cooler air. The capacitance, time constant, effectiveness of heat exchange for the server are calculated using the equation shown in Section 4.2. The heat transfer coefficient between the hot server and cooling air stream is calculated as shown below (Sparrow, 1992, Heat transfer correlation for flat packs):

$$h = \frac{\dot{m}c_{p,air} \ln(1 - \varepsilon)}{0.39 * 0.434}$$

The output values for the conditions given are shown in Table 4.1 below:

Table 4.2: Server parameters calculated through MLE+

Parameter	Unit	Value from MLE+
Server Mass, M	kg	24
Time Constant, τ	minutes	4.84
Effectiveness, ε	dimensionless	0.9029
Capacitance, Cs	J/K	15456
Heat Transfer Coefficient, h	W/m ² .K	811.27

4.4.2 Un-modified Power

A comparison of the results from EnergyPlus are shown in Figure. 4.2 - 4.7 below. The simulation is run for a 5-hour period from midnight till 5am on a randomly chosen date. Figure 4.2 shows the CPU loading schedule, where a value of 0 means that the CPU is idling while a value of 1 means that the CPU is running at full load. Currently a load value of 0.5 is chosen for the purpose of analysis.

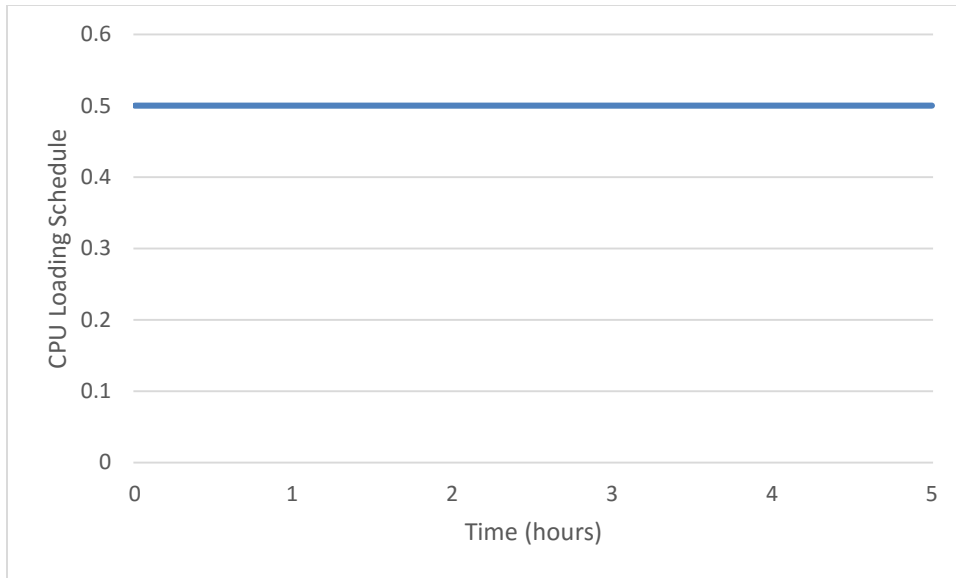


Figure 4.2: CPU loading schedule

Within EnergyPlus, there are two ways to actuate the CPU power. One is to either change the load profile which is shown in Fig. 2. Increasing or decreasing the loading schedule value will result in a change in CPU power. The other is through a CPU power modifier curve, such as the one shown in Figure 4.3 below.

A typical CPU power modifier curve is a biquadratic function of the CPU loading schedule value (x) and the server inlet air temperature (y). The general form of a biquadratic curve is:

$$\text{Curve} = C1 + C2*x + C3*x^2 + C4*y + C5*y^2 + C6*x*y$$

The original and modified loading curve coefficients are shown in Table 4.2 below:

Table 4.3: CPU power modifier curves – original and modified

Coefficient	Original	Modified
C1	-1	-1
C2	1.0	1.6
C3	0.6	0.6
C4	0.06667	0.06667

Table 4.3 continued

C5	0	0
C6	0	0

The output from the two curves are shown in Figure 4.3 below, calculated using the above six coefficients and the CPU loading schedule (x) and server inlet temperature (y) at each time step. The modified curve produces a greater output between 3:00 – 4:00 am and hence this would result in enhanced CPU power during this time interval. This is equivalent to increasing the loading value i.e. the CPU load increasing from 0.5 to a higher value which corresponds to the curve output, showing a greater demand from the cloud. Using the modified curve, the CPU power was actuated from 11 to an average of 13.6 kW during the time interval stated above.

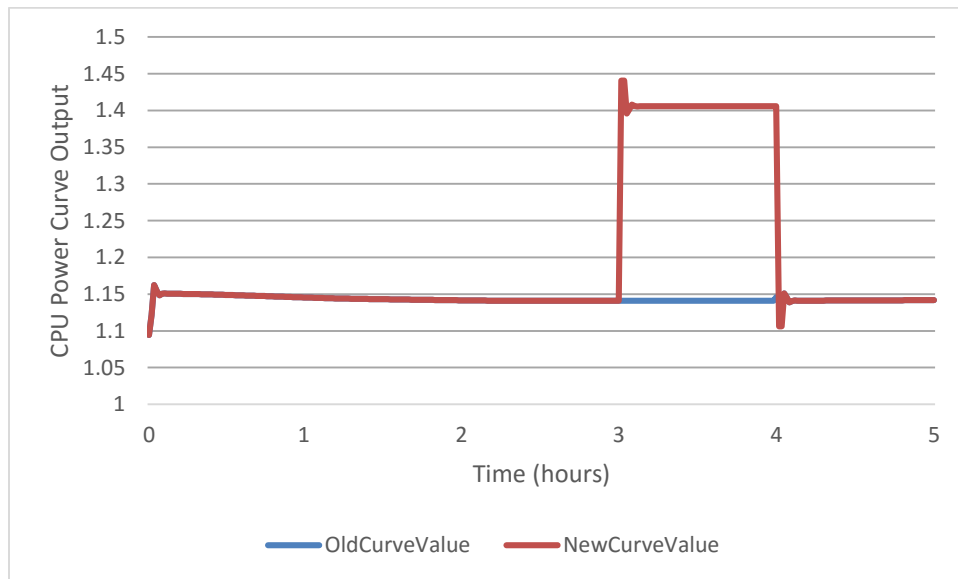


Figure 4.3: CPU power modifier curve output

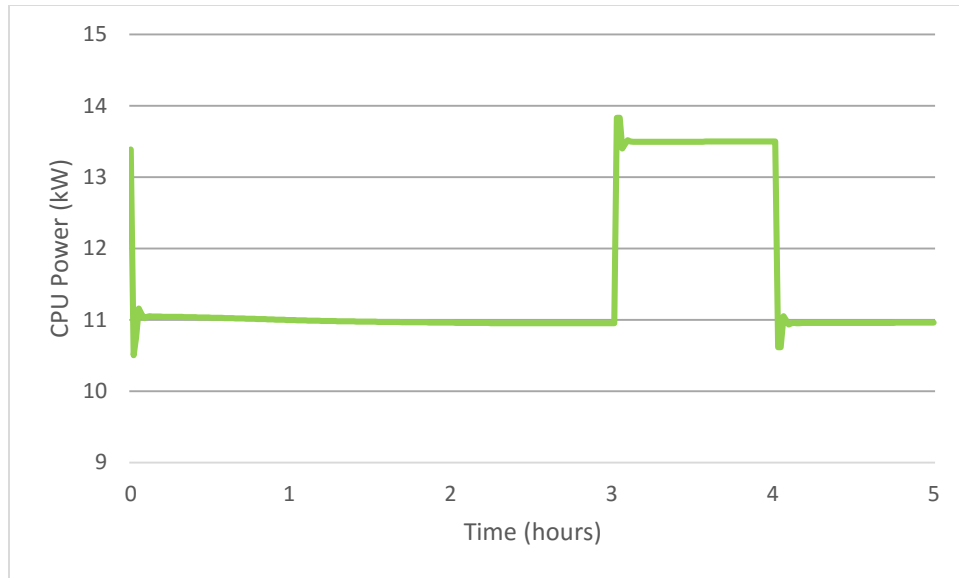


Figure 4.4: CPU power dissipation

The corresponding HVAC power is calculated by EnergyPlus using the total heat gain to zone from the IT equipment and any other electrical and thermal heat loads, such as lights and people. However, since we are dealing with modular data centers, the number of people within the data center is kept to zero and lighting load is kept to a minimum of 300 W, which is only 2.7% of the original IT load. Hence the HVAC power that is calculated by EnergyPlus for the total zone cooling load (IT + lights) is shown in Figure 4.5 below.

The trend to note is the rapid increase in HVAC power as the demand and hence the CPU power goes up. The HVAC system in EnergyPlus follows the total heat gained by the zone and calculates the required HVAC power at the current timestep based on the zone heat gain from the previous time step.

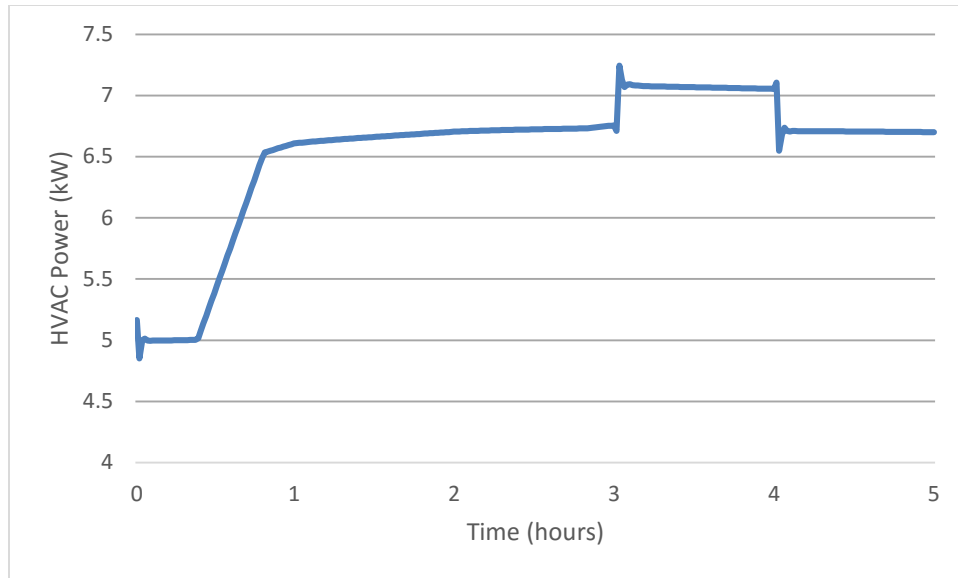


Figure 4.5: HVAC power consumption

The corresponding server inlet and exit air temperatures are shown in Figure 4.6 below. The HVAC system adjusts the inlet air temperature to the servers based on the total cooling load. Hence, if the CPU demand goes up, the convective heat gain to the zone increases, and the DX cooling system increases its cooling rate to supply colder air to the servers in order to maintain the zone and return air temperatures. This rapid fluctuation in inlet and exit air temperature increases the cooling and hence the HVAC power.

However, when contrasted with the transient results from MLE+ as shown in Figure 4.6 below, the outlet air temperature in fact does not rise as sharply as is expected. There is a clear lag in the rate of change of exit air temperature as calculated by MLE+, as opposed to EnergyPlus. This perceived lag is due to the server's thermal mass i.e. its ability to store heat when heated up and release the stored heat when cooling down. This is evident from the results of Figure 4.7, where the server temperature does not rise up instantly nor linearly; rather it increases at a decreasing rate when the CPU power goes up sharply and similarly cools down to a lower level with a considerable lag when the excess load is removed, as shown by the time stamps marked in Figure 4.7. The reason for the difference in exit air temperatures calculated between EnergyPlus and MLE+ is due to a difference in initial conditions in the Matlab calculation. Since the two exit air temperature is

calculated differently by both software, the initial value or initial condition becomes different and that difference propagates evenly throughout the calculation.

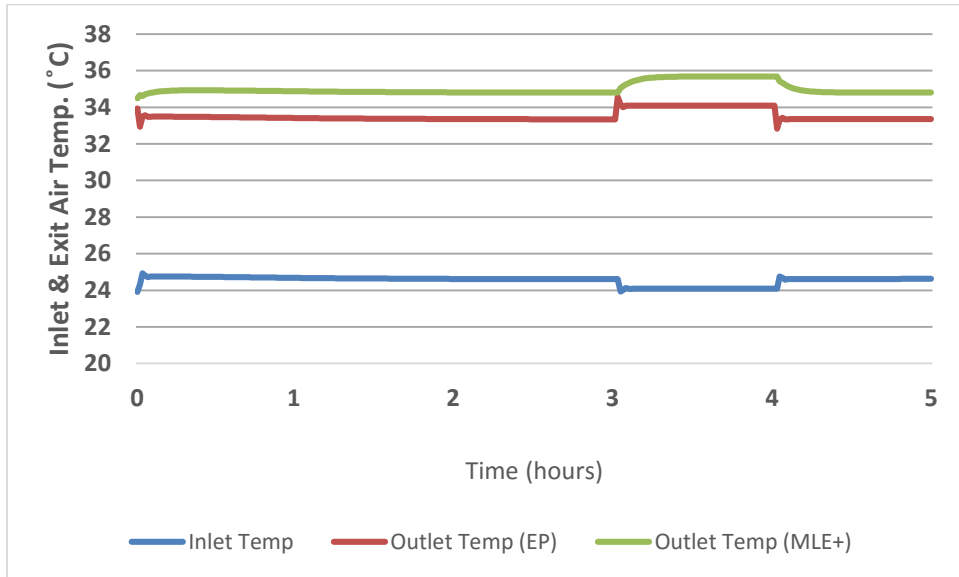


Figure 4.6: Server Inlet and Exit Temperature

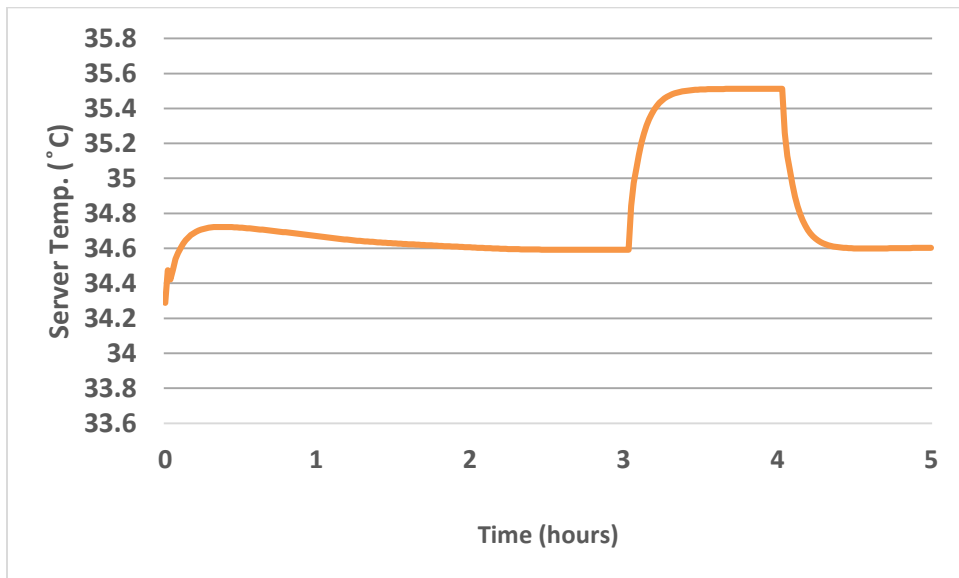


Figure 4.7: Server Temperature calculated using MLE+

4.4.3 Power Savings

When demand goes up, the CPU temperature follows the trend as shown until it reaches a steady-state value. Since the server is heating with the trend shown in Figure 4.8, the CPU power dissipation will hence not rise immediately to the higher level, but will gradually increase at a decreasing rate, similar to that of the server. Hence the cooling system should follow the modified curve of Figure 4.9.

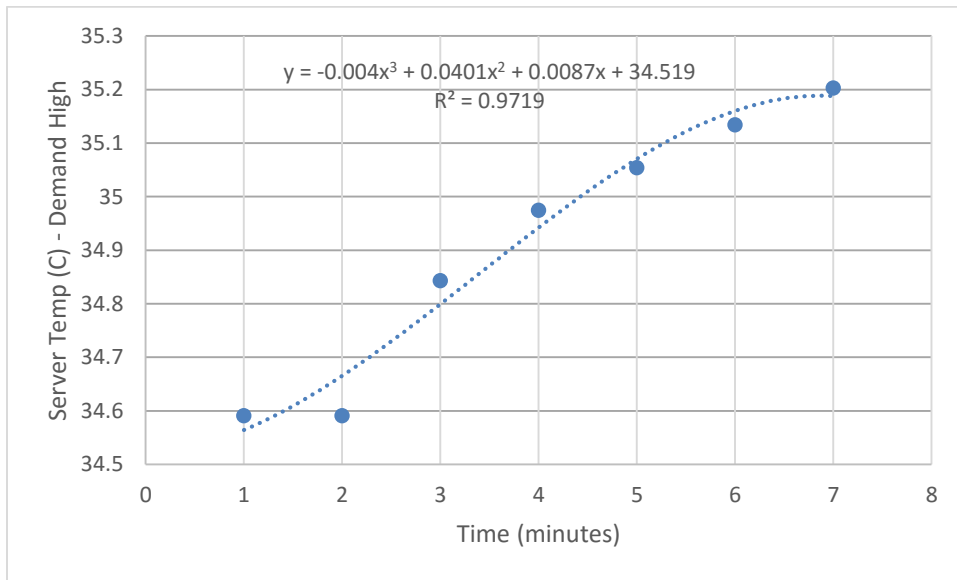


Figure 4.8: Server Temperature increasing with rising demand

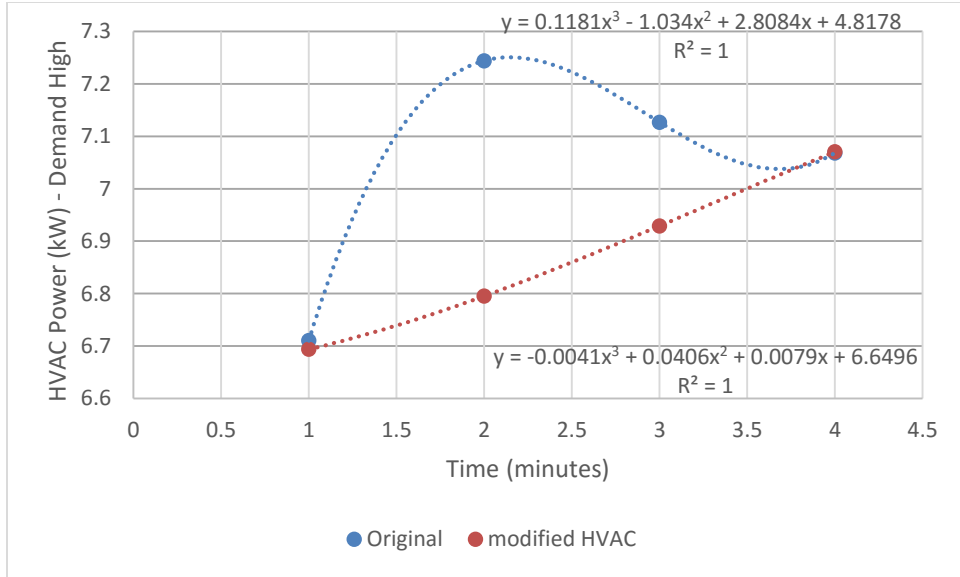


Figure 4.9: Comparison of HVAC power between EP & transient model

Similarly, when the demand goes down, the server temperature and hence power dissipation decay to a lower value, rather than falling abruptly. Hence, here the trade-off occurs. If the cooling system follows the profile depicted by the server temperature, it will use more power as compared to dropping the power instantly. It is feasible as long as the server and exit air temperatures are not near the manufacturer's specified limit, which in the case of a Dell R210 server is 50°C.

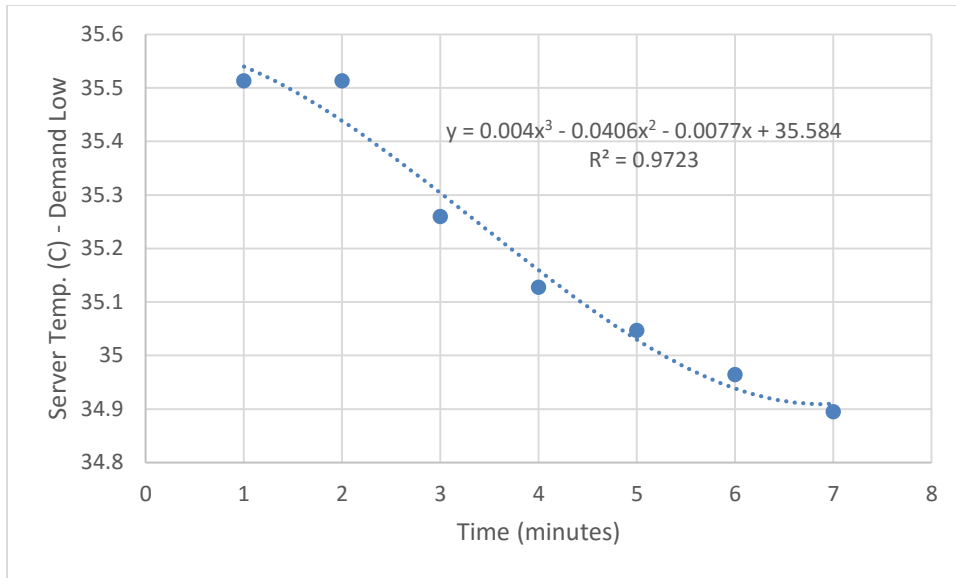


Figure 4.10: Server Temperature decreasing with a drop in demand

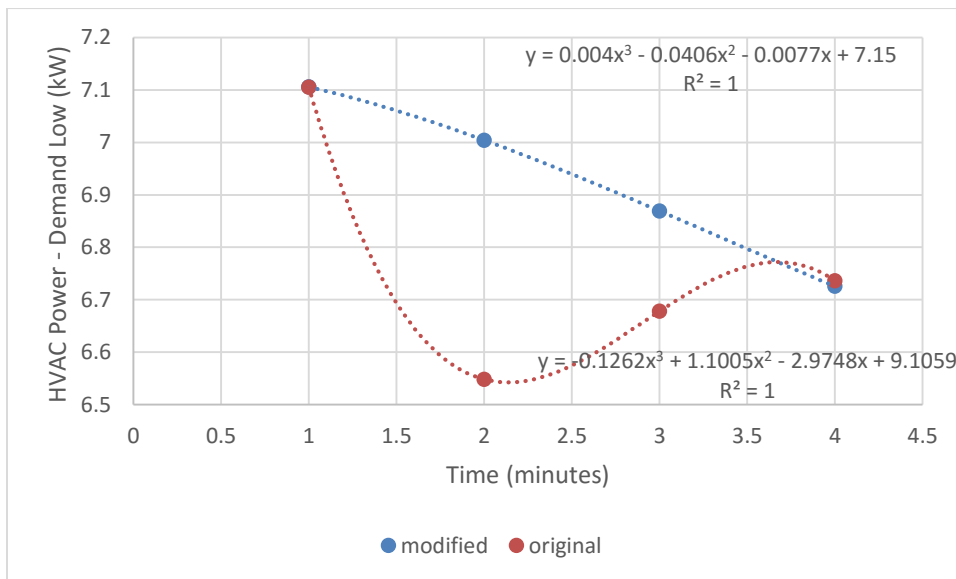


Figure 4.11: Comparison of HVAC power between EP & transient model - decreasing power

For a 5-hour period with a single rise & fall in demand/server load, average power savings of 660W (0.034% of total) if server temperature profile is followed by HVAC system for rise in demand only and instant drop of HVAC power with a drop in demand. However, average power

savings of 24W (0.0012% of total HVAC power used) if server temperature profile is followed by HVAC system for both rise & drop in demand. A graph of the expected power savings by following the server transient temperature trend is depicted in Figure 4.12.

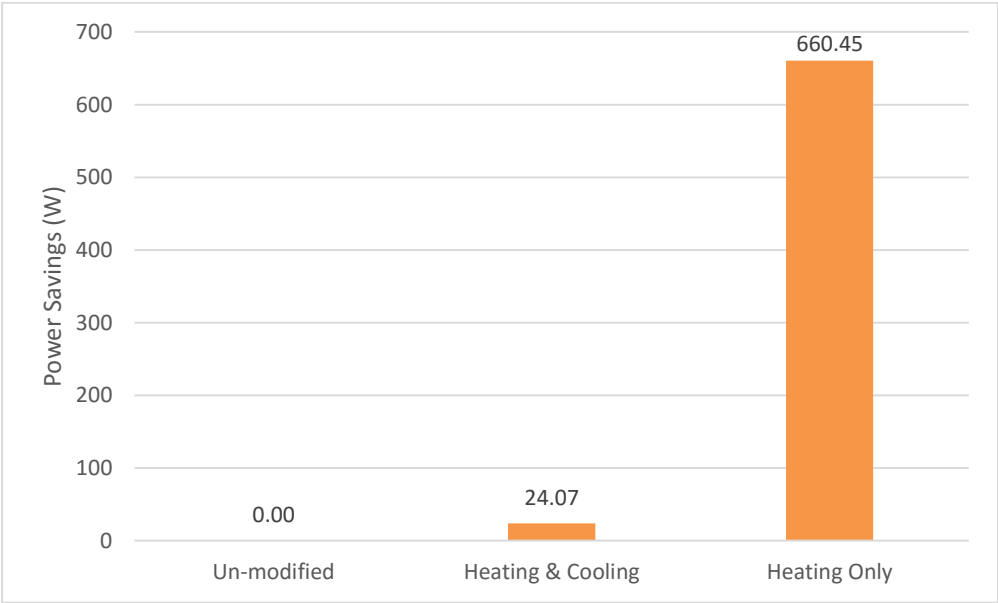


Figure 4.12: Power Savings by following transient server profile

Extrapolating this trend on an annual basis yields the following energy savings, which at 8c/kWh translates into \$92.51 of monetary savings for the first case and just \$3.36 of savings for the second case. These results are graphically depicted in Figure 4.13 & 4.14 below.

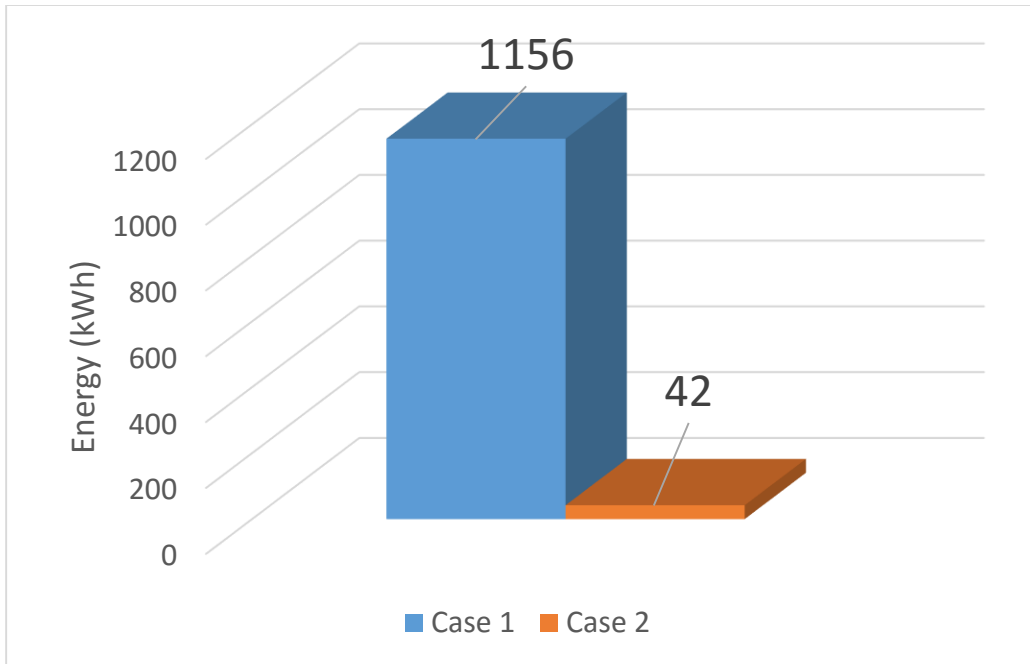


Figure 4.13: Extrapolated annual energy savings for both cases

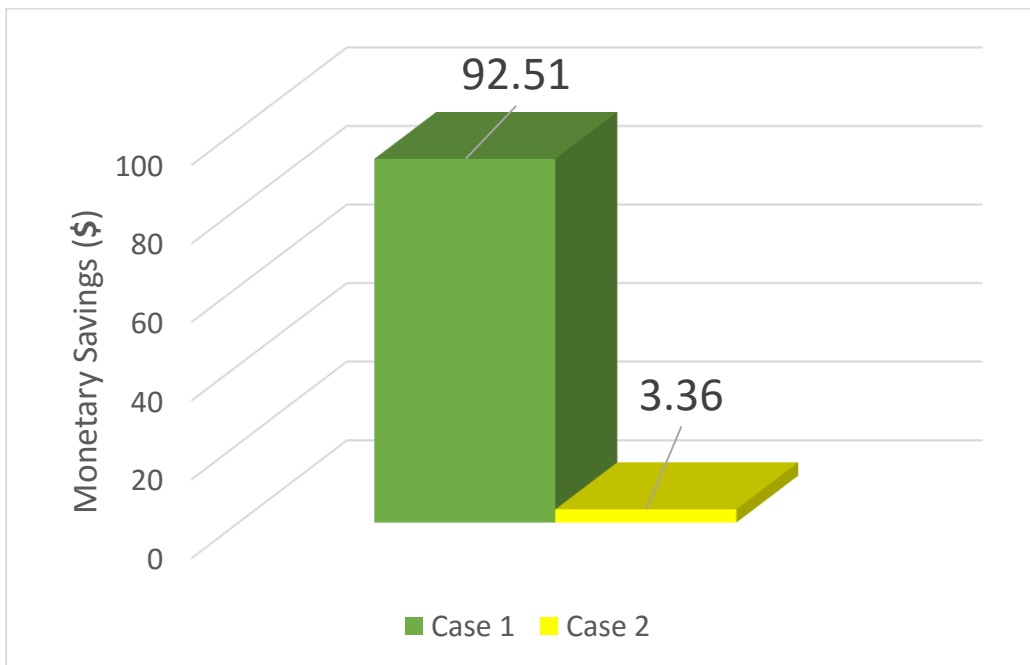


Figure 4.14: Expected financial savings for both cases

4.5 Timestep analysis for transient server model

The base timestep used for the transient model simulations is 1 minute, which is the lowest timestep that EnergyPlus can utilize. However, in order to assess the influence of timestep on EnergyPlus output, a timestep analysis was performed using a 2-minute & 4-minute timestep. The percentage error for the results of these two cases versus the base case of 1-minute is shown in Figure 4.14-4.18 below. These results are for the server temperature and exit air temperature as calculated by Matlab (MLE+), the exit air temperature as calculated by EnergyPlus and the total HVAC power consumed for each case.

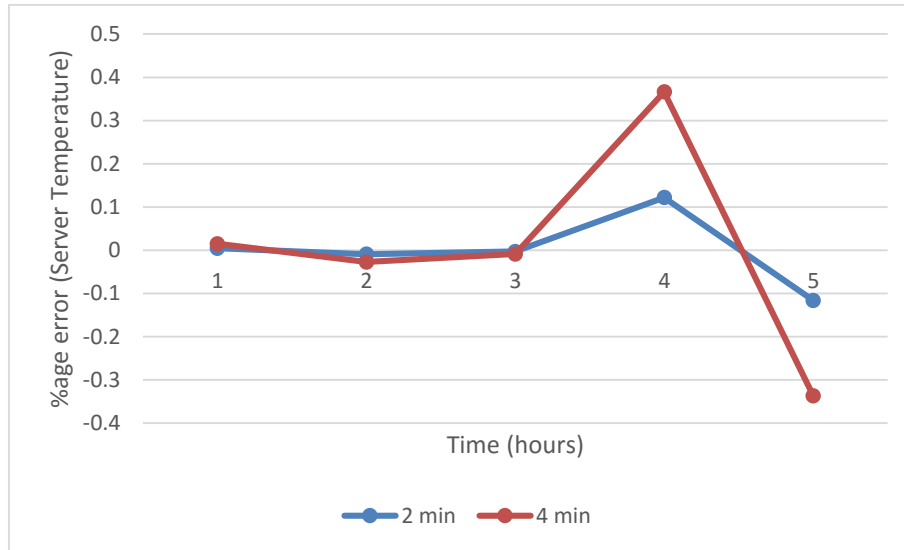


Figure 4.15: Variation in percentage error of server temperature with timestep

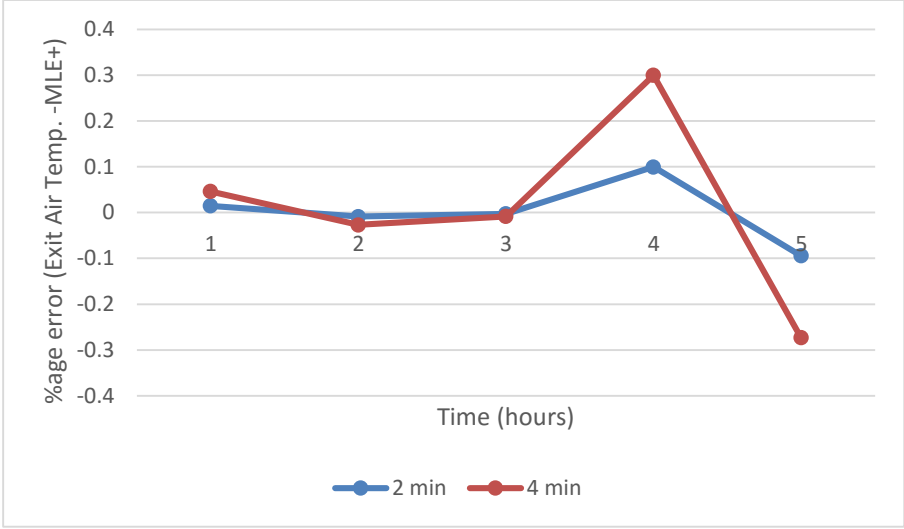


Figure 4.16: Variation in percentage error of exit air temperature as calculated by MLE+ with timestep

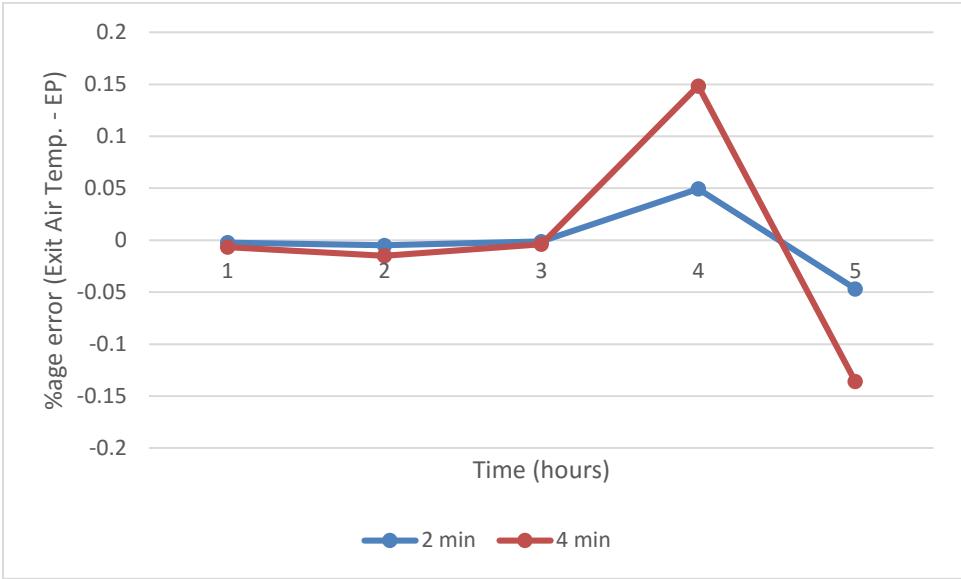


Figure 4.17: Variation in percentage error of exit air temperature as calculated by EnergyPlus with timestep

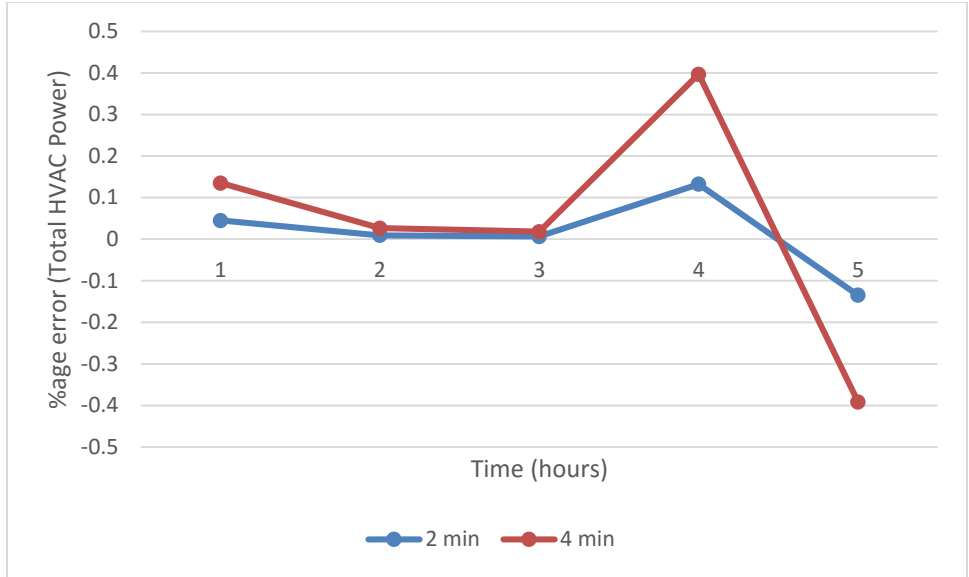


Figure 4.18: Variation in percentage error of total HVAC power with timestep

Furthermore, a comparison of the values for server capacitance, time constant, heat transfer effectiveness and heat transfer coefficient between the server and cooling airstream are presented in Table 4.4 below:

Table 4.4: Comparison of server transient parameters with varying timestep

Timestep (minutes)	Tau (minutes)	Effectiveness	Capacitance (J/K)	Heat Transfer Coefficient (W/m ² .K)
1	4.9970	0.8753	15456	724.3852
2	4.9971	0.8753	15456	724.3703
4	4.9973	0.8753	15456	724.3415

These results show that there is no difference at all in the server capacitance and effectiveness values; the two values of interest for the transient model. Moreover, the time constant and heat transfer coefficient is also the same for all practical purposes.

Hence, the timestep does not impact the results in any significant way and in any case, the chosen timestep is the lowest that can be used within EnergyPlus and hence a higher degree of accuracy cannot be achieved anyways while using this software.

4.6 Summary & Conclusion

The results of this work show that by recognising that the servers in a data center have a thermal mass associated with them. This results in slowly increasing server and exit air temperature, which gives weight to the fact that when demand through the cloud goes up, the CRAC power can be increased slowly to the desired higher level, rather than ramping up abruptly. This will result in power savings at each time step since the actual HVAC power will be lower than what is perceived to be, as long as the server and exit air temperatures are kept in check. Frequently exceeding manufacturer's recommended limits can result in reliability issues in the long run, leading to degradation of server running life, frequent downtimes and eventual failure.

Similarly, when the demand goes down and hence the CPU power, the server and exit air temperatures do not immediately drop down to the lower level, rather they exhibit the same lag as before. This is again due to the server's thermal mass, whereby the heat absorbed in the ramping up process is now gradually released to the environment and hence the server temperature drops slower than expected and a time lag is observed. Here, the data center operator has a choice. He can either choose to immediately drop the CRAC power at the next cycle (timestep for EnergyPlus), thereby elevating the zone air temperature slightly or drop it gradually to follow the exit air temperature. In the first case, the savings in terms of power gained when the demand went up will be off-set by the gradual decline in power, resulting in 0.0012% of total power savings. In the latter case, however, they will manifest as additional savings from not choosing to operate at a higher power level, with resulting power savings of 0.034%. However, this should not be the case if the initially higher server temperatures are frequently near the manufacturer's prescribed limits, which will again result in reliability issues in the long run. Lastly, however small the power savings may be by adapting to the dynamic power dissipation of the server, it does result in some savings that over the course of a year will result in savings in terms of utility costs.

CHAPTER 5

CONCLUSIONS

This study aimed to develop steady-state energy and exergy models for modular data centers, as well as a transient model to predict dynamic cooling requirements. This study concludes that under steady-state operating conditions, the locations near the southern border of the United States are in general too hot for efficient cooling of data centers using Direct Expansion (DX) cooling alone. In general, these locations are not preferred for construction of regular data centers but since modular data centers are mobile and cloud based infrastructure capacity can be needed anywhere, such as an oilfield or military base located in the desert, it is recommended to retrofit these container facilities with passive cooling techniques such as evaporative and free air cooling. This will not only help the facilities to perform more efficiently, they can also reduce their power consumption by up to 38% in selected areas. Also, having the provision of an air-side economizer can allow these facilities to operate energy free by utilizing the cooler night air or whenever the ambient conditions permit. Furthermore, through second-law analysis, it has been found that the server inlet-exit temperature difference is the biggest source of exergy destruction in a data center. The operating goal should be to minimize this temperature difference by setting a lower return air temperature for the CRAC system. However, since this in itself is power consuming and costly, the use of passive cooling techniques is suggested where conditions permit in order to augment base cooling without utilizing significantly more energy and producing extra emissions. Lastly, it should be noted that in general, increasing the zone and inlet air temperature don't necessarily lead to savings in power, since after an optimum setpoint, the savings in power from the CRAC unit are offset by energy consumption from the server fans in order to cool the servers. This optimum temperature is determined to be around 74 F though trial and error in various simulations.

In terms of dynamic loading, it should be realized that the servers in a data center have an associated thermal mass which allows for fluctuations or swings in their temperature. Thus in times of rising demand over the cloud, the servers will heat up slowly rather than instantly, as suggested by the transient model explored in this study. The CRAC system can potentially save up to 0.03% of the total power by following the transient server temperature and power dissipation. However small this power saving may be, it can amount to a considerable number of Watts saved during the course of a year. This will not only offset the utility costs slightly but will also save on harmful

emissions emitted by burning carbon-based fuels. In a world where data center trend is on the rise and their capacity is increasing by the year, apparently small savings in power locally can amass to significant number of kilowatts globally.

Appendix A: PERFORMANCE CURVES FOR DX SYSTEM MODELED AS A CRAC UNIT

Quadratic Curves:

Curve Name: HPACCoolCapFFF

0.8	Coefficient1 Constant
0.2	Coefficient2 x
0.0	Coefficient3 x**2
0.5	Minimum Value of x
1.5	Maximum Value of x

Curve Name: HPACCOOLEIRFFF

1.156	Coefficient1 Constant
-0.1816	Coefficient2 x
0.0256	Coefficient3 x**2
0.5	Minimum Value of x
1.5	Maximum Value of x

Curve Name: HPACCOOLPLFFPLR

0.85	Coefficient1 Constant
0.15	Coefficient2 x
0.0	Coefficient3 x**2
0.0	Minimum Value of x
1.0	Maximum Value of x

Curve Name: ECM FanPower fFlow

0.0	Coefficient1 Constant
1.0	Coefficient2 x 1.0
0.0	Coefficient3 x**2
0.0	Minimum Value of x
99.0	Maximum Value of x

Curve Name UPS Efficiency fPLR

1.0	Coefficient1 Constant
0.0	Coefficient2 x
0.0	Coefficient3 x**2
0.0	Minimum Value of x
99.0	Maximum Value of x

Biquadratic Curves:

Curve Name: Liebert Econophase quadratic fit

0.1416159	Coefficient1 Constant
0.0	Coefficient2 x
0.0	Coefficient3 x**2
0.013828452	Coefficient4 y
0.00023872	Coefficient5 y**2
0.0	Coefficient6 x*y

12.77778	Minimum Value of x
23.88889	Maximum Value of x
-10	Minimum Value of y
46.11111	Maximum Value of y
0.04	Minimum Curve Output
1.4	Maximum Curve Output
Temperature	Input Unit Type for X
Temperature	Input Unit Type for Y
Dimensionless	Output Unit Type

Curve Name: Data Center Servers Power fLoadTemp

-1.0	Coefficient1 Constant
1.0	Coefficient2 x
0.0	Coefficient3 x**2
0.06667	Coefficient4 y
0.0	Coefficient5 y**2
0.0	Coefficient6 x*y
0.0	Minimum Value of x
1.5	Maximum Value of x
-10	Minimum Value of y
99.0	Maximum Value of y
0.0	Minimum Curve Output
99.0	Maximum Curve Output
Dimensionless	Input Unit Type for X
Temperature	Input Unit Type for Y
Dimensionless	Output Unit Type

Curve Name: Data Center Servers Airflow fLoadTemp

-1.4	Coefficient1 Constant
0.9	Coefficient2 x
0.0	Coefficient3 x**2
0.1	Coefficient4 y
0.0	Coefficient5 y**2
0.0	Coefficient6 x*y
0.0	Minimum Value of x
1.5	Maximum Value of x
-10	Minimum Value of y
99.0	Maximum Value of y
0.0	Minimum Curve Output
99.0	Maximum Curve Output
Dimensionless	Input Unit Type for X
Temperature	Input Unit Type for Y
Dimensionless	Output Unit Type

Curve Name: Data Center Recirculation fLoadTemp

1.0	Coefficient1 Constant
-----	-----------------------

0.0	Coefficient2 x
0.0	Coefficient3 x**2
0.0	Coefficient4 y
0.0	Coefficient5 y**2
0.0	Coefficient6 x*y
0.0	Minimum Value of x
1.5	Maximum Value of x
-10	Minimum Value of y
99.0	Maximum Value of y
0.0	Minimum Curve Output
99.0	Maximum Curve Output
Dimensionless	Input Unit Type for X
Temperature	Input Unit Type for Y
Dimensionless	Output Unit Type

Table: Two Independent Variables

Cool Cap Mod func of

Temperature	Name
Biquadratic	Curve Type
Linear Interpolation Of Table	Interpolation Method
13.0	Minimum Value of X
23.89	Maximum Value of X
-10.0	Minimum Value of Y
46.11	Maximum Value of Y
	Minimum Table Output
	Maximum Table Output
Temperature	Input Unit Type for X
Temperature	Input Unit Type for Y
Dimensionless	Output Unit Type
	Normalization Reference
13.0	X Value #1
-10.0	Y Value #1
1.00	Output Value #1
13.0	X Value #2
15.0	Y Value #2
1.00	Output Value #2
13.0	X Value #3
18.0	Y Value #3
1.00	Output Value #3
13.0	X Value #4
24.0	Y Value #4
0.924738271	Output Value #4
13.0	N20

30.0	N21
0.883909339	N22
13.0	N23
35.0	N24
0.835522309	N25
13.0	N26
38.0	N27
0.800222635	N28
13.0	N29
46.0	N30
0.683109499	N31
17.0	N32
-10.0	N33
1.00	N34
17.0	N35
15.0	N36
1.00	N37
17.0	N38
18.0	N39
1.00	N40
17.0	N41
24.0	N42
1.00	N43
17.0	N44
30.0	N45
0.976933863	N46
17.0	N47
35.0	N48
0.937696593	N49
17.0	N50
38.0	N51
0.907886775	N52
17.0	N53
46.0	N54
0.805413255	N55
19.4444	N56
-10.0	N57
1.00	N58
19.4444	N59
15.0	N60
1.00	N61
19.4444	N62
18.0	N63

1.00	N64
19.4444	N65
24.0	N66
1.00	N67
19.4444	N68
30.0	N69
1.00	N70
19.4444	N71
35.0	N72
1.00	N73
19.4444	N74
38.0	N75
0.9718	N76
19.4444	N77
46.0	N78
0.8782	N79
21.0	N80
-10.0	N81
1.00	N82
21.0	N83
15.0	N84
1.00	N85
21.0	N86
18.0	N87
1.00	N88
21.0	N89
24.0	N90
1.00	N91
21.0	N92
30.0	N93
1.00	N94
21.0	N95
35.0	N96
1.0385	N97
21.0	N98
38.0	N99
1.0142	N100
21.0	N101
46.0	N102
0.9264	N103
23.9	N104
-10.0	N105
1.00	N106

23.9	N107
15.0	N108
1.00	N109
23.9	N110
18.0	N111
1.00	N112
23.9	N113
24.0	N114
1.00	N115
23.9	N116
30.0	N117
1.00	N118
23.9	N119
35.0	N120
1.110828252	N121
23.9	N122
38.0	N123
1.090488436	N124
23.9	N125
46.0	N126
1.013268253	N127

Table:TwoIndependentVariables

Liebert Econophase EIR Func T	Name
Biquadratic	Curve Type
LinearInterpolationOfTable	Interpolation Method
12.7	Minimum Value of X
23.8	Maximum Value of X
-50	Minimum Value of Y
50	Maximum Value of Y
0.03	Minimum Table Output
1.5	Maximum Table Output
Temperature	Input Unit Type for X
Temperature	Input Unit Type for Y
Dimensionless	Output Unit Type
	Normalization Reference
12.7	X Value #1
-50	Y Value #1
0.042	Output Value #1
12.7	X Value #2
-4.0	Y Value #2
0.042	Output Value #2
12.7	X Value #3

-1.2222	Y Value #3
0.084	Output Value #3
12.7	X Value #4
1.5555	Y Value #4
0.084	Output Value #4
12.7	N20
4.3333	N21
0.2269	N22
12.7	N23
7.1111	N24
0.2395	N25
12.7	N26
9.8888	N27
0.311	N28
12.7	N29
12.6667	N30
0.3697	N31
12.7	N32
15.4444	N33
0.4454	N34
12.7	N35
18.222	N36
0.5462	N37
12.7	N38
21.0	N39
0.6723	N40
12.7	N41
23.777778	N42
0.7227	N43
12.7	N44
26.55556	N45
0.7773	N46
12.7	N47
29.33333	N48
0.8193	N49
12.7	N50
32.11111	N51
0.895	N52
12.7	N53
34.88889	N54
1.0	N55
12.7	N56
50.0	N57

1.5	N58
23.8	N59
-50	N60
0.042	N61
23.8	N62
-4.0	N63
0.042	N64
23.8	N65
-1.2222	N66
0.084	N67
23.8	N68
1.5555	N69
0.084	N70
23.8	N71
4.3333	N72
0.2269	N73
23.8	N74
7.1111	N75
0.2395	N76
23.8	N77
9.8888	N78
0.311	N79
23.8	N80
12.6667	N81
0.3697	N82
23.8	N83
15.4444	N84
0.4454	N85
23.8	N86
18.222	N87
0.5462	N88
23.8	N89
21.0	N90
0.6723	N91
23.8	N92
23.777778	N93
0.7227	N94
23.8	N95
26.55556	N96
0.7773	N97
23.8	N98
29.33333	N99
0.8193	N100

23.8	N101
32.11111	N102
0.895	N103
23.8	N104
34.88889	N105
1.0	N106
23.8	N107
50.0	N108
1.5	N109

Appendix B: SIMPLE TRANSIENT SERVER EXPERIMENT TO VALIDATE TRANSIENT MODEL

Description of Problem:

Simulated experiment for a 1-D finite difference model using a 2U server to determine its transient parameters. The model is implemented in Matlab. Independent parameters to characterize a server are:

1. Thermal Capacitance, C_s (including Time Constant, τ)
2. Heat transfer effectiveness, ϵ

For a single server, experiment constitutes keeping the server inlet temperature constant while increasing the flow rate from zero to a desired steady-state value. Then, the inlet air temperature is suddenly or linearly raised from the initial constant value to a higher final value, while keeping the power at zero (server off) and flow rates constant. Then the inlet air temperature is kept at that higher value while keeping the mass flow rate constant and noting the exit air temperature. The transient characteristics such as the time constant can be obtained from the mathematical model using the data. Note that in this case the server is powered off i.e. CPU & fan power is zero.

%% *****%%

```

%declare variables
%air characteristics
rho_air = 1.1610;           %density of air
m_dot_ss = rho_air*(100/3600); %mass flow rate of air
c_p_a = 1006.5;           %specific heat of air
C_a_dot = m_dot_ss*c_p_a;
U = 2;                    %2U server; 1U = 1.75"

%server characteristics
Mass = 24.2;              %mass of server in kg
C_s = 644*Mass;          %server thermal capacitance
effectiveness = 1-(13*((Mass/U)^(-1.87))); %effectiveness of server
K = effectiveness*m_dot_ss*c_p_a;
Tau = C_s/K;             %time constant in seconds
Tau_minutes = Tau/60;    %time constant in minutes
h = -C_a_dot*log(1-effectiveness)/(0.39*0.434); %heat transfer coefficient, W/(m^2.K)

%declare transient time
t_f = 5000;              %ending time in seconds
time = 1:t_f;

```

```

delta_t = 1;                %time step - 1 second

%declare temperatures
T_h = 40;                  %steady-state exit temp in deg. C
T_c = 22;                  %steady-state inlet temp in deg. C
T_a_in = zeros(1,t_f);    %inlet air temp
T_a_ex = zeros(1,t_f);    %exit air temp
T_s = zeros(1,t_f);       %server temp
q_dot_cpu = zeros(1,t_f); %CPU power
q_dot_fan = zeros(1,t_f); %fan power
q_dot_s = zeros(1,t_f);   %server power
q_dot_ss = 304.5;         %steady-state server power in Watts
q_fan = 0;                %fan power
delta_T_fan = q_fan/C_a_dot; %temperature rise of the fan

%inlet temperature profile      %air temp at inlet of server in Kelvin
for t = 1:t_f
    if t <= 1000
        T_a_in(t) = T_c;
    elseif (t > 1000) && (t <= 1500)
        T_a_in(t) = 0.036*t - 14; %transient event-alpha = 2.16 C/min
    else
        T_a_in(t) = T_h;
    end
end
plot(time,T_a_in)
xlabel('Time (s)')
ylabel('Inlet Air Temperature (C)')
title('Inlet Air Temperature vs time')

%power dissipation in server
for tt = 1:t_f
    if tt<=1000
        q_dot_cpu(tt) = 0;
        q_dot_fan(tt) = 0;
        q_dot_s(tt) = q_dot_cpu(tt) + q_dot_fan(tt);
    else
        q_dot_cpu(tt) = 0;
        q_dot_fan(tt) = 0;
        q_dot_s(tt) = q_dot_cpu(tt) + q_dot_fan(tt);
    end
end
figure
plot(time,q_dot_s,time,q_dot_fan)
xlabel('Time (s)')
ylabel('Power Dissipation (W)')

```

```

title('Server and Fan Power Dissipation vs time')
legend('Server','Fan')

% *****%

delta_T_ss = q_dot_s(1)/(m_dot_ss*c_p_a); %temp difference in steady-state

%Initial Conditions
T_s(1) = T_a_in(1) + delta_T_ss/effectiveness;
T_a_ex(1) = T_a_in(1) + delta_T_ss + delta_T_fan;

%Temperatures
for ttt = 2:t_f
    T_s(ttt) = ((Tau./(Tau+delta_t)).*T_s(ttt-1)) +
(delta_t/(Tau+delta_t)).*(T_a_in(ttt)+(delta_T_ss/effectiveness));
    T_a_ex(ttt) = (1-effectiveness)*T_a_in(ttt) +
(delta_t/(Tau+delta_t)).*(effectiveness*T_a_in(ttt)+ delta_T_ss) +
(effectiveness*(Tau/(Tau+delta_t))*T_s(ttt-1))+delta_T_fan;
end

% *****%

%%Plot the output
%Plot T_out vs T_in
figure
plot(time,T_a_in,time,T_a_ex)
xlabel('time (s)')
ylabel('Air Temperature (C)')
title('Air Temperature vs Time')
legend('T_a_in','T_a_ex','Location','northwest')

%Plot T_s vs time
figure
plot(time,T_s)
xlabel('time (s)')
ylabel('Server Temperature (C)')
title('Server Temperature vs Time')

%Plot T_s vs time
figure
plot(time,T_s,time,T_a_ex)
xlabel('time (s)')
ylabel('Temperature (C)')
title('Server & Outlet Air Temperature vs Time')
legend('T_s','T_a_ex','Location','northwest')

m_dot = m_dot_ss*3600; %mass flow rate in m3/hr

```

```

%Display Output
display(m_dot_ss)
display(m_dot)
display(Tau_minutes)
display(effectiveness)
display(C_s)
display(h)

```

```

%% *****end of program*****

```

Results for un-powered server

Table B.1 : Transient server parameters for an unpowered server

Vol. Flow Rate (m ³ /hr)	Tau (minutes)	Effectiveness	Capacitance (J/K)	Heat Transfer Coefficient (W/m ² .K)
100.00	9.12	0.88	15585	402.22

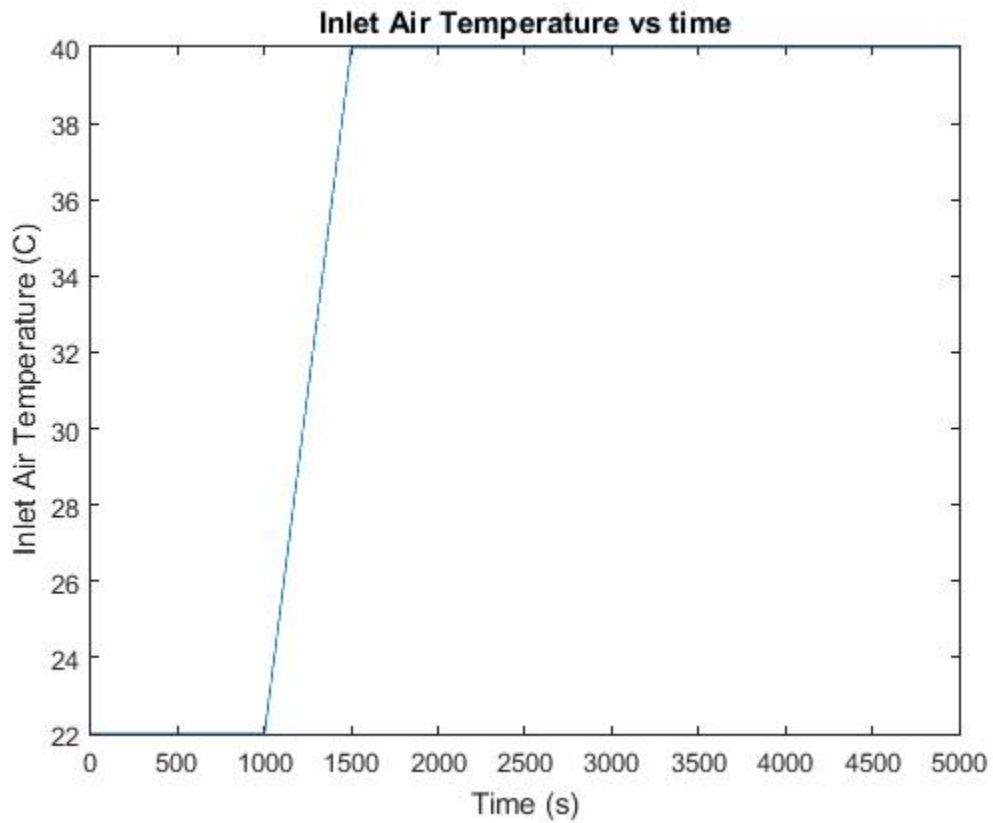


Figure B.1: Variation of server inlet air temperature with time

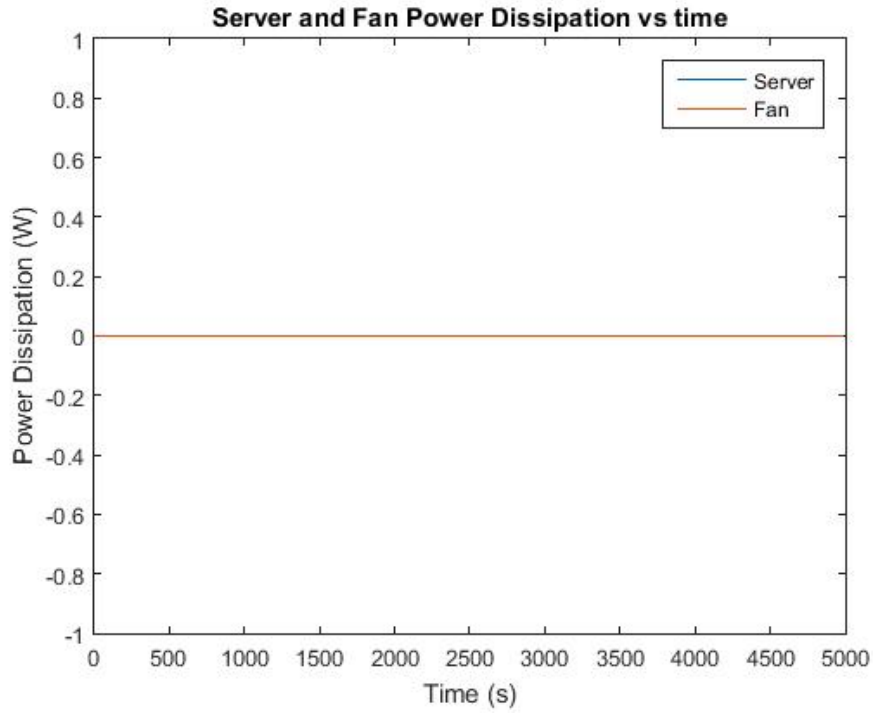


Figure B.2: Variation of CPU & fan power dissipation with time for an unpowered server

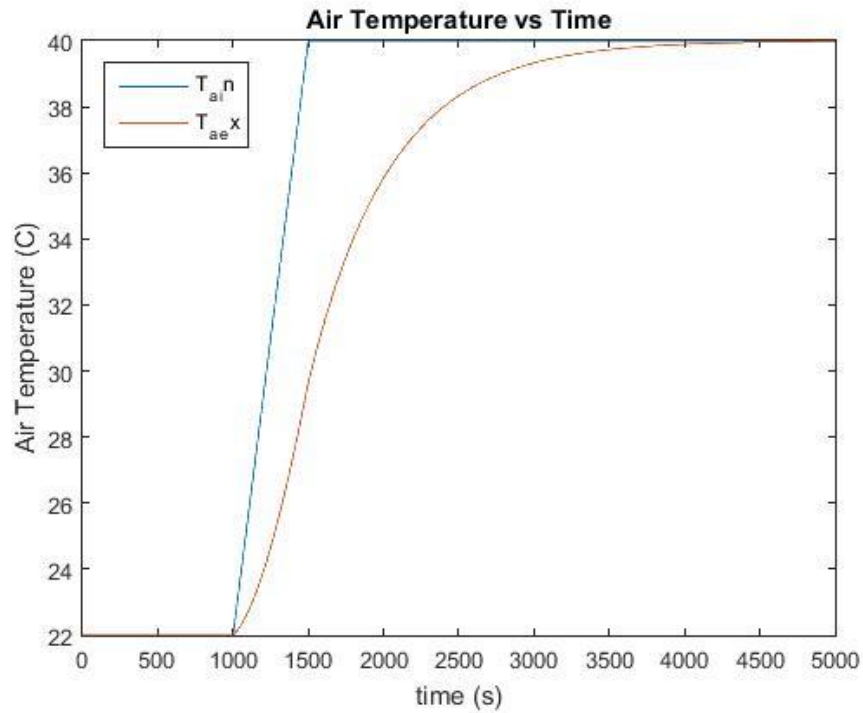


Figure B.3: Variation of server inlet & exit air temperature with time for an unpowered server

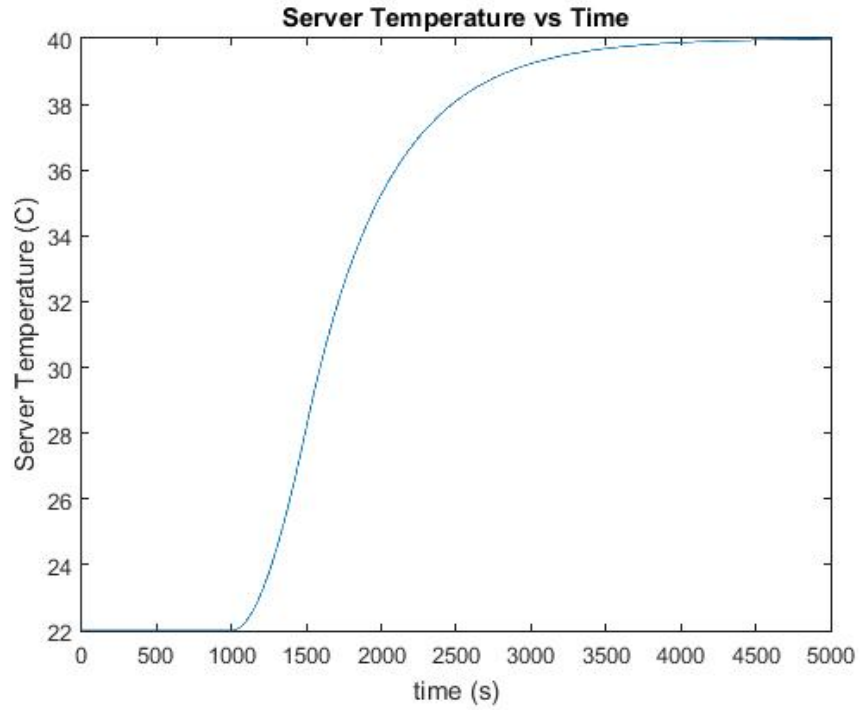


Figure B.4: Variation of server temperature with time for an unpowered server

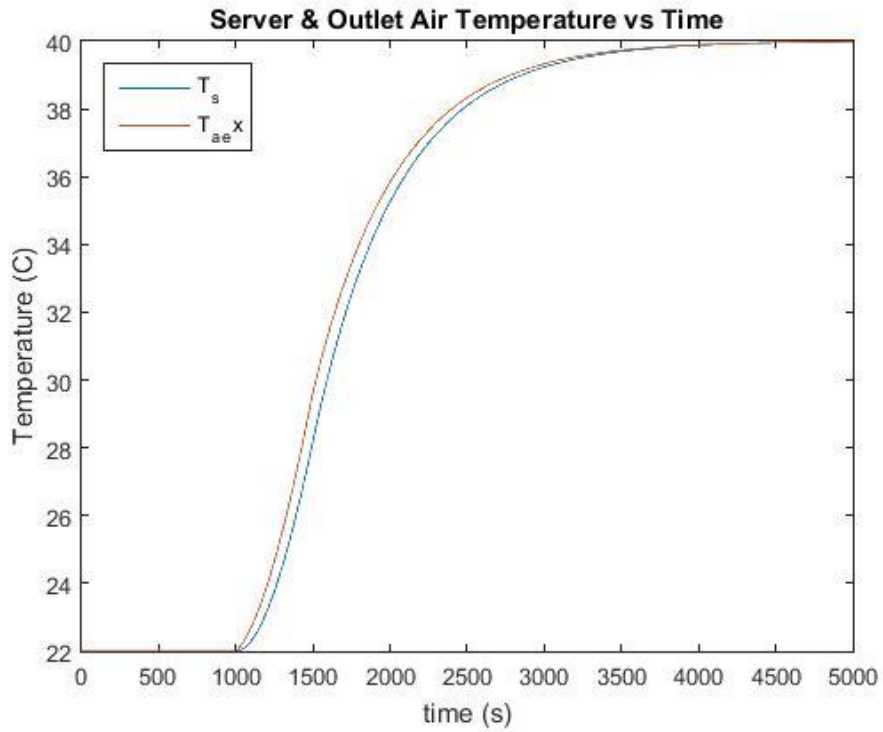


Figure B.5: Variation of server & exit air temperature with time for an unpowered server

Initially powered on server

Here is the combined power dissipation of all the server components, barring the fan, is 350W. The fan dissipation itself is 32W, making a total of 382W of power dissipation for the entire server.

Results for server initially powered on

Table B.2: Transient server parameters for an initially powered server

Vol. Flow Rate (m ³ /hr)	Tau (minutes)	Effectiveness	Capacitance (J/K)	Heat Transfer Coefficient (W/m ² .K)
100.00	9.12	0.88	15585	402.22

The graphs for the resulting server, inlet & exit air temperatures are shown on the following page, along with a graph for the server power dissipation.

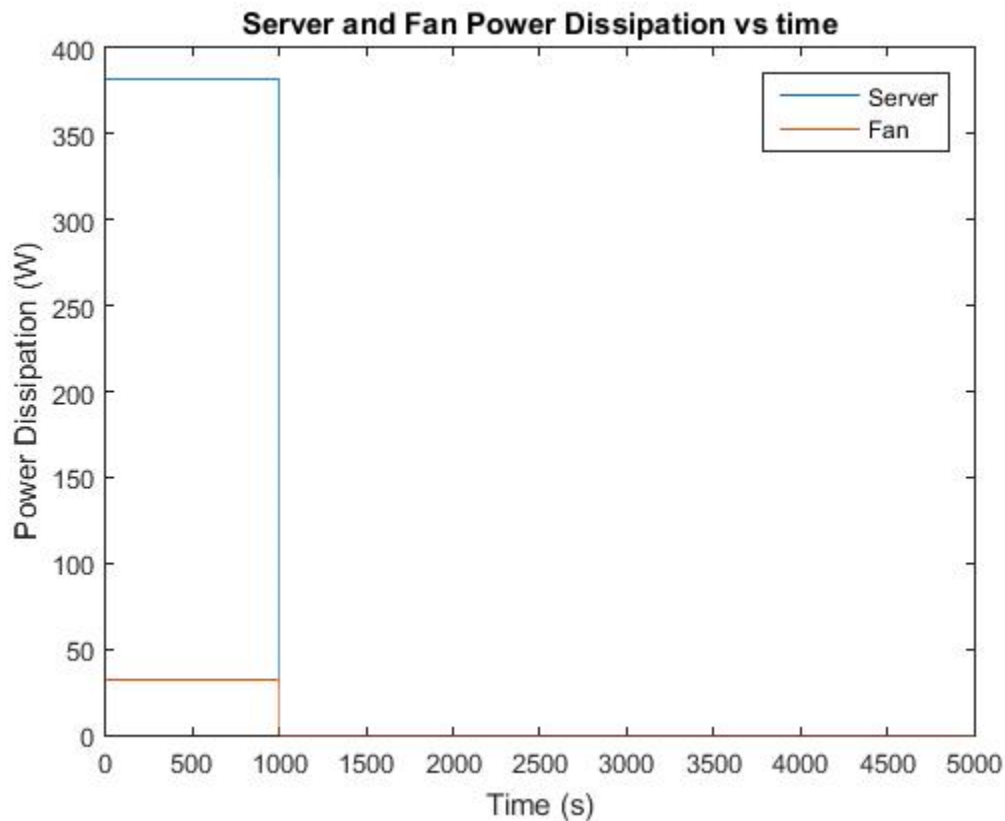


Figure B.6: Variation of CPU & fan power dissipation with time for an initially powered server

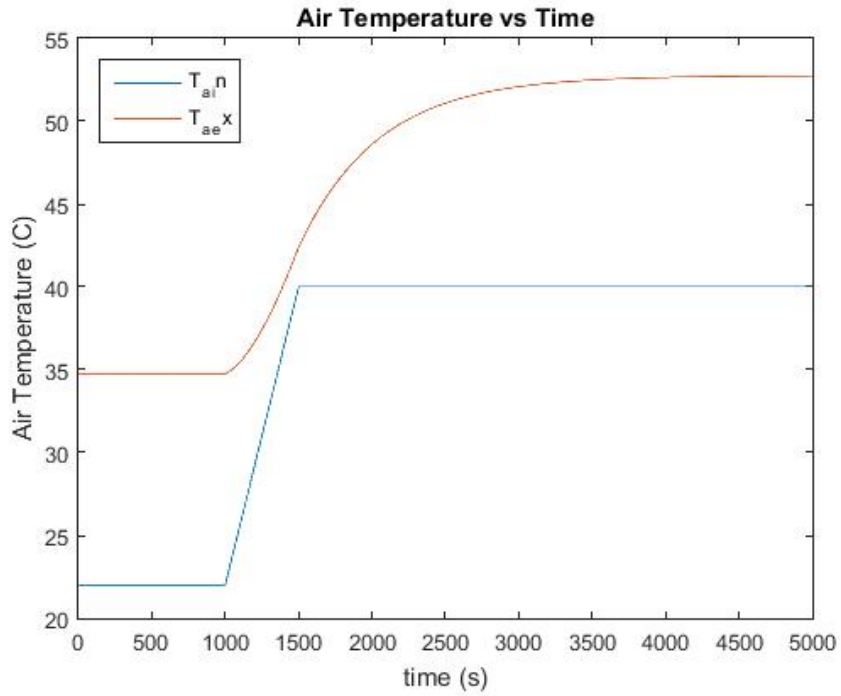


Figure B.7: Variation of server inlet & exit air temperature with time for an initially powered server

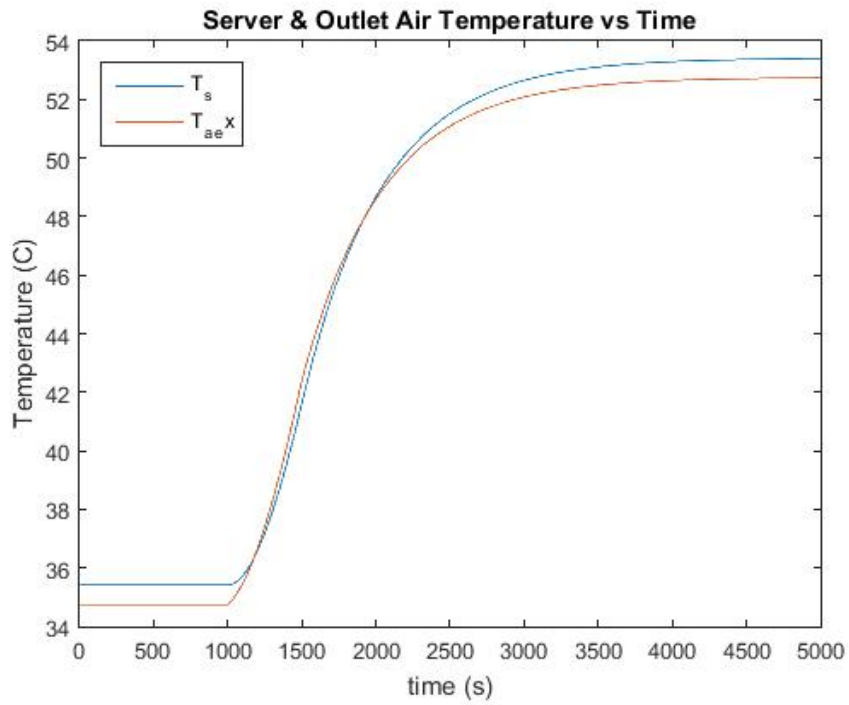


Figure B.8: Variation of server & exit air temperature with time for an initially powered server

Comparison with Khalifa paper results

Comparing the results of this model with the parameters provided in the Khalifa paper, the following results are obtained.

Table B.3: Comparison of numerical vs empirical transient server parameters

Source	Vol. Flow Rate (m ³ /hr)	Tau (minutes)	Effectiveness	Capacitance (J/K)	Heat Transfer Coefficient (W/m ² .K)
Author	68.0	13.42	0.88	15585	273.51
NY Lab	68.0	9.3	0.94	17500	Not Given
MA Lab	68.0	8.2	0.91	14500	Not Given

The capacitance value calculated is in the 15000 range, which is normally what is expected from a 2U server. This value lies in the middle range of the values determined at the two labs. The effectiveness and time constant values are different, however. The reason for this discrepancy is the fact that capacitance and effectiveness are calculated from the given correlations which are obtained using curve fitting of the experimental data, with R^2 values of 0.89 & 0.66 respectively. Since the R^2 values significantly deviate from 1, especially in the effectiveness case, hence there will be significant discrepancy between the experimental and analytical values (those obtained using the curve-fitting correlations). And since the time constant is a ratio of the capacitance and K , (effectiveness times the flow rate & specific heat), the time constant will significantly deviate as well. However, the model stands since the results obtained from it are close the experimental values and in essence, based on the correlations which are curve-fitted from the experimental data itself. Any discrepancy is attributed to the precision of the curve-fitting method in order to obtain the best-fit curve. The temperature profiles for the given volumetric flow rate are shown in Figure B.9 - B11 below:

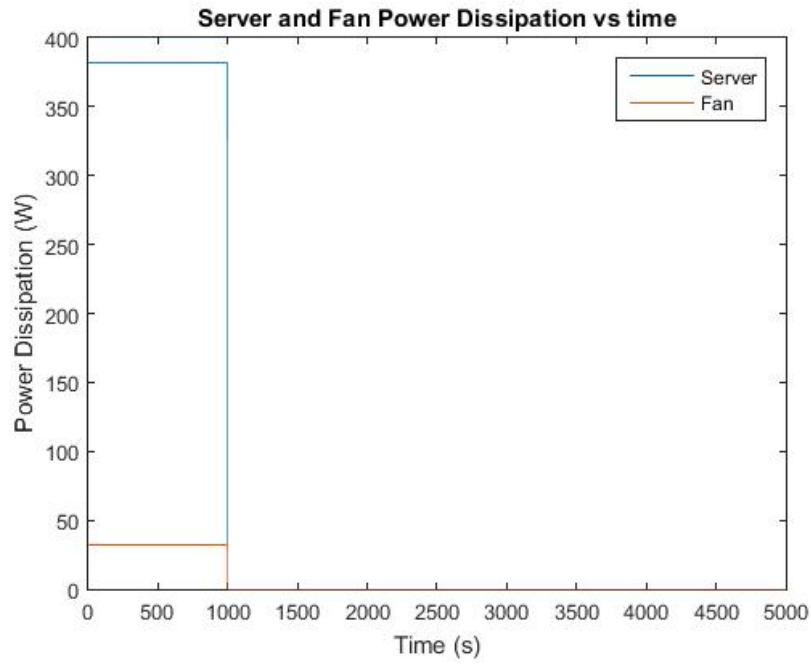


Figure B.9: Variation of CPU & fan power for an initially powered server; flow rate of 68m³/hr

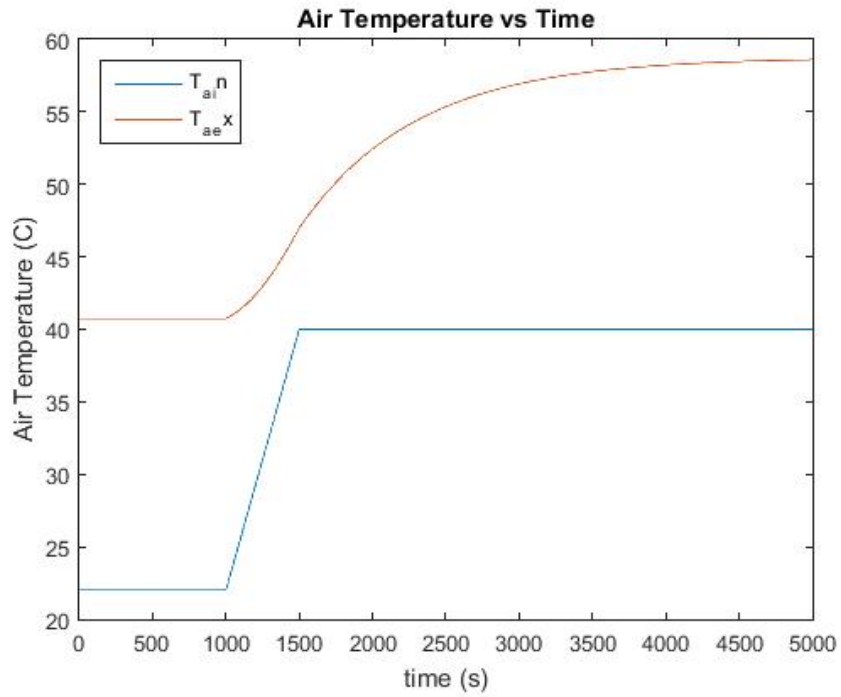


Figure B.10: Variation of server inlet & exit temperature for an initially powered server; flow rate 68m³/hr

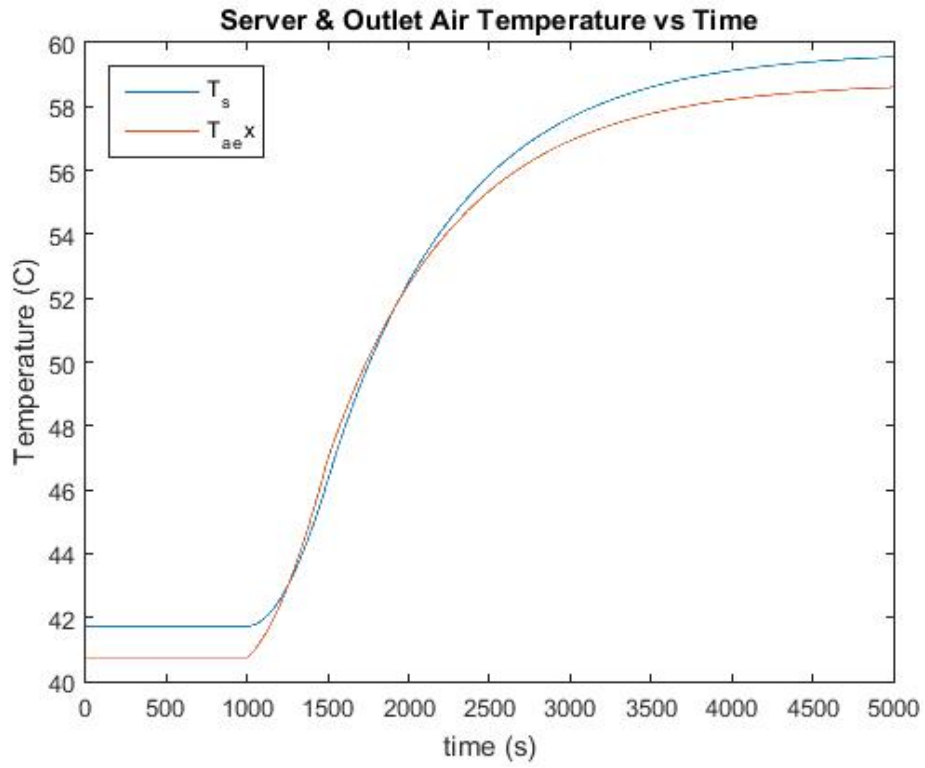


Figure B.11: Variation of server & exit air temperature for an initially powered server; flow rate $68\text{m}^3/\text{hr}$

REFERENCES

- [1] https://en.wikipedia.org/wiki/Modular_data_center
- [2] <http://siliconangle.com/blog/2014/03/05/the-evolution-of-the-data-center-timeline-from-the-mainframe-to-the-cloud-tc0114/>
- [3] http://www.theregister.co.uk/2009/12/07/ibm_data_center_containers/
- [4] <http://www.datacenterknowledge.com/microsofts-next-generation-data-centers/>
- [5] <http://www.datacenterknowledge.com/archives/2016/04/20/microsoft-moves-away-from-data-center-containers/>
- [6] <http://www.datacenterdynamics.com/rackable-systems-unveils-ice-cube-modular-data-center/30169.fullarticle>
- [7] <http://www.datacenterknowledge.com/archives/2008/03/05/verari-offers-data-center-in-a-container/>
- [8] <http://www.schneider-electric.com/en/product-range/61783-ecobreeze-air-economizers/>
- [9] <https://www.hpe.com/us/en/integrated-systems/pods.html>
- [10] https://en.wikipedia.org/wiki/HP_Performance_Optimized_Datacenter
- [11] <http://www.asetek.com/press-room/blog/2014/liquid-cooling-delivering-on-the-promise/>
- [12] http://www.megatel.com.pl/megatel/download/RD100_HP_NREL.pdf
- [13] www.nrel.gov/news/features/feature_detail.cfm
- [14] <https://www.youtube.com/watch?v=soVDoqRVP5c>
- [15] Huawei IDS1000 Container Data Center Solution
- [16] <https://energyplus.net/>
- [17] ASHRAE Publication, “2008 ASHRAE Environmental Guidelines for Datacom Equipment- Expanding the recommended environmental envelope”, Atlanta, 2008
- [18] AHRAE TC 9.9 Publication, “2011 Thermal Guidelines for Data Processing Environments- Expanded Data Center Classes and Usage Guidance”, Atlanta, 2011

- [19] ASHRAE Publication, “ANSI/ASHRAE/IES Standard 90.1-2010 Applicability to Datacom”, Atlanta 2010
- [20] ASHRAE Publication, “ANSI/ASHRAE/IES Standard 90.1-2010”, Atlanta, 2010
- [21] S.-W. Ham, M.-H. Kim, B.-N. Choi, and J.-W. Jeong, “Energy saving potential of various air-side economizers in a modular data center,” *Appl. Energy*, vol. 138, pp. 258–275, Jan. 2015.
- [22] S.-W. Ham, J.-S. Park, and J.-W. Jeong, “Optimum supply air temperature ranges of various air-side economizers in a modular data center,” *Appl. Thermal Engineering*, vol. 77, pp. 163–179, Jan. 2015.
- [23] H. Endo, H. Kodama, H. Fukuda, T. Sugimoto, and T. Horie, “Effect of climatic conditions on energy consumption in direct fresh-air container data centers,” *Sustainable Computing: Informatics & Systems*, vol. 6, pp. 17–25, 2015.
- [24] H. Zhang, S. Shao, H. Xu, H. Zou, and C. Tian, “Free cooling of data centers: A review,” *Renewable & Sustainable Energy Reviews*, vol. 35, pp. 171–182, 2014.
- [25] A. Qouneh, C. Li, and T. Li, “A quantitative analysis of cooling power in container-based data centers,” *IEEE Transactions*, pg. 61-71, 2011.
- [26] V. Depoorter, E. Oro, and J. Salom, “The location as an energy efficiency and renewable energy supply measure for data centers in Europe,” *Appl. Energy*, vol. 140, pp. 338-349, 2015.
- [27] <http://www.utopiatechnology.co.uk/storage/containerised-data-centre/>
- [28] Department of Energy, “EnergyPlus Engineering Reference,” 2010.
- [29] Wemhoff, A. P., del Valle, M., Abbasi, K., Ortega, A. (2013) Thermodynamic modeling of data center cooling systems. Proceedings of the 2013 International Technical Conference and Exhibition on Packaging and Integration of Electronic and Photonic Microsystems (InterPACK), 73116.
- [30] Zachary M. Pardey Dustin W. Demetriou, Hamza Salih Erden, James W. VanGilder. Ezzat Khalifa, Roger R.Schmidt, Proposal for Standard Compact Server Model for Transient Data Center Simulations, *ASHRAE Transactions*, 121(1)
- [31] Hamza Salih Erden, Ezzat Khalifa, Roger R.Schmidt, 2014, Determination of the Lumped Capacitance Parameters of Air-Cooled Servers through Air Temperature Measurements, *Journal of Electronic Packaging*, 136

[32] Application Guide for EMS, *EnergyPlus Version 8.3*

[33] Dell, PowerEdge R210 II, *Technical Guide*

[34] W. Bernal, M. Behl, T. Nghiem, and R. Mangharam, “MEL: a tool for integrated design and deployment of energy efficient building controls,” Real-Time and Embedded Systems Lab (mLAB), October 1, 2012, http://repository.upenn.edu/mlab_papers/51.